Republic of Iraq
Ministry of Higher Education & Scientific
Research
Al-Furat Al-Awsat Technical University
Engineering Technical College Al-Najaf

EXPERIMENTAL STUDY OF UNDERGROUND HEAT EXCHANGER WITH DOUBLE LAYERS

A Thesis

Submitted To the Department Of Mechanical Engineering Techniques of Power in Partial Fulfillment of the Requirements for Master of Thermal Technologies Degree in Mechanical Engineering Techniques of Power

BY
Zahraa Saleh Abdzaid

(B.Tch. Automotive. Eng.)

Supervised by:

Assist. Prof. Dr.
Tahsean Ali Hussain

Assist. Prof. Dr.
Ali Najah Kadhim

August 2020

بِسْمِ ٱللَّهِ ٱلرَّحْمَٰنِ ٱلرَّحِيمِ

أَلَمْ نَشْرَحْ لَكَ صَدْرَكَ ۝ وَوَضَعْنَا عَنْكَ وِزْرَكَ ۝ الَّذِي أَنْقَضَ ظَهْرَكَ ۝ وَرَفَعْنَا لَكَ ذِكْرَكَ ۝ فَإِنَّ مَعَ الْعُسْرِ يُسْرًا ۝ إِنَّ مَعَ الْعُسْرِ يُسْرًا ۝ فَإِذَا فَرَغْتَ فَانْصَبْ ۝ وَإِلَىٰ رَبِّكَ فَارْغَبْ ۝
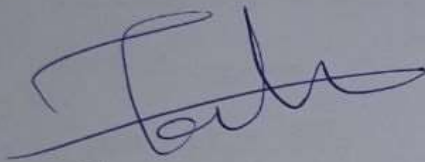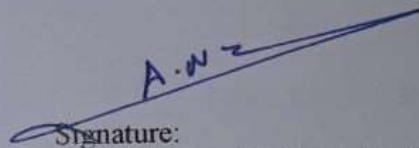
صدق الله العلي العظيم

سورة الشرح

Supervisor's Certification

We certify that this thesis titled "**EXPERIMENTAL STUDY OF UNDERGROUND HEAT EXCHANGER WITH DOUBLE LAYERS**"submitted by **Zahraa Saleh Abdzaid** has been prepared under our supervision at the Department of Mechanical Engineering Techniques of Power, College of Technical Engineering / Najaf⸴ AL-Furat Al-Awsat Technical University, as a partial fulfillment of the requirements for Master of Thermal technologies degree.

Signature:
Asst. Prof.Dr. Tahsean Ali Hussain
(Supervisor)
Date: 2٩/ 9 / 2020

Signature:
Asst. Prof.Dr. Ali Najah Kadhim
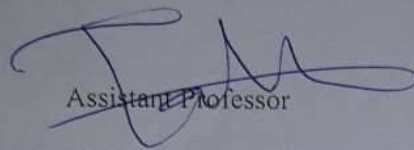(Co-Supervisor)
Date: 2٤/٩ / 2020

In view of the available recommendation, we forward this thesis for debate by the examining committee.

Signature:
Asst. Prof.Dr. Dhafer Manea Hachim
Head of power mechanic Tech. Eng. Dept.
Date: /   / 2020

Committee Report

Committee Report

We certify that we have read this thesis entitled " EXPERIMENTAL STUDY OF UNDERGROUND HEAT EXCHANGER WITH DOUBLE LAYERS" submitted by **Zahraa Saleh Abdzaid** and as Examining Committee, examined the student in thesis contents. In our opinion, the thesis is fully adequate in scope and quality for a master degree in Thermal Technologies Engineering.
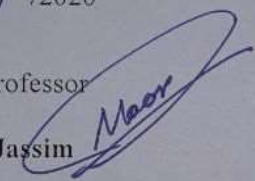
Assistant Professor

Dr. Tahsean Ali Hussain
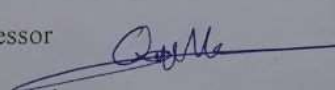
Supervisor

Date: 24/ 9 /2020

Assistant Professor

Noor M. Jassim

Member

Date: 24/ 9 /2020

Assistant Professor

Dr. Ali Najah Kadhim

Co-Supervisor

Date: 24/ 9 /2020

Assistant Professor

Dr. Ahmed H. Ali

Member

Date: 24/ 9 /2020

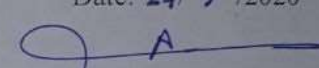Assistant Professor

Dr. Qahtan A. Abd

Chairman

Date: 24/ 9 /2020

Approval of the Najaf Engineering Technical College

Signature:

Assistant Professor Dr. Hassanain Ghani Hameed

Dean of the Engineering Technical College – Najaf

Date: / /2020

Acknowledgements

Above all, praise be to my God for mercy, blessing and assistance during the preparation of this work and supporting me in all aspects of my life.

I also extend my thanks and gratitude to my parents, who are my first support and inspiration for all the knowledge I gained, in my life.

My thanks go to my project supervisors for their support in completing the project, Special thanks go to the Head and staff of the Techniques Power Mechanic Engineering Department in Al-Najaf Technical College, Al-Furat Al-Awsat Technical University for their support and advice.

Thanks also to my sisters, brothers, family, and all of my colleagues for their continued encouragement to me.

I also thank everyone who helped me to complete this project.

Abstract

Several techniques have been tested to transfer heat and over a period of years for purpose of obtaining a good heat transfer and a low operating cost, and of these technologies the underground heat exchangers for various types and purposes for their use, which depend on the transfer heat of fluid inside them to the depths of the soil and vice versa

A two-layer horizontal underground heat exchanger was designed and tested as a closed system to reduce the required area. The installation of a single layer horizontal heat exchangers, needs to sufficient area to bury the exchanger, which increase the economic cost of this type of underground heat exchangers that is one of the disadvantages of a horizontal heat exchangers (not having enough space at times).

The temperature gradient of the soil was recorded during the year, and its relative stability was observed at the specified depth from 2m to 3.5 m, in addition to measuring the thermal conductivity of a sample of the same soil and knowing its properties.

Polyethylene MLC pipes have been used with an external diameter of 16 mm and a thickness of 2 mm and a length of 100 m for each layer.

Two networks are designed in the form of a serpentine each network is 100 m long, where the pipes of the two networks facing each other in a staggered arrangement (at V shape side view) to increase the contact area of the pipes to obtain a greater heat transfer. And by using the COMSOL program, assuming 2D system and inserting the design properties of the pipes and soil, fined the optimum distance between the pipes was proposed to be (0.3-0.5) m, the dimension 0.4m was chosen for the design ground heat exchanger GHE.

The first layer of the system pipes was buried at a depth of 3 meters and the second layer system pipes buried at a depth of 2.5 meters, from the ground surface.The tests were done on every layer separately and then for the two layers together, by changing the inlet water temperature approximately from 30, 40 and 50°C and with different flow rates from 2, 3, 4 and $5\ell/min$, that was achieved at the period (12/6/2019 - 22/7/2019).for the purpose of cooling in the hottest months of the region.

When operate the system in a double layer mode a high temperature difference was obtained (the average is 15.96 °C), and when operate the system with single layer mode the average of high temperature difference obtained is (15.8) and (13.4) °C for the first and the second layer, respectively, under different circumstances

In order to record the coefficient of performance (COP), the system was tested for both layers to record the highest value, the (COP) was 8.59 in the double-layers mode of operation and‹5.9, 5.2 for the first and second layers respectively in the same conditions, Due to the increased flow when testing each pipe layer separately, compared with testing the double-layers together.

TABLE OF CONTENTS

Contents

LIST OF TABLES

LIST OF FIGURES

Nomenclature

Symbols	Meaning	Unit
Cp_{mean}	Mean heat capacity of working fluid	kJ/kg.°C
D_i	Pipe inside diameter	mm
D_o	Pipe outside diameter	mm
k_w	Thermal conductivity of water inside the pipe	W/m.°C
k_{pipe}	Thermal conductivity of pipe	W/m. °C
$\dot{V}$	Volumetric flow rate	m^3/s
T_s	Temperature of soil surface	°C
T_{amb}	Temperature of surrounding air	°C
T_i	Temperature of water inlet the pipe	°C
T_o	Temperature of water outlet the pipe	°C
u	Velocity of water inside the pipe	m/s
L	Length of the pipe	m
U	Overall heat transfer coefficient	W/m^2.K
$\dot{m}$	Mass flow rate of fluid	kg/s
K_{soil}	Thermal conductivity of soil	W/m.K
C_w	Specific heat of water	kJ/kg.K
q	Total rate of heat transfer	W
A_i	Inside surface area of pipe	m^2
A_o	Outside surface area of pipe	m^2

d	depth of soil	m
T_0	is the initial temperature of the ground ($d = 0$)	°C
T_b	fluid bulk temperature	K
q'	is the heating rate per unit length of the line source	W/m
Δp	Pressure drop	Bar
I	electrical current supply	Amber
V	electrical voltage (220)	Volte
e	Roughness inside pipe	mm
ΔT ($T_{in}-T_{out}$)	Overall temperature difference of fluid	°C
T_T	Temperature of film between solid and fluid	°C
Q	Heat transfer	W
Re	Reynold number	-
Pr	Prandtle number	-
R_{soil}	Thermal resistance of soil	K/W
$R_{conv.}$	Thermal resistance convection	K/W
R_{pipe}	Thermal resistance conduction	K/W
h_w	heat transfer coefficient	W/m.K
Nu	Nusselt number	-
E	energy	W

Symbols	Meaning	Unit
μ	Dynamic viscosity	kg/m.s
∇x	Depth gradient	m
ρ	Density of water in the pipe	kg/m^3
α	thermal diffusivity	m^2/s

Abbreviations

Symbols	Meaning
COP	The coefficient of performance
EER	energy efficiency ratio
GHE	Ground heat exchanger
GSHP	Ground source heat pump
MLCP	Multi-layer composite pipe
R.O	reverse osmosis system for water

Chapter One
Introduction

CHAPTER ONE

INTRODUCTION

1.1   HISTORY OF ENERGY USE

Since the beginning of the existence of human on the surface of the earth, the first kinds of energy that he knew was his kinetic energy and his ability to accomplish work, which is the result of the chemical energy of the food he consumes. Then he used energy in its various forms to be able to withstand and live. As he used Animal energy and water energy for mobility.

Next, he developed the use of energy; solar energy used in many purposes as drying crops before storage, water heating, and other purposes. The energy of the earth used to obtain sources of heating and cooling for various application, as well as wind energy was used in the rotation of windmills and water energy to rotate the watermills. Grease extracted from animal used for lighting, cooking, etc. [1]

From that we conclude, that the energy adhered the existence of human to facilitate his life, and without it could not withstand and live.

During the industrial revolution, and the discovery of fossil fuels (crude oil), which first used before 3000 BC by the ancients Iraqis (Babylonians)[2].Then the world began to use this kind of energy in various life applications; The ease of use and high efficiency of Fossil fuels led to it's widespread, Fossil fuel energy was the first essential energy source that still being used to this day.

After the development of energy generation systems using multiple fossil fuel components, fossil fuel consumption provided incredible benefits to humidity as this enabled the development of reliable long-term transport.

 Also led to providing various goods and replacing that goods which made from natural resources, by others composite of petrochemical materials, such as the industry of tissues, furniture, and wide range of applications depend on natural sources.

 That mentioned was in the Holy Quran, which revealed was in 635 AD in Surat al-Nahl (verse 80)

(﴿وَاللَّهُ جَعَلَ لَكُمْ مِنْ بُيُوتِكُمْ سَكَنًا وَجَعَلَ لَكُمْ مِنْ جُلُودِ الْأَنْعَامِ بُيُوتًا تَسْتَخِفُّونَهَا يَوْمَ ظَعْنِكُمْ وَيَوْمَ إِقَامَتِكُمْ ۙ
وَمِنْ أَصْوَافِهَا وَأَوْبَارِهَا وَأَشْعَارِهَا أَثَاثًا وَمَتَاعًا إِلَىٰ حِينٍ﴾)

((And Allah has made for you from your homes a place of rest and made for you from the hides of the animals tents which you find light on your day of travel and your day of encampment; and from their wool, fur and hair is furnishing and enjoyment <u>for a time</u>))[3]

 Then the usage of energy types was developed to facilitate life and make it the most comfortable and developed forms of energy used and prospered.

But, in recent decades, there have been many disadvantages to the use of oil and its derivatives appeared, on the earth's environment in general, the climate in particular, and the extent of its effect on the deterioration of the health of human. In addition to being that the fossil fuels are from the depleted sources of energy, that can run out after a certain period. Now the human begins to replacing fossil fuels with other sustainable sources of energy that have no negative effect on the climate and environment of the globe.

Renewable resources are unlimited natural resources, which can replenish in a very short amount of time, such as solar energy, wind energy, hydropower, biomass, ocean energy, geothermal energy, and waste energy. The principal of using ground inertia for heating and cooling is not a new concept, but rather a modified concept that goes back to the ancients. This technology has been used throughout history from the ancient Greeks and Persians in the pre-Christian era until recent history. For instance the Italians in the middle ages used caves, called colvoli, to precool / preheat the air before it entered the building. The system which is used nowadays consists of a matrix of buried pipes through which air is transported by a fan. In the summer the supply air to the building is cooled due to the fact that the ground temperature around the heat exchanger is lower than the ambient temperature. During the winter, when the ambient temperature is lower than the ground temperature the process is reversed and the air gets preheated [4]

The percentage of current use the geothermal energy in the world is 1.5% from the renewable energy and 0.3% from the total electrical energy produced, The geothermal energy distribute on a wide range of application as shown in the figure 1.1 [5].
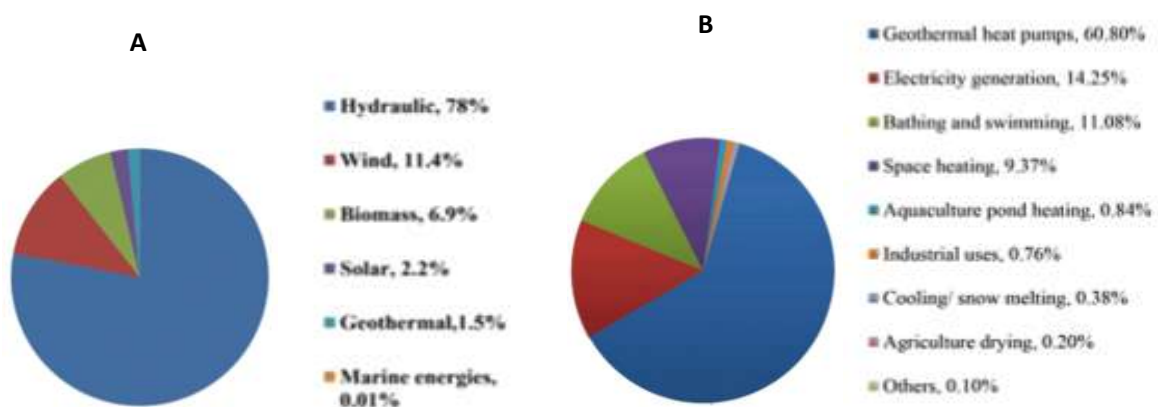
Figure 1.1 A-the worlds electricity production from renewable sources, B- Geothermal energy applications worldwide in 2014. [5]

1.2   GEOTHERMAL ENERGY

geothermal energy is considered one of the most important sources of sustainable energy, for the reason of stability, and relatively constant temperature due to variations of annual weather the temperatures, and low effect of different climate factors. Which is the main factor to influence the rest of the other forms of sustainable energy in most regions of the globe, also it will be an important power source for billions of years to come.

Is defined as the terrestrial generated heat keep in, or discharged from rocks and fluids (water, brines, gasses) saturated pore house, cracks, and cavities and is wide harnessed in two ways: for power (electricity) generation and for direct use, e.g., heating, cooling, agricultural processes, spas, and a wide range of commercial processes, as well as drying [6].

Since ancient times underground energy has been used for, heating, cooling, and other functions, which related to the cultures of the world. New Zealand and Native Americans have used water from hot springs for cooking and health purposes, for thousands of years. The Greeks and Romans had used groundwater energy from hot spas to treat the problem of eyes and skin. The Japanese have enjoyed energy spas for hundreds of years.as shown in figuer1.2

Figure 1.2 one of manifestations of hydrothermal vents [2]

The underground temperature varies from the center of the earth to the surface, whereas the temperature of the center earth is 6,000 degrees Celsius i.e same to the temperature of the surface of the sun. The rise in temp for the depths of up to kilometers or thousands of kilometers is enough to evaporate the fluid used and increase the temperature and the speed of the steam produced which is used to rotate the turbines of the stations of electric power generation, which is one of the indirect ways to benefit from the energy of the core of the earth. This heat has transmitted from the heart of the earth for 4.5 billion years [7]. As shown in the figure 1.3
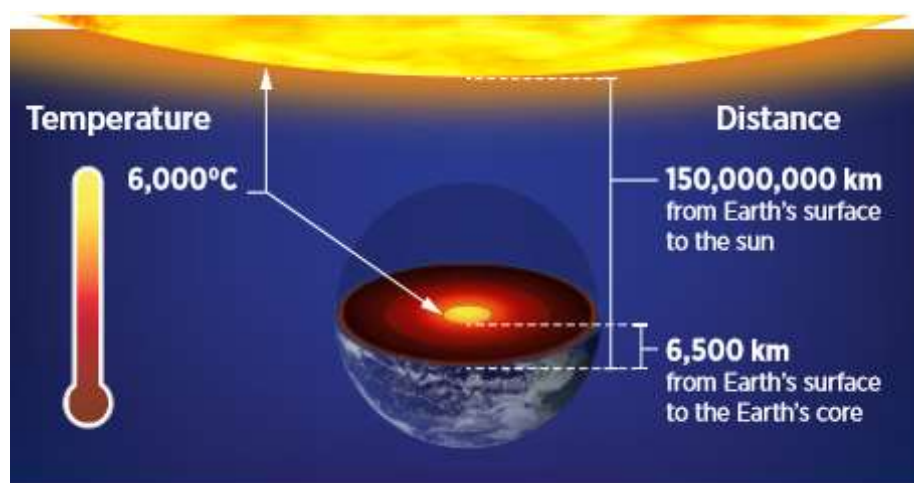
Figure 1.3 The underground temperature varies from the center of the earth to the surface, [7]

Popiel et al. (2001) has divided the distance between the surface and the core into many zones, depending on the temperature variation of the earth and in the sandy soil at low depths [8].

1. Surface zone, reaching a depth of 1m, within which the soil temperature is incredibly sensitive to short-time changes of climatic conditions.

 2. Shallow zone, ranging from the depth of one to eight-meter (for dry lightweight soils) or twenty-meter (for wait sandy soils) where the soil temperature is nearly constant and close to the normal annual air temperature; throughout this zone, the distributions soil temperature, depend primarily on the cycle seasonal of climatic conditions.

3. The deep zone flowing the depth of the shallow zone, where the soil temperature is relatively constant (very slowly rising with the depth in keeping with the geothermal energy raise).

   The second zone is suitable for direct subtraction or withdrawal of heat due to the relative stability of temperatures, in this region over the annual term, it is suitable in the applications of heating and cooling systems for homes where the heat is subtracted or withdrawn from the soil through heat exchangers or system of pipes buried at depths of up to 4 meters or more, depending on the type of heat exchanger and other factors, through which a medium (fluid) circulates heat from the ground to the use area or vice versa [9].

There are many definitions to the Underground heat exchangers rely on its design some of them called buried pipe systems, underground air tunnels, geothermic heat exchangers, device for earth pipes, and earth air tunnels [10]

The types of underground heat exchangers are divided according to the ground heat exchanger types, [8] can be shown in the following scheme figuer4.1.
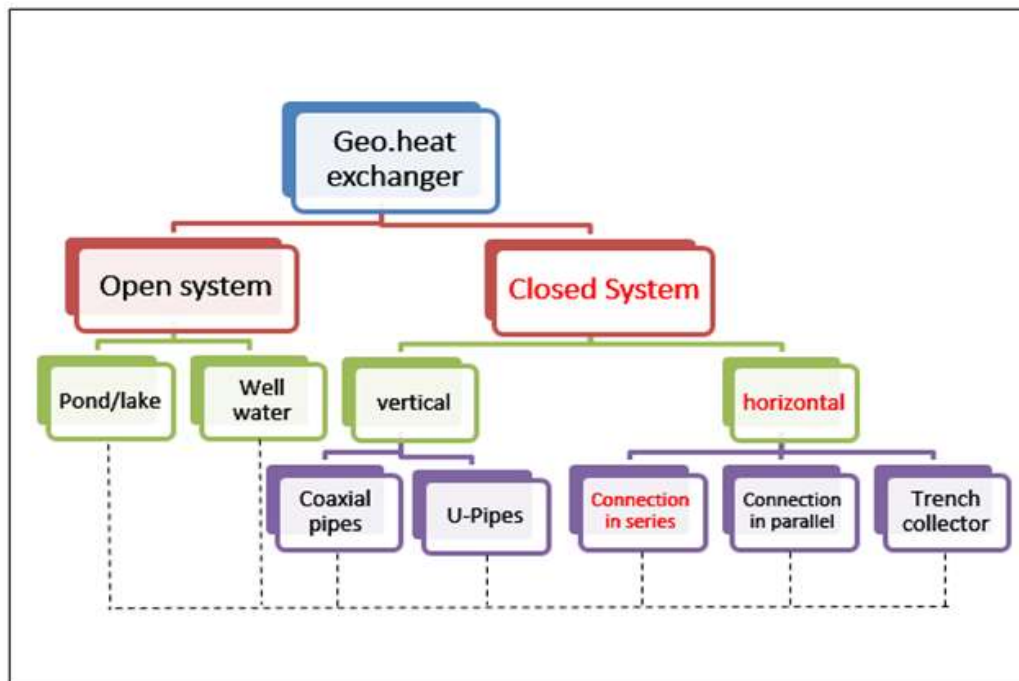
Figure 1.4 Types of underground heat exchangers

Closed systems are very suitable for heating and cooling applications using water as the primary medium for heat transfer in systems, residential homes, zero-energy homes, and greenhouses.[11,12,13,14,15,16,17,18,19,20,21]

1.3   RESEARCH OBJECTIVE:

- The current research aims to exploit the underground energy to cooling and heating the buildings as Zero Energy Houses under the local conditions of the Najaf governorate / Iraq.

- Design of two layers of piping system buried in a 2.5m and 3m depths because of the relative stability of ground temperature in this depths of the light sandy soil, and at appropriate dimensions to reduce its operating cost of the underground heat exchanger. in order to use the Najaf Zero Energy House in the city of Holly Najaf, Iraq.

- Test the performance of a two layers horizontal underground heat exchange buried in a different depths when operating as a double-layers together and when operating as a single pipes layer.

- The place of the research completion is the open area which suggested to construct the Najaf Zero Energy House Project (NZEHP) in the Najaf Engineering Technical College which follows the Al-Furat Al-Awsat Technical University, the (31.9760718 ° N 44.364692 ° E).

CHAPTER TWO

LITERATURE REVIEW

2.1 INTRODUCTION

Energy consuming comfort humans in a world is increased in multifold about the past. 80% of the global energy required to come as of fossil fuel and involvement only 20% commencing sources renewable energy because of huge use for fossil fuels, there is a huge increase in carbon dioxide emissions, which is one of the greenhouse gases that cause global warming. Many countries developed new techniques about the problem so, beginning to introduce emission control measures. The energy Spent in the buildings sector around 30%, most for heating and cooling as well as can be replaced using sources of renewable energy. One of the most common types of alternative energy used in heating and cooling systems is underground heat exchangers.which has been used since ancient times in direct and simple ways for use, before a discovery for fuel, and its use remained in areas that lack fossil fuels or found the little amount of it and with development for methods for using, after that a development for forms and types Exploiting underground energy and increasing its efficiency and ability for its systems and it is still developing [22],[23],[24][5] One of the efficient and promising technologies that used in most countries that can be used for heating and cooling

8

processes is a ground heat exchanger GHE and ground source heat pump GSHP technology [24],[10]

2.2 Literature Survey

Many researchers around the world have presented studies on geothermal heat exchangers of various kinds and under different conditions. Below are some of those researches:

Esen, Inalli et al. (2007) Presented comparison between an air-coupled heat pump ACHP and ground-coupled for heat pump GCHP system. An experimental results taken in cooling season of June until September in 2004. A performance of average cooling coefficient for GCHP system for horizontal ground heat exchanger in various trench , at 1 and 2m depth, obtain to be 3.85 and 4.26, respectively and average cooling coefficient for ACHP system determine is 3.17. A result illustrated parameter significant impact in performances, and GCHP system are economical better than ACHP system at space cooling purpose.[25]

Figure. 2.1 Photographs for condenser (a) GCHP (b) ACHP[25]

Demir, Koyun et al. (2009) presented heat conduction equation solved in finite difference formulation developed in MATLAB environment and effects for solution parameters. Experimental study A GSHP having 4 kW heating and 2.7 kW cooling capacity is used for the experimental study. The ground heat exchanger consists of three parallel pipes which have 40

m length and1/2" diameter buried in the soil at 1.8m depth. illustrated a testing for model. Ground source heat pump GSHP Pilot System Yildiz Technical University in Davopasa over an area for 800 square meters with no special rotor cover. Using a double-shielded in a soil horizontal and vertical in different distance from center of the tubes, in inlet and outlet of ground heat exchangers and temperature data are collected. And obtain a comparison for experimental and numerical simulations using experimentally water inlet temperature. A high difference among numerical result with experimentally information about 10.03%. Soil temperatures considered and then compared with experimentally information. Horizontal and vertical temperatures features match well with experimentally information. A simulation result compared with other studies.[26]

Eicker and Vorschulze (2009) presented a geothermal low-depth heat exchanger is used efficiently heat sink of buildings energy produced in summer. When ambient temperature annually average is low enough, buildings cool down directly. A cooling tower is replaced by a heat exchanger in conjunction with an active cooling system. A performance for a double heat exchanger gave results for a ground analysis a better performance coefficient ranging between 13-20 ,as an annual average rate for use for cold produce electricity. Maximum corruption per meter is less than planned geothermal heat exchanger and varies among 8W/m at low-depth horizontal heat exchanger but up to 25W/m at vertical heat exchanger. Waste energy by -30% depend in conductivity of soil. Used polyethylene U-tubes in vertical boreholes of 75–220 mm diameter. A thermal conductivity for vertical tube filling material presentation affect 30% for different materials. Depending on temperature for inlet to heat exchanger on ground, energy spaced increase 2 W/m in direct cooling application in 20 ° C to 52 W/m in alternative to cooling towers at 40 ° C.[27]

Shua'a and Sabeeh (2009) presented results for a heat transfer characteristics in underground heat exchanger. An experimental test section is made for 50 m carbon steel pipe for 26.6, 52.5, 77.9 and 102.3 mm inner diameters and 33.5, 60.5, 88.9 and 114.3 mm outer diameters, respectively. A pipe is buried 2 m deep below ground surface. Hot water is used as working fluid in a tube. Experiments are performed under conditions for volumetric flow rates varying from 0.25 to 1 m3/h and an inlet hot water temperature is between 50 to 80 °C. Water temperature is measured at five points with equal length by arm couples placed inside a pipe. A metical model was developed on this purpose, which allows foreseeing a temperature distribution for a water in a system. Using a model, parametric analysis is carried out to investigate an effect for water flow rate, pipe material type, and pipe length and diameter on overall performance for an earth tube. [28]

Ozgener and Ozgener (2010) presented study performance for energetic characteristics for greenhouses cooling of underground air tunnel 47 m in horizontal, but in nominal diameter 56 cm galvanized U-bend buried in the soil at about 3 m in depth for ground heat exchangers. System installed and designed in Solar Energy Institute, Ege University, Izmir, Turkey. An exergy transport among component and destructions in each component for system is determined for average measured parameter illustrated from experimental results. A daily maximum coefficient cooling for performances (COP) value for system obtained 15.8. An average total of experimental period COP establish is 10.09. System COP calculate depended on amount for cooling produce using air tunnel and amount for power required to move air during a tunnel, but efficiency of energetic for air tunnel is 57.8-63.2%. A total exergy efficiencies on product/fuel is about 60.7%.[29]

Fujii, Okubo et al. (2010) evaluated applicability for horizontal Ground Heat Exchangers (GHEs) on Geothermal Heat Pump (GHP) systems for a

use in greenhouse farming. The depth and length for each trench were1.5 m deep and 70 m, respectively with diameter 0.8m for coil shape, 0.034 m and 0.024 m, for pipe. A GHEs were connected to heat pump and circulation pump become pelted as GHP system. Using GHEs, thermal response tests and air-conditioning test carried out from summer 2008 to spring 2009 for collecting operation testimony for system and ground temperature information in operation. An information examined for evaluating heat exchange capacity for horizontal GHEs and compared heat exchange performances with vertical GHEs. A test illustrated that horizontal installation for slinky coil in superior performance to vertical installation for energy efficiency, due to a lesser amount for influence atmospheric temperature change. The results of field tests showed that horizontal installation of slinky coils is superior to vertical installation in terms of energy efficiency, due to more stabilized ground temperatures. The comparison of heat medium temperatures within the air-conditioning test showed that horizontally-installed slinky coils have a comparable heat exchange capacity with vertical U-tube GHEs drilled during a formation with favorable thermal conductivity.[30]

Miyara, Tsubaki et al. (2011) presented study for several installed types ground heat exchanger (GHE) of steel pile basis, include multi-tube GHEs, U-tube, as well as double-tube in Saga University. Water flow during heat exchanger and exchange heat ground. A performance GHEs investigate in actual procedure for cooling form through flow rate 2, 4, and 8 l/min. The double-tube GHE has the highest heat exchange rate, followed by the multi-tube and U-tube. For example, with a flowrate of 4 l/min, the heat exchange rate is 49.6 W/m for the double-tube, 34.8 W/m for the multi-tube, and 30.4 W/m for the U-tube. Temperature for ground and GHE tube wall is calculated for discover temperature distribution for depth ground and GHE tube wall. A temperature for inlet and outlet for circulate water measured

for calculating heat exchange rate. A heat exchange rate better significantly for flowrate raise 2 to 4 l/min, except faintly altered 4 to 8 l/min.[31]

Wu, Gan et al. (2011) presented thermal performance for horizontal-coupled ground-source heat pump system. Studied in UK climate. Numerical simulation for a thermal behavior for a proposed heat exchanger in ambient air temperature, wind speeds, coolant temperature, and thermal properties for an experiment using a transient two-dimensional model. Simulation shows that there was no significant effect of wind speed on the specific heat extraction for the horizontal heat exchanger. The specific heat extraction by the heat exchanger increased with the ambient temperature and soil thermal conductivity but decreased with increasing refrigerant temperature. A specific heat extraction for a heat exchanger increases.[32]

Zukowski, Sadowska et al. (2011) presented simulation and experimental investigations for earth to air heat exchanger (EAHE) .A geothermal system reduces a heating load and greatly reduces air temperature during a summer season. A program used – Energy Plus to estimate a cooling potential for an air and ground piping system in apartment buildings with different Polish climate conditions. Simulate three important annual average factors for the soil as follows: surface temperature, surface temperature capacity and phase constant relative to a temperature calculated by CalcSoil SurfTemp. A result for a long-term experimental measurement for a double-pass ground air heat exchanger (ETHE and EAHE) made for PCV tube. The experimental data and calculations results indicate that earth tube is an energy saving solution. We can reduce cooling energy load by about 595 kWh due to this system. As mentioned before, the underground channels reduce the operative temperature inside the tested building by average 1.9°C. This effect has positive influences on improving person's thermal comfort. [33]

Congedo, Colangelo et al. (2012) studied a behavior for efficiency and energy of Heating and cooling for Ground Source Heat Pumps (GSHPs). The result indicated that heat fluxes transmitted from a ground and an efficiency for a system. Fluently calculating CFD code and simulation covers 1 year for system process, in summer and winter from typically climatic condition for souarn Italy. In particular three different geometry configura- tions (linear single tube, helical and slinky) have been analyzed for different working conditions (winter and summer) and varying: burying depth of the heat exchanger inside the ground (from 1.5 to 2.5 m); heat transfer fluid velocities (from 0.25 to 1 m/s); thermal conductivities of the ground around the heat exchangers (from 1 to 3 W/m K).The main factor for a heat transfer performance system led to a thermal conductivity for an earth during a heat exchanger and an optimum earth type with a maximum thermal conductivity (3 W / m.K). A choice for a rapid fluid heat transfer surrounded by tubes is major advantage. A depth installation for a horizontal geothermal heat exchanger didn't take part in performance system. Comparing the geometry arrangements leads to the choice of the helical heat exchanger as the best performing one.[34]

Naili, Attar et al. (2012) studied the evaluation for Tunisian geothermal energy and performance test for a horizontal ground heat exchanger. The results illustrated that an existing efficiency ranges from 14% to 28%. A total rejected heat using a Geothermal Heat Exchanger (GHE) system was compared with a total cold requirements in a room tested with a surface for 12 square meters. the results illustrated that GHE, with a length for 25 meters buried at a depth for 1 meter, covered 38% for a total cooling requirements for a tested room[35]
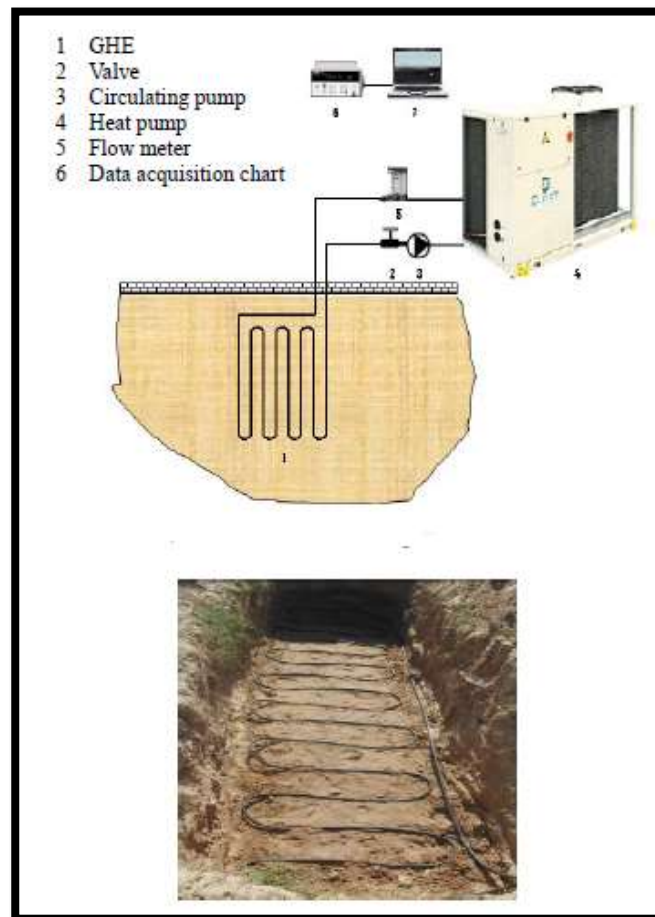
Figure 2.2 A GHE buried 1 m depth [35]

Abdul Rahman .O, et al. (2012) investigated a coefficient of performance (COP) for earth tube heat exchanger (ETHE) on sandy soil on desert arid climate. In an ETHE air was withdrawn from an exit for a greenhouse and pushed through a pipes under the ground to go in from our side to greenhouse. During this process heat is exchange among air and wall for a pipe to reduce temperature for air through summer or raise it during winter. An ETHE system is able to attained an average COP for 6.32 and peak for 6.89 during heating test despite occasional heat losses to a surrounding soil. It has achieved a maximum COP for 5.5 in August during a cooling tests with mean for 1.75. During a sensitivity analysis, a difference for approximately 3 in COP value found to varying from specific volume 0.6 m3/kg - 0.95 m3/kg. This signifies importance for incorporating effect for condensation flow fluid.[36]

15

Naili, Hazami et al. (2013) studied two experimental systems are performed at the Research and Technology Center of Energy (CRTEn), in Borj Cédria, northern Tunisia. Firstly, to evaluate optimal parameters of the GHE (ground heat exchanger), the performance of the GHE with horizontal configuration was analyzed experimentally and analytically. The effect of various parameters such as mass flow rate of circulating water, length, buried depth and inlet temperature of the GHE on the heat exchange rate were examined. Second, water-to-water GSCS (Ground Source Cooling System) with HGHE (Horizontal Ground Heat Exchanger) was performed. The results obtained from this experimental study, are used to evaluate the COP hp (coefficient of performance of the heat pump) and the COP sys (coefficient of performance of the overall system) of the GSCS, which are ranged between 3.8-4.5 and 2.3-2.7, respectively. In the first part of the present study the thermal performance of three GHEs with horizontal arrangements installed at the Center of Researches and Energy Technologies (CRTEn), in Borj Cédria, northern Tunisia, was investigated. The effect of various parameters such as mass flow rate of circulating water, length and buried depth of the GHE was examined. In the second part of this study, an experimental setup of a GSCS.show in Figure 2.3 [37]
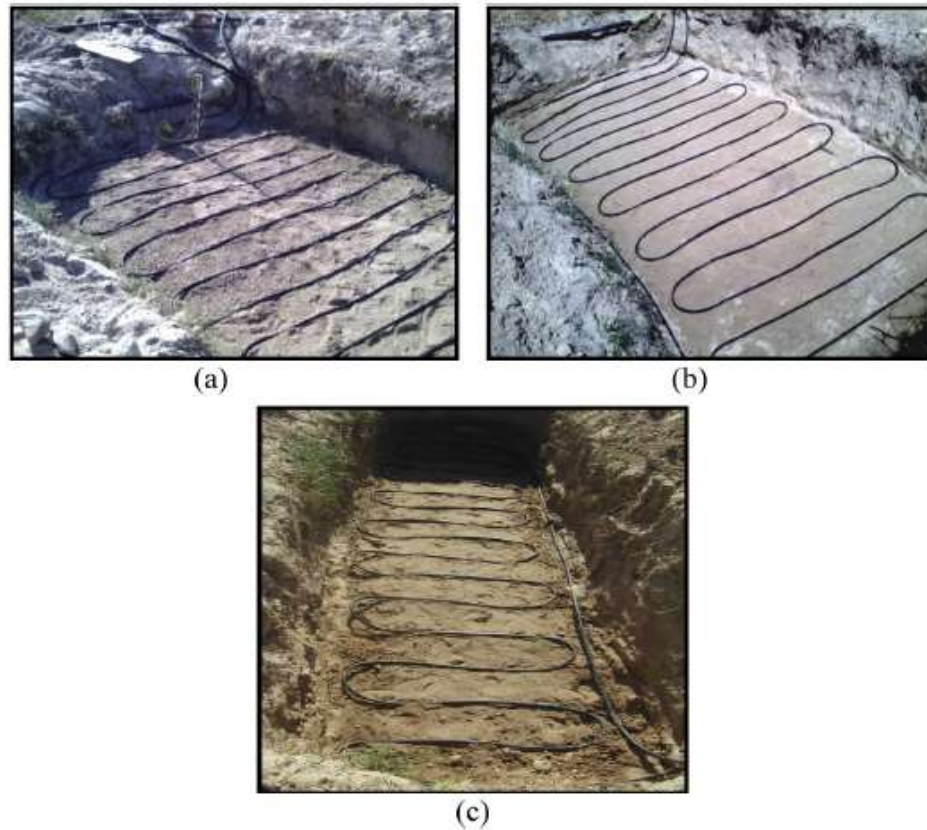
Figure 2.3. A GHE, 50 m (a) buried 0.6 m, (b) buried 1 m and (c) buried at 1 m in 25 m. [37]

Nikiforova, Savytskyi et al. (2013) studied thermophysical characteristics for different soil type and developed method for Soil to determines thermal conductivity. The study has stated analytical accreditation for estimating a coefficient for thermal conductivity for a different type (sand, clay and silt) and moisture for an obtained soil. This accreditation used for a technical thermal calculation for a ground-protected buildings[38]

NAILI, HAZAMI et al. (2013) stated that ground heat exchangers (GHE) consist of length Pipes buried at a reasonable depth below a surface for an earth, and a ground is used as a source of heat (in winter) or heat sink (in summer). This design takes advantage for moderate ground temperatures to enhance efficiency and reduce operational costs for heating and cooling systems. An aim for this study is to test a thermal performance for a horizontal ground heat exchanger (GHE) for space cooling. An experimental group constructed for translated climatic conditions in north

Tunisia. Result an Earth's temperature is illustrated at several depths (Ground thermal gradient), and a total heat transfer coefficient (U) is used to evaluate a system's efficiency, so energy efficiency is found from 14 to 28%.[39]

Bošnjaković, Lacković et al. (2013) presented the use of sources for geothermal energy to heat a greenhouse. Using geothermal energy for conventional purposes is a very acceptable and excellent option for a greenhouse design power source. Sources are not available throughout the Republic of Croatia, and they are useful and profitable on a sites that have been found. Obtaining an analysis for green house heating techniques has an advantage and disadvantages he use of thermal energy in greenhouses to reduce production costs, which amounts to 35% of the total costs of production. One of the major disadvantages of using geothermal water in greenhouses is the high investment cost.[40]

Chen, Xia et al. (2015) presented GHE Prototype Heat Transfer Model. Simulation for the results illustrated that in a vertical 100 meters GHE, a first 70 meters for a vertical buried GHE has an ability to transfer high temperatures from a last 30 meters. A validation model is used to verify an optimum depth for a vertical GHE in 5 case studies along a length for 60 - 100 m. But a result for a GHE with buried depth for 70 m provides a maximum rate for heat exchange in   depth (54.1 and 47.0 W / m in refusal / heat extraction modes). This results the   shortest whole length for GHE for 11,388 meters, the lowest cost for 1.82 million yuan(17136.51$), and optimum burial depth for a vertical state UH tube tubes studied is 70 meters if plenty for space is allocated for a construction for a well. the outcomes of simulation are compared with the measurement results. This comparison reveals a good correlation between the results of simulation and experiment. It shows that the maximum relative error between the simulated and measured soil temperature is 3.6% under heat extraction mode and 4.2% under heat rejection mode, which indicates the reliability

of the developed model. In addition, the validated model is used to investigate the optimal depth of GHEs. The heat transfer rates as well as the costs of GHEs for a set of five buried depth (60, 70, 80, 90 and100 m) schemes are investigated.[41]

Yusof, Anuar et al. (2015) presented a review for implementation GHE for thermal comfort and agricultural greenhouses cooling. A ground temperature difference used in many researches that reviewed is important part for identifying potential implementation GHE. So it illustrated a review for Design and performance GHE as well as summarizes potential and advantage GHE implementation in Malaysian climate for cooling application for decrease energy that used in building and greenhouses gas emission [10].

Boughanmi, Lazaar et al. (2015) presents analysis experimental for examine performance for New geothermal conical basket (CBGHE) to cool greenhouses. An experimental system that designs, installs and tests in an Energy Technology and Research Center (CRTEn) in BorjCedria. For the exploitation of the soil thermal potential for Chapel greenhouses cooling, a geothermal system is used. Experiments were performed in June. This system consists of a geothermal heat pump, a heat exchanger in the form of a conical basket buried in the ground, and a multilayer heat exchanger installed in the green-house. A composition consists of: A series for parallel coil planting at a depth for three meters. An experiment is conducted between 7 and 8 June 2014. A result obtained in CBGHE system applied in Mediterranean region for Tunisia to cool a greenhouse. A maximum amount for heat transmitted from a ground by CBGHE is 8 kW. A maximum temperature different for an inlet and outlet CBGHE system is approximate 30 ° C, and a mass flow rate is 0.08 kg / s. the air temperature inside greenhouses decreases by 12 ° C. CBGHE stability, coefficients for a geothermal heat pump and whole system around 3.9 and 2.82, in contrast.[42]

Naili, Hazami et al. (2016) presented an evaluation for geothermal resource in Tunisia and test deployment for surface geothermal energy for application cooling. A GSHP collected with a ground heat exchangers horizontal (GHE) with reverse geothermal heat pump (GHP), it connects with a cryogenic ceiling plate (CCP) that is installed in a room climate test. The results illustrated (1)Tunisia benefits from important geothermal resources, but its use remains very limited, (2) the only useof the (GHE) has reduced the average temperature inside the climate test room of about 2◦C during 1day. (3) The test of the GSHP system proves that it is a profitable solution in Tunisia, the coefficient of the performance of the GHP and the all system are found to be 4.46 and 3.02, respectively.[43]
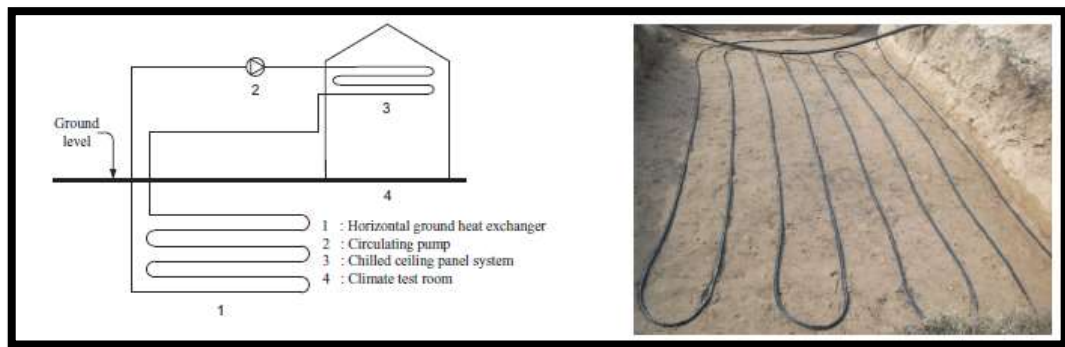
Figure 2.4 Experimental setup surface geothermal energy for direct test [43]

Patel and Ramana (2016) presented optimum dimension for Buried tube Heat Exchanger (BTHE) in Indian climate condition to decrease conservative air load and put aside energy source to decrease heating and load cooling for inhabited and building. BTHE consist of tube (one or more) that lying underground deep in a cooling in summer and heating at winter, as well as an air supplied in a building. The results illustrated that a constant temperature at a depth for 3 meters from a ground level through an experimental setting to measure a temperature during a year in Vallabh Vidyanagar in India situated at 22 ° N latitude and 72 ° E longitude by RCC pipe. Computational Fluid Dynamics (CFD) is applied to evaluation with experimental information to help in ANSYS. The results illustrated that an optimum performance for a BTHE system at a depth for 3 meters is called

(Buried Depth) and Experimentally it is observed for pipe of 25m length and 0.11m inner diameter with 0.006m pipe thickness, the temperature drop from 41°C to 26.15°C and 28.10°C for the flow of velocity 3m/s and 10m/s respectively could be achieved. 3 m/s air velocity and 26°C to 28°C temperature is human comfort condition, in summer at Indian climate condition. BTHE can be very useful to society and economically affordable.[44]

Sivasakthivel, Philippe et al. (2017) presented effectiveness, temperature, extraction and injection for heat rate that effect on surrounding ground formation. Study performance for ground heat exchanger GHX mono and double tube at bureau of geological and mining research (BRGM), France. The result illustrated that an effectiveness for a mono tube heat exchanger is approximately 0.34 and 0.40 in heating and cooling modes but a double U tube is 0.46 and 0.57 respectively. The results also illustrated that an average efficacy is noticeable in a running mode for cooling, but the difference in temperature between a heat carrier liquid and a ground is higher compared to a marked difference in a process heating mode.[45]

Song, Shi et al. (2017) studied unsteady-state 3D numerical model to explain flow for fluid and process thermal for DHE system. A validity for a form is verified by field experimental data. Three types for DHE are formed, as well as vortex and multiple tubes in a parallel connection, but multiple tubes are in a serial connection. The result illustrated that an external temperature and thermal energy for a serial conduction is higher than that for DHE when compared to parallel conduction at an equal number for tubes, but a DHE screw forming tube gives maximum heat extraction performance.[46]

Ceylan (2017) studied, ground heat exchanger for condenser temperature in ground source heat pumps (TKIP) ground heat exchanger (TID) length and an effect for heat pump on performance coefficient (COP) for four different refrigerants (R134a, R407C, R4010A and R404A) were examined

during a cooling period. Heat transfer to soil with TID while experimentally investigating, calculations related to a heat pump supposed to work in connection with TID theoretically done. Horizontal laying under a ground in Çorlu district for Tekirdağ for heat transfer to soil36 m polyethylene TID embedded by a method was used. It was measured using appropriate probes and all data were recorded via data-logger. 1kW cooling load using COP value for a vapor compression heat pump and a TID length using an amount for heat transferred to the ground. An average TID has been determined using water inlet temperatures .The results obtained, compressor power increases with increasing condenser temperature and TID and length was reduced. The greatest coefficient for performance among a coolants examined (COP) and the smallest pipe length was obtained for R134a. TID water inlet temperature is 39.54 from 31.34 ° C. When it increased to ° C, an increase in compressor power for R134a was found to be 38% and a decrease in pipe length was 48%.[47]

Popovici, Mateescu et al. (2017) presented Common type for Geothermal, surface and depth heat exchange is characterized by difficult irregular ground. Uncommon thermal heat exchanger solution, variable spatial water engineering, using cylindrical or tapered, compared to geothermal prospecting and a pilot project, represents an important term recovery for a geothermal land. To maintain a behavior for spiral tubes with a fixed diameter is to maintain a loading / unloading for a rough ground, a position is radically changed when a spiral geometry for a pointed and cylindrical charge transfer area is used to direct proportional to lower a working temperature, evolution and discharge for a lead charge regularly. From a functional and energy point for view, a solution is better clear for any usual deep and surface, heat transfer in a changeable heat exchanger.[48]

Neupauer, Pater et al. (2018) presented long-term change in temperature for ground in Horizontal geothermal heat exchanger, it is useful to implement a simplified digital heat transfer model. Using a thermal

conductivity for a one-dimensional equation, but a heat transfer in a geothermal heat exchanger is illustrated in horizontal tubes. The result concluded that the features for an Earth's temperature in a parallel tube heat exchanger are not significantly different from heat exchangers coil as plate that indicates large distances in level that pipe is placed, a small distance among axes for tubes and a length for time operation. The differences between considered temperatures increase in tube and plate exchanger differed appreciably in individual time periods, and approximately 20-30%. Experiments performed in parallel tubes of heat exchangers illustrate the temperature field that can be described using a linear heat source model. Compatibility with theoretically and experimentally determined temperature maps was satisfactory with a good degree of accuracy.[49]

Habibi and Hakkaki-Fard (2018) presented 3-D simulation modal for GHE using a CFD software for computational fluid dynamics to assess an initial fixing and cost performance for horizontal GHE. 4 types for horizontal GHE: are presented linear, spiral, also horizontal with vertical, soil types considered. The result illustrated that spiral and linear configuration is less expensive for a primary composition in individual and parallel arrangement, by the design based on an application for secondary soil by better property by GHE tubes. It revealed that the application for resultant soil can lead to a development for GHE thermal performance and reduce a cost for an initial composition for a horizontal GHE, but a conductivity and the thermal capacity for a secondary soil is better than that found in a previous soil.[50]

M.JunKim, et al. (2018) designed proposed horizontal solenoids GHEs using modified boundary condition for the current equation. To verify the applicability for a proposed design for an equation, laboratory reaction thermal examination is performed to confirm a finite element form. by modifying the boundary conditions of an existing equation, a novel design method in the form of an equation was proposed for a horizontal spiral-coil

GHE, which can be solved using the building load, heat-pump specification, pipe dimension, and ground thermal properties. To verify the applicability of the proposed equation, A validated model is the use for computational fluid dynamics simulation (CFD) in arbitrary construction where it operates in a GSHP system in a GHE spiral horizontal. The entering water temperature EWT of 32.09 °C from the simulation result was lower than the design EWT criteria of 32.2 °C, implying that the thermal performance of the GHE for a month of operation is sufficient to cover the building load. The results provide an applicability for a proposed design.[51]

Gao, Li et al. (2018) reviewed a search for geothermal heat exchangers from a new perspective and explains air potential in building zero energy. First, a geothermal heat exchanger is classified: water-based and air-based heat transfer medium. Applicable research and project are entered into each approach and analyst. An integration for geothermal heat exchangers in different cooling and heating techniques and connected studies is also evaluated. The technologies include solar thermal collector, cooling tower, night cooling radioactive technology, solar chimney, etc. As well as geothermal heat exchanger technology helped to achieve zero energy construction, that provide talented solution to advance energy efficiency in buildings.[52]

Revesz, Chaer et al. (2018) described numerical investigation in Recover thermal energy from underground railways at near vertical geothermal heat exchangers (GHE). An examination used at London Underground Station (LU) for case study but findings generated worldwide. An obtained result is that a rate for heat extraction for GSHP devices installed near UR tunnels will be significantly enhanced to around 43%. By improving the efficiency for a generally GSHP system, this results   significant saving in operating cost and emission carbon. The result used to improve the relationship that allows the heat recovery process for GHEs to resemble an improvement in

a convection (lights) for a thermal tunnel. That gives direction to an operational engineer in a field where thermal reactions arise between URs and nearby GHEs.[53]

Hassanzadeh, Darvishyadegari et al. (2018) presented new proposal for dissipating higher amount for thermal energy to improve horizontal directly ground basis heat exchanger (GSHE) compared to conservative GSHE. The result demonstrated   one time a buried pipe for a GSHE is equipped in galvanized bridge, a heat transfer rate between a pipes and a ground is greatly enhanced compared to a traditional GSHEs. It has been illustrated that the method used to improve heat transfer is effectual at lesser conductive than high-conductivity soils. Finally, the maximum improvements in thermal energy dissipation were set at 90.46%, 28.84% and 12.58% of Soil I, Soil II and Soil III correspondingly.[54]

Omer's (2018) study examined the reduction energy consumption in building, recognize GSHP As an environmentally friendly technology to provide energy efficiency in a construction sector, he supported the use for a GSHP application as an ideal method for heating and cooling, and provided a model application and modern progress for direct expansion (DX) GSHPs. The demonstrated the most prominent potential energy savings that can be achieved while using a ground power source. In addition to focusing on improving and developing an operating state for a DX GSHP heat and performance cycle. The results illustrated that a direct expansion for a GSHP, a built-in and ground heat exchanger in a foundation pile and a storage for seasonal energy in a solar thermal complex, are fully applicable.[55]

Shi, Song et al. (2018) studied 3D unsteady state Model a couple liquid flow state and a heat transfer process for a DHE systems. Heat performance extraction for 3 different DHE structure, include comparison for single U tube, double U tube and spiral tube. Simulation results illustrated that a helix tube is greatest heat performance extraction. As a flow rate for a liquid

mass increases to work, the outlet temperature decreases and the heat energy increases. As an inlet temperature rises, an outlet temperature rises while reducing thermal energy. The effect for tank porosity and heat conductivity wall tube on slight DHE performance. High-speed surface water and greater rock-thermal conductivity improve a performance for DHE, but a previous effect is more important. A direction for subsurface water flow neglected its performance impact on single and double U tubes, but a tangible effect on spiral tube.[56]

Boughanmi, Lazaar et al. (2018) examined performance for conic helicoidally geothermal heat exchanger (CHGHE) in greenhouses heating. They used composed for CHGHE fixed in 3m depth linked to geothermal heat pump that linked to ceiling panel installed in greenhouses. A ceiling unit is made up for exchanger suspended in indoor air and oars located on a floor. A permissible state system allows a recovery for excess energy from greenhouses during a day using exchanger on the ground, and energy stored is heated to heat the greenhouses by using suspended exchangers at night. The result illustrated that an average recovery temperature for Earth using CHGHE is 4.7 Kw also, at 12 kW and 10 kW in greenhouse. The performance for a coefficient for heat pump (COPhp) with total system (COPsys) is 3.93 and 2.64, in contrast. A geothermal system ensures an equal amount for heat is 692.208 kW which exchanges letters to the temperature that rises 3 ° C below the greenhouse to obtain optimum water flow rate for 0.6 kg / s.[57]

Noorollahi, Saeidi et al. (2018) presented a review for Previous research in various parameters GHE to improve efficiency and impact factor such as type for heat exchanger, heat exchange rate, heat outlet, loss pressure, thermal resistance, interference, conductivity, soil temperature, economic arm and others. They illustrated three parts. The first part is dedicated inside a pipe parameter (speed, temperature, working means inlet). Pipe parameter including diameter, pitch, center from center to distance, arrangement and

material review for tubes in Part Two. Outside parameter pipes including length, well depth, pipe diameter, and backfill materials are reviewed in Part Three. Inside the GHE pipe, there are more restricts to checking the parameters than the other two parts, including the fluid which is often a mixture of water and antifreeze. Changing the fluid velocity and the initial temperature corresponds to change the energy consumption .Generally, the velocity reduction causes an increase in temperature difference between inputs and outputs fluid, but another parameter, including thermal interference, should be considered to reach optimum velocity. Also, the inlet temperature directly affects the temperature of the outlet and the amount of heat transfer .The results illustrated that a fluid entering speed and fluid circulation, a higher distance from a center to a middle for a vertical tube and a spiral tube, and thermal conductivity for a backfill materials, are a maximum strength when increasing performance when compared to other parameters.[58]

Lamarche (2019) presented simulate GHE on a clock, geothermal heat exchangers are in a horizontal configuration. An analytical model based on a new formulation of the finite line source associated to horizontal configurations was developed to simulate the heat transfer between a horizontal heat exchanger and the surrounding ground. The model was compared to a finite element simulation in the case of a simple configuration and display excellent agreement given that the model is 500 0times faster than the numerical simulation. While the configuration may be simple, it illustrates a very important aspect of horizontal systems, namely, different local ground temperatures around pipes at different heights and how this can affect the thermal behavior of the ground exchanger. The model can easily be extended to different inline configurations, which can have parallel branches as well. Extensions to slinky or spiral configurations can also be considered, but in that case, the thermal response factor between pipe sections would be more complex. An

extension of the classical work of Claesson and Dunand was also presented as part of this study. It is a future goal to use it to provide potentially better guidelines for horizontal design procedures. The last study to drill a vertical well and adapt it to a horizontal system, Simulation for intended value tool around a clock, and response time to a ground heat exchanger coupled with equipped buildings and heat pump.[59]

Atwany, Hamdan et al. (2019) investigated two-dimensional model using ANSYS Fluent to study the performance for horizontal earth water heat exchanger (EWHE). An effect for inlet water temperature, water velocity, soil thermal conductivity and ground surface temperature on a rate for heat transfer have been analyzed. The results have indicated a direct relation between soil thermal conductivity and a rate for heat transfer.[60]

2.3 SUMMARY OF SURVEY

Below is a numbered table showing the researches that is close to our research.

Table (2.1) Summarize of Literature Survey				
No	Author	Title	Methods	Results
1	**Naili, Attar et al. (2012)**	**Experimental Analysis of Horizontal Ground Heat Exchanger for Northern Tunisia**	Study to evaluate the Tunisian geothermal energy and second to test the performance of horizontal ground heat exchanger	Results show Efficiency Found to range From 14% to 28%.
2	**NAILI, HAZAMI et al. (2013)**	**Experimental performance of horizontal ground heat exchanger for space cooling**	Study is to test the thermal performance of horizontal ground heat exchanger (GHE) for space cooling.	Results obtained during experience were presented and discussed. The coefficient of the performance of the GHP and the whole system are found to be 4.46 and 3.02, respectively.
3	**Naili, Hazami et al. (2013)**	**In-field performance analysis of ground source cooling system with horizontal ground heat exchanger in Tunisia**	Study the effect of various parameters such as mass flow rate of circulating water, length, buried depth and inlet temperature of the GHE on the heat exchange rate	The results show to evaluate the COPhp ranged between 3.8- 4.5 and 2.3-2.7, respectively

4	**Ceylan (2017)**	**Experimental Study on the Change of Ground Heat Exchanger Length with Condenser Temperature**	Study ,the ground heat exchanger of the condenser temperature in ground source heat pumps (TKIP) (TID) length and the effect of the heat pump on the performance coefficient (COP) different refrigerants, the experimental setup, horizontal paving pipe serpentine shap	The efficiency coefficient of the heat pump and the required TID length were found for the condenser temperatures determined according to the TID inlet. The effect of condenser temperature on soil heat exchanger length in horizontal tube ground source heat pumps was investigated
5	**Esen, Inalli et al. (2007)**	**A techno-economic comparison of ground-coupled and air-coupled heat pump system for space cooling**	comparison between a ground-coupled heat pump (GCHP) system and an air-coupled heat pump (ACHP) system. The average cooling performance coefficients (COPsys) of the GCHP system for horizontal ground heat exchanger (HGHE) in the different trenches, at 1 and 2 m depths, were obtained to be 3.85 and 4.26.	The result indicate that parameters have effect on performance, and that GCHP systems are economically preferable to ACHP systems for cooling
6	**Atwany, Hamdan et al. (2019)**	**Performance of earth-water heat exchanger for cooling applications**	investigated two-dimensional, using ANSYS Fluent to study the performance of a horizontal earth water	The results have indicated direct relation between soil thermal conductivity and rate of heat transfer, inverse relation observed between ground

			heat exchanger (EWHE)	surface temperature and the rate of heat exchanged.
7	**Lamarche (2019)**	**Horizontal ground heat exchangers modeling**	Presented to simulate GHE on an hourly basis, ground heat exchangers having a horizontal configuration	Result show response of GHE coupled with a building equipped with heat pumps.
8	**Shua'a and Sabeeh (2009)**	**Analysis The Performance of Underground Heat Exchanger**	The experimental test section is made of 50 m carbon steel pipe The pipe is buried 2 m deep below ground surface using Hot water.	Experiment show that water flow rate and pipe dimensions are the major variables affect the overall heat transfer process for cooling hot fluids that circulate into pipe
9	**Demir, Koyun et al. (2009)**	**Heat transfer of horizontal parallel pipe ground heat exchanger and experimental verification**	An experimental GSHP system is installed at Yıldız Technical University Davupasa Campus on 800 m2 surface area with no special surface cover.	The results show maximum difference between numerical results and the experimental data is 10.03%.
10	**Habibi and Hakkaki-Fard (2018)**	**Evaluation and improvement of thermal performance of different types of HGHE based on techno-economic analysis**	Presented numerical modal based on 3-Dsimulation of GHE with computational fluid dynamics methods. Four different types of horizontal and different soils types are considered.	Results showed that spiral and linear configurations have lowest initial installation costs in single and parallel arrangements. secondary soil with better thermal properties
11	**Congedo, Colangelo et al. (2012)**	**CFD simulations of horizontal ground heat exchangers: Acomparison**	CFD code of Fluent and the simulations covered one year of system operation of HGHE, both in summer	The depth of installation of the horizontal ground heat exchangers did not play an important role on the system performance HGHE.

		among different configurations	and winter for typical climate conditions of the South of Italy	
12	**Alghanna m (2012)**	**Investigations of Performance of Earth Tube Heat Exchanger of Sandy Soil in Hot Arid Climate**	Investigate the coefficient of performance (COP) of earth tube heat exchanger(ETHE) on sandy soil on desert arid climate ,used air as fluid circulating	The ETHE attained an average COP of 6.32 and peak of 6.89 during heating tests despite occasional heat losses to surrounding soil. And achieved a maximum COP of 5.5 in August during cooling tests with a mean of 1.75.
13	**Hassanza deh, Darvishy adegari et al. (2018)**	**A new idea for improving the horizontal straight ground source heat exchangers performance**	Dissipating higher amounts of thermal energy with enhanced horizontal straight ground source heat exchangers (GSHEs) comparing to conventional GSHEs	Results show that once the buried pipes of GSHEs were equipped with galvanized bridges, the rate of heat transfer between the pipes and ground enhances significantly in comparison to conventional GSHEs
14	**Fujii, Okubo et al. (2010)**	**Field Tests of Horizontal Ground Heat Exchangers**	Field tests were carried out in Japan, Two types of installations of slinky coils were examined, namely, horizontal and vertical setting in trenches excavated in the shallow ground. record of the system and ground temperature data during	The result showed horizontal installation of slinky coils results in superior performance to vertical installation in terms of energy efficiency, due to the less influence of atmospheric temperature changes.
15	**Naili, Hazami et al. (2016)**	**Assessment of surface geothermal energy for air**	The aims of this paper are (1) to evaluate the geothermal resources in Tunisia and (2) to test	(1)the only use of the (GHE) has reduced the average temperature inside the climate test room of about 2-C during 1

		conditioning in northern Tunisia: Direct test and deployment of ground source heat pump system	the deployment of the surface geothermal energy for cooling application.	day (2) The test of the GSHP system proves that it profitable solution in Tunisia, the coefficient of the performance of the CHP and the whole system are found to be 4.46 and 3.02, respectively
16	**Ozgener and Ozgener (2010)**	**An experimental study of the exegetic performance of an underground air tunnel system for greenhouse cooling**	Study exegetic performance characteristics of underground air tunnel for greenhouse cooling U-bend buried galvanized ground heat exchanger.	The exegetic efficiency of air tunnel is found range among 57.8 – 63.2%. The overall exergy efficiency value for system on a product/fuel is 60.7%.
17	**Patel and Ramana (2016)**	**Experimental Performance of Buried Tube Heat Exchanger Validated by Simulation Performance in Heating Climate Condition**	Presented to find optimum dimension of BTHE at Indian climate condition for that BTHE is used to reduce conventional air conditioning load	Concluded the comparison of the simulation results and experimental result that optimum performance of the BTHE system is at 3m depth from the ground this called buried depth and horizontal 25m buried length at specific
18	**Bošnjako vić, Lacković et al. (2013)**	**The Greenhouses Soil Heating By Geothermal Energy**	Study geothermal energy for conventional purposes in the whole area of the Republic of Croatia	The result soil heating technology with geothermal energy which, its further improvement, brings considerable economic benefits.

19	**Kim, Lee et al. (2018)**	**An applicable design method for horizontal spiral-coil-type ground heat Exchangers**	The horizontal spiral-coil GHEs by modifying the boundary conditions of an existing equation and The simulation result	a useful and reliable method for calculating the trench length of a horizontal spiral-coil GHE was developed.
20	**Boughanmi, Lazaar et al. (2015)**	**Thermal performance of a conic basket heat exchanger coupled to a geothermal heat pump for greenhouse cooling under Tunisian climate**	The configuration typically consists of a series of parallel coil implanted in 3 meter depth. The experiments are conducted between 7th and 8th June 2014.	The results obtained show that the CBGHE system can be used in the Mediterranean regions such as Tunisia for greenhouses cooling. During the experimental period the maximum quantity of heat transferred to the ground by the CBGHE is about 8 kW
21	**Boughanmi, Lazaar et al. (2018)**	**A performance of a heat pump system connected a new conic helicoidally geothermal heat exchanger for a greenhouse heating in the north of Tunisia**	Examine performance of new conic helicoidally (CHGHE) for greenhouse heating. Using composed of CHGHE implanted in 3m depth connected to a geothermal heat pump which is connected to a ceiling panel installed into a greenhouse	The results showed The coefficient of the performance of the heat pump (COPhp) and the overall system (COPsys) were found to be 3.93 and 2.64 respectively
22	**Neupauer, Pater et al. (2018) Poland**	**Study of Ground Heat Exchangers in the Form of Parallel Horizontal Pipes Embedded in the Ground**	predict long-term changes in the temperature of the ground in which a horizontal ground heat exchanger has been installed	prove the possibility to use a one-dimensional heat transfer equation in a model of a horizontal Ground exchanger.

23	**Eicker and Vorschulze (2009) Germany**	**Potential of geothermal heat exchangers for office building climatisation**	Performance of vertical and horizontal geothermal heat exchangers implemented in two office building climatisation projects is evaluated.	The experimental results were used to validate a numerical simulation model. The earth heat exchangers reach excellent annual coefficients of performance above 20 using a low pressure drop design. The power dissipation of heat exchanger is rather low at 8 W m for low depth horizontal heat exchangers and 26 Wm for 80 m deep vertical heat exchangers.
24	**Miyara, Tsubaki et al. (2011) Japan**	**Experimental study of several types of ground heat exchanger using a steel pile foundation Kentaro Yoshida**	The performance of three types GHEs was investigated under actual operation in the cooling mode with flow rates of 2, 4, and 8 l/min	The double-tube GHE has the highest heat exchange rate, followed by the multi- tube and U-tube. For example, with a flowrate of 4 l/min, the heat exchange rate is 49.6 W/m for the double-tube, 34.8 W/m for the multi-tube, and 30.4 W/m for the U-tube
25	**Wu, Gan et al. (2011) UK**	**Prediction of the thermal performance of horizontal-coupled ground-source**	thermal performance of a horizontal-coupled ground-source heat pump system has been assessed both experimentally and numerically in a UK climate	The specific heat extraction by the heat exchanger increased with ambient temperature and soil thermal conductivity, however it decreased with increasing refrigerant temperature
26	**Zukowski, Sadowska**	**Assessment of The Cooling Potential of an Earth-Tube**	Used energy simulation software –Energy Plus to estimate the cooling potential of earth–air–	Estimation of the cooling potential of EAHE system for Polish climate conditions. The experimental data and

	et al. (2011) Poland	**Heat Exchanger In Residential Buildings**	pipe systems in residential buildings.	calculations results indicate that the earth tube is an energy-saving solution.
27	**Chen, Xia et al. (2015)**	**Simulation and experimental analysis of optimal buried depth of the vertical U-tube ground heat exchanger for a ground-coupled heat pump system**	Presents a numerical heat transfer model for vertical U-(GHE). The optimal depth of vertical GHEs in five case studies ranging from 60 to 100 m length. Among them, the simulation results demonstrate that the GHE with buried depth of 70 m	The simulation results show that for 100-m vertical GHE, the first 70 m of the vertically buried GHE has higher heat transfer capability than its last 30-m section.
28	**Sivasakth ivel, Philippe et al. (2017)**	**Experimental thermal performance analysis of ground heat exchangers for space heating and cooling applications**	Performance of single and double U-tube GHX at bureau of geological and mining research (BRGM), France is explained	Results show the average effectiveness of single U-tube in heating and cooling modes are 0.34 and 0.40 respectively and double U-tube, it is 0.46 and 0.57 respectively.
29	**Song, Shi et al. (2017) chain**	**Heat extraction performance simulation for various configurations of a downhole heat exchanger geothermal system**	study 3D unsteady-state numerical models to describe fluid flow and thermal processes of DHE system	The results show that outlet temperature and thermal power of serial connection DHE higher than those of parallel connection with equal number of tubes

30	**Popovici, Mateescu et al. (2017) Romania**	**Innovative solutions for geothermal heat exchangers**	Functional and numerical simulation results of the machine ground heat exchanger used to build the type of geothermal equipped with reversible heat pumps. presents significant recovery in terms of thermal capacity of the ground	This solution is obvious superior to any surface or deep usual, the heat transfer in the heat exchanger is variable
31	**Gao, Li et al. (2018) china**	**Ground heat exchangers: Applications, technology integration and potentials for zero energy buildings**	Reviews latest research on ground heat exchangers	Technical route for GHE to help realize zero energy buildings is presented, which provides a promising solution to improve energy efficiency of buildings.
32	**Revesz, Chaer et al. (2018) UK**	**Modelling of Heat Energy Recovery Potential form Underground Railways with Nearby Vertical Ground Heat Exchangers in an Urban**	Describes numerical investigation, vertical (GHEs).in London Underground (LU)	The results showed that heat extraction rates of GSHPs installed near UR tunnels can be significantly improved by up to ~ 43%. This will enhance overall GSHP system efficiencies
33	**Omer (2018)**	**Heat exchanger technology and applications: ground source heat pump**	GSHPs as an environmental friendly technology able to provide efficient	The direct expansion of the GSHP, combined with ground heat exchanger in foundation piles and seasonal thermal energy storage from solar

		system for buildings heating and cooling.	utilization of energy in the buildings	thermal collectors, is extendable to more comprehensive applications
34	**Shi, Song et al. (2018) china**	**Numerical investigation on heat extraction performance of a downhole heat exchanger geothermal system"**	Study 3D unsteady state numerical model is established to couple fluid flow and heat transfer processes of DHE system. including single U-tube, double U-tube and spiral tube	Results show fluid mass flow rate rises, outlet temperature declines and thermal power increases
35	**Noorollahi, Saeidi et al. (2018)**	**The effects of ground heat exchanger parameters changes on geothermal heat pump performance – A review**	Carried out on various parameters which are affecting the GHE performance for different types of GHE.	Inlet temperature and circulating fluid velocity, higher center-to-center distance of vertical pipe and pitch for spiral pipe and, thermal conductivity of backfill material, have the greatest impact on increasing system performance compare to other parameters.
36	**(Yusof, Anuar et al. 2015) Malaysia**	**A Review of Ground Heat Exchangers For Cooling Application In The Malaysian Climate**	Reviews several important ways of implementing GHE in order to supply passive cooling for any application	Summarizes the potential and benefit of GHE implementation in Malaysian climate for cooling applications to reduce the energy used in buildings and greenhouse gas emission.
37	**Nikiforova, Savytskyi**	**Methods and results of experimental researches of thermal**	Study thermo physical characteristics of different soil types and to develop methods for the soils thermal	Analytical dependence of heat conductivity coefficient determination for different types (sand, clay and loam) and humidity of soil. The

	et al. (2013)	**conductivity of soils**	conductivity determination	dependence can be used for thermal-technical calculations of earth sheltered buildings.

CHAPTER THREE

METHODOLOGY

3.1   OVERVIEW

In this chapter we will mention the most important equations used to calculate the geothermal heat performance coefficient and the performance coefficient of the geothermal heat exchanger in our region conditions, in addition to the most important design equations used to determine the dimensions of the heat exchanger designed for testing and determine the water flow rate of inside them to optimize the utilization of heat exchange with soil, And get the highest temperature difference possible.

3.2   NEAR-SURFACE THERMAL PROPERTIES.

The soil and rocks which exist in the 200-300 meters under the surface of the Earth act as a heat sink that develops in response to two heat sources .gradients result from the surface temperature which rests between $(5-50)$ °C. This gradient will differ from region to other worldwide, also it is differs seasonally due the variation of the ambient temperature.

$$(\nabla x \times q)/\nabla T = k_{soil} \quad ………….…..3.1$$

The above equation shows that as the thermal conductivity decreases, the thermal gradient(∇T) must increase. [61]

     The researches indicates that, at the certain depth in the ground, the temperature fluctuations observed near the surface of the ground diminish Figure 3., and the temperature remains relatively constant at the depth (2- 5) meters. This is due to the high initial heat content of the Earth's surface, as well as the effect of time lag between the surface temperature fluctuations, on the soil temperature in the depths of the ground. As a result, the heat from solar irradiation is not absorbed at very deep layers with in the earth [62] as shown in figure 3.1
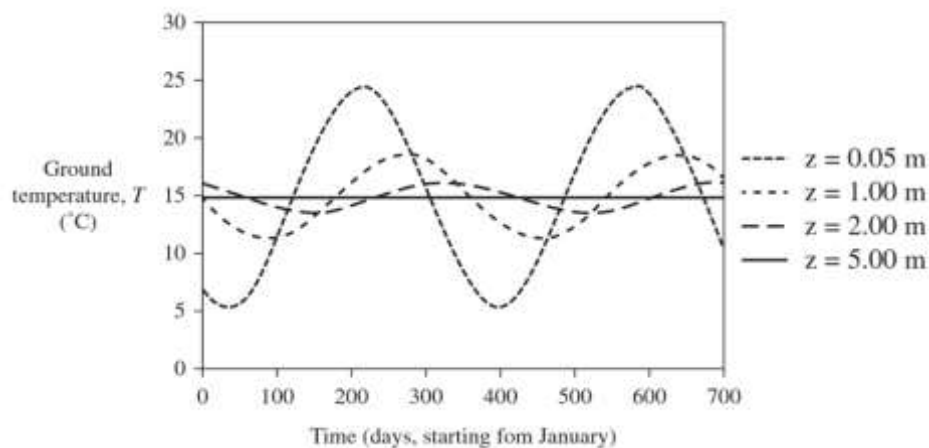
Figure 3.1 Relation between ground temperature and time at a different depths [62]

     For this reason and after reviewing a set of research for a soil type similar to that of the work area the depth chosen for the burial of the geothermal exchanger should be between 2-4 meters ,Due to the relative stability of temperatures at these depths throughout the year.

3.3   COEFFICIENT OF PERFORMANCE COP.

The coefficient of performance (COP) for the heat pump is a number resulted from the comparison between the energy required to drive this cycle to the amount of heat transferred [63]

$$COPHP_{space\ cooling} = \frac{Heat\ removed\ from\ cooled\ space}{Electricity\ consumption} \quad \text{……. (3.2) a}$$

$$COPHP_{space\ heating} = \frac{Heat\ provided\ to\ heated\ space}{Electricity\ consumption} \quad \text{…… (3.2) b}$$

Electric power can be calculated from the following term:

$$Power = IV \quad \text{………………. 3.3}$$

The high COP, means that the system was efficient. The temperatures of the high and low-temperature media within which the heat pump operates directly affect the COPHP. The COPHP decreases at larger temperature differences between the high-and low-temperature media. In an ideal heat pump, the coefficient of performance of the heat pump (COP rev) is only dependent on the high-and low-temperature media. Specifically,

$$COP_{cooling} = \frac{1}{1 - \frac{Tcooling\ coil}{Tf}} \quad \text{…….…… (3.4) a}$$

$$COP_{heating} = \frac{1}{1 - \frac{Tf}{T_{heating\ coil}}} \quad \text{……….. (3.4) b}$$

The efficiency of heat transfer process has been measured by comparing the energy required to drive this cycle to the amount of heat transferred.

The most important term observed in the study of any heat exchanger, is known as the energy efficiency ratio (EER) or coefficient of performance (COP) for cooling and heating,

$$EER = E_{total} / E_{consumed} \quad \text{……… (3.5)}$$

The EER values for ground source heat pumps are generally in the range of 15 to 25. [61]

The quantity of heat transferred from the working fluid to the soil   through the ground heat exchanger. [64]

$$Q = \dot{m}Cp \ (T_{in} - T_{out}) \ \dots\dots \ (3.6)$$

3.4   MATHEMATICAL MODEL

3.4.1   Energy Equation

The general heat conduction equation in cylindrical coordinates appears in the following form

$$\frac{\partial^2 T}{\partial r^2} + \frac{1}{r}\frac{\partial T}{\partial r} + \frac{1}{r^2}\frac{\partial^2 T}{\partial \varphi^2} + \frac{\partial^2 T}{\partial z^2} + \frac{\dot{q}_{gen}}{k} = \frac{1}{\alpha}\frac{\partial T}{\partial t} \quad \dots\dots \ (3.7)$$

Assuming the GHE as an infinite line-source in the ground which is regarded as an infinite medium with an initial uniform temperature. Due to its minor order, heat transfer in the axial direction along the heat exchanger, which accounts for the heat flux across the ground surface and down to the depth of GHE, can be neglected. This assumption is valid for a length of the borehole distant enough from the borehole top and bottom. Therefore, heat conduction in the ground is an unsteady radial heat conduction problem, that is, T(r, t), and the following simplified heat conduction equation can be derived:

$$\frac{\partial^2 T}{\partial r^2} + \frac{1}{r}\frac{\partial T}{\partial r} = \frac{1}{a}\frac{\partial T}{\partial t} \quad \dots\dots\dots \ (3.8)$$
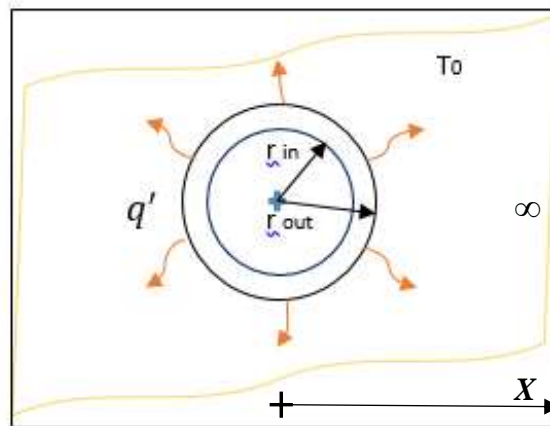
Figure 3.2 Explain the transfer of heat from inside the tube to the soil

The boundary conditions for a line source of heat are introduced as:

$$-2\pi r k \frac{\partial T}{\partial r} = q' \qquad r \to 0 \qquad \text{……….. (3.9) a}$$

$$T - T_0 \to 0 \qquad r \to \infty \qquad \text{……….. (3.9) b}$$

$$T - T_0 = 0 \qquad t = 0 \qquad \text{……..… (3.9) c}$$

  The first boundary condition in equation (3.9) is related to the heat flow rate per unit length at the wall conducted in the ground, which is derived from Fourier's law of heat conduction (Eskilson 1987). At larger distances $(r \to \infty)$ the temperature of the ground is not affected by the line source of heat and remains equal to the initial condition. The last condition relates to the initial temperature of the ground at $t = 0$. The temperature response in the ground due to a constant heat flow rate per unit length of the line source (q') is given by [62].

$$T(r,t) - T_0 = \frac{\dot{q}}{4\pi k} \int_{\frac{r^2}{4at}}^{\infty} \frac{e^{-u}}{u} \, du \qquad \text{……. (3.10)}$$

3.4.2   GHE Length Equation.

To determine the length of the pipes used in the horizontal geothermal heat exchanger, we can assume the pipe is a cylindrical wall with core temperature equal to the fluid temperature, as shown in figure 3.3
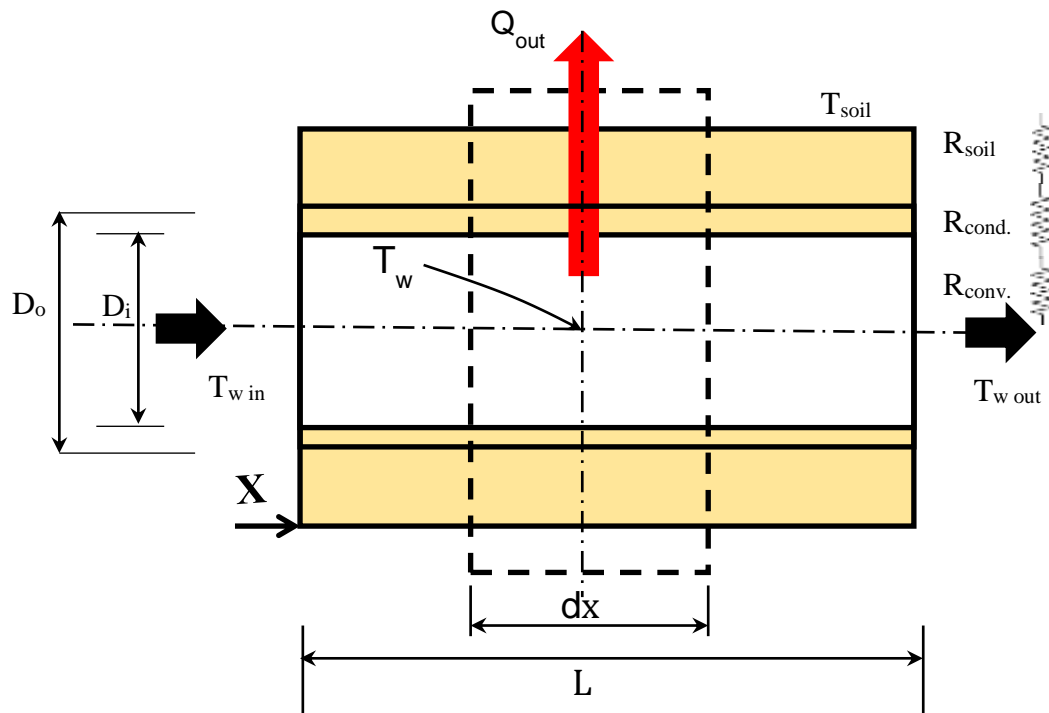
Figure 3.3 the pipe control element

Calculate the length of the horizontal HE we must first assess the thermal resistance of the system:

$$R_{conv.} = \frac{1}{\pi D_i h_w} \quad \ldots\ldots\ldots\ldots\ldots (3.11)$$

$$R_{cond.} = \frac{\ln\left(\frac{D_o}{D_i}\right)}{2\pi k_{pip}} \quad \ldots\ldots\ldots\ldots\ldots (3.12)$$

$$R_{soil} = \frac{1}{S k_{soil}} \quad \ldots\ldots\ldots\ldots\ldots (3.13)$$

$$R_{total} = R_{conv} + R_{pip} + R_{soil} \ldots\ldots\ldots\ldots (3.14)$$

Where *S* is the conduction shape factor of the pipe given determined from the following formula (Incropera and DeWitt-2002): [65]

$$S = \frac{2\pi}{\ln\left[\left(\frac{2d}{D_o}\right) + \sqrt{\left(\frac{2d}{D_o}\right)^2 - 1}\right]} \quad \ldots\ldots\ldots\ldots\ (3.15)$$

To calculate the R_{conv} we must calculate the heat transfer coefficient h_w is evaluated by using the following *Nusselt Number* empirical formula (for turbulent flow and forced fluid), $(2000 \leq Re \leq 32000)$.

$$Nu = \frac{h_w D_i}{k} = 0.023 \left(\frac{\rho V D_i}{\mu}\right)^{0.8} (Pr)^{0.3} \ \ldots\ldots\ (3.16)$$

Using the energy balance equation on the control element dL shown in figure (3.3), the differential heat transfer is expressed as:

$$dq = -\dot{m}_w c_{p.w} dT_w = \frac{T_w - T_{soil}}{R_{total}} dx \quad \ldots\ldots\ldots\ (3.17)$$

Assume that θ_w is the difference between the fluid and the soil temperature then:

$$\theta_w = T_w - T_{soil} \quad \ldots\ldots\ (3.18) \quad \text{and} \quad X = \frac{dx}{\dot{m}_w c_{p.w} R_{total}} \quad \ldots\ldots(3.19)$$

then the equation *3.17* can be written as:

$$\frac{d\theta_w}{dX} = \theta_w \quad \ldots\ldots\ldots\ (3.20)\ a$$

The boundary conditions are:

At $\quad x = 0 \quad \rightarrow \quad X = 0 \quad , \ \theta_w = T_w - T_{win} = \theta_{w\ in} \ \ldots\ldots\ (3.20)\ b$

At $x = L \rightarrow X = \frac{L}{\dot{m}_w c_{p.w} R_{total}} \quad , \ \theta_w = \theta_{wout} = T_{wout} - T_w \ \ldots\ldots\ (3.20)\ c$

Solving the equation 3.19 the pipe length and the temperature distribution along the pipe can estimated: [65]

$$\frac{\theta_w}{\theta_{w\ in}} = e^{\left(\frac{-x}{\dot{m}_w c_{p.w} R_{total}}\right)} \quad \ldots\ldots\ldots\ldots\ (3.21)$$

$$L = \left(\dot{m}_w c_{\text{p.w}} R_{total}\right) ln \left(\frac{\theta_{wout}}{\theta_{win}}\right) \quad \ldots\ldots\ldots (3.22)$$

3.4.3   Simplified Method

Ingersoll et al. (1954) uses a simple steady state heat transfer equation to solve for the shorter term variation

$$q = L\ (T_{soil} - T_w)\ /\ R \quad \ldots\ldots (3.23)$$

This equation can be rewritten as (Braud, et al., 1988). [66]

$$q = L(U.\Delta T)\ldots\ldots (3.24)$$

The overall heat transfer coefficient *(U)* should be determined using the following equation [67].

$$U = \frac{k_w\left(\frac{F}{8}\right)(Re-10^3)Pr}{d\left[1+12.7\left(\frac{F}{8}\right)^{0.5}\left(Pr^{\frac{2}{3}}-1\right)\right]} \quad \ldots\ldots\ldots (3.24)\ a$$

$$\Delta T = \frac{T_{wout}-T_{win}}{2} - T_{soil} \quad \ldots\ldots (3.24)\ b$$

$\dfrac{T_{wout}-T_{win}}{2}$ is the fluid temperature difference in the pipes.

$$T_b = \frac{T_{in}+T_{out}}{2}\ldots\ldots\ldots\ldots (3.25)$$

3.5   THE DISTANCE BETWEEN PIPES CENTER

In order to knowing the appropriate distance to ensure that heat does not accumulate around the pipes, which is reduces the efficiency of the geothermal heat exchanger, the COMSOL program was used to simulate the heat flow between the parallel pipes to obtain the optimum distance between them, which represent the heat transfer in on line source (one dimension) with time depending. Assuming the pipe in a two dimensional domain and the heat was transferred

radially, the pipe section is a circle with a highest temperature which recorded annually. [49], [68].

For determine the distance between the pipes centers *(H)*, there was two arrangement depended (parallel, and staggered), of course the staggered arrangement is the best for the two layers GHE Figure 3. represent side view of the double-layers GHE, When drawing in COMSOL with the same dimensions of the pipes that were used (D=16 mm) and entering the soil properties in working area . The different horizontal and vertical distances from (0.1 - 0.6) m (with increment 0.1m) obtains a different cut-point (center point) temperature *(T$_{cp}$)*,as shown in figuer3.4, the optimum distance is selected when:

$$T_{cp.} = T_{soil} \quad \ldots\ldots\ldots.. \quad (3.26) \text{ a}$$

$$\text{Or} \qquad T_{cp.} \leqq T_w \quad \ldots\ldots\ldots\ldots \quad (3.26) \text{ b}$$
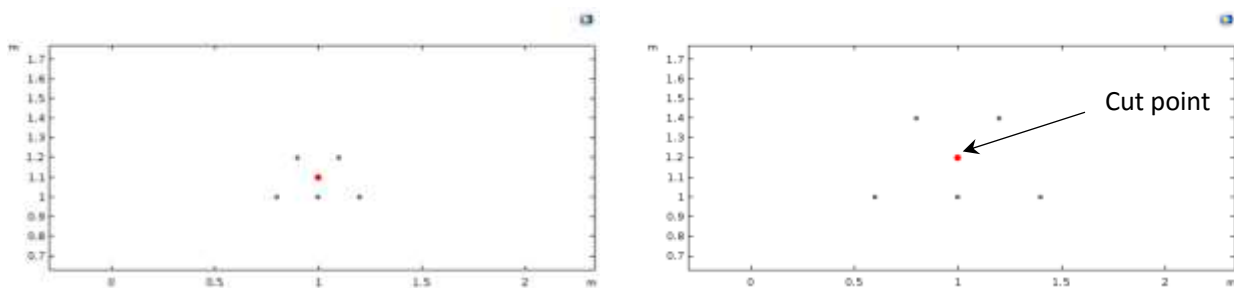
Figure 3.4 Shows the midpoint of the shape of the pipes M

Where , the temperature at the midpoint should be less than the temperature of the tube surface, to ensure that the heat dissipation continues and that there is no thermal accumulation occurs that may lead to a decrease in the efficiency of the heat exchanger after a period of operation.

Figure 3.5 shown the shape of mesh that taken for represent the accurately results of heat transfer around pipes surface through soil.
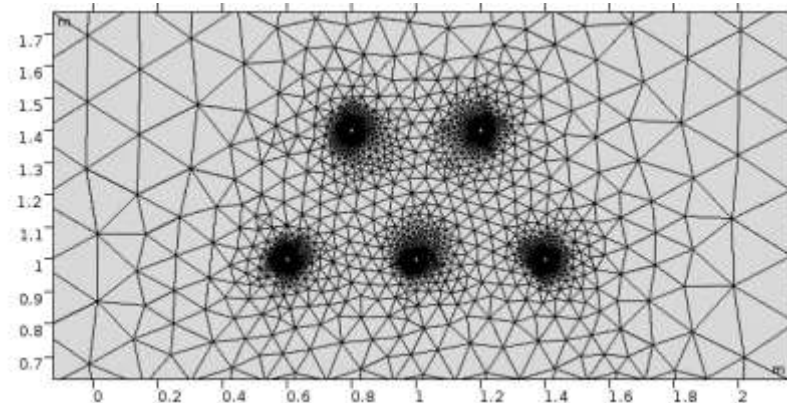
Figure 3.5 show the mesh shape around pipes

Figure 3.6 shown the following temperature contours shows the temperature distribution of the area around the pipe $(T_{soil} = 25\ {}^oC)$, with pipe surface temperature $(T_{pip}=30\ {}^oC)$.
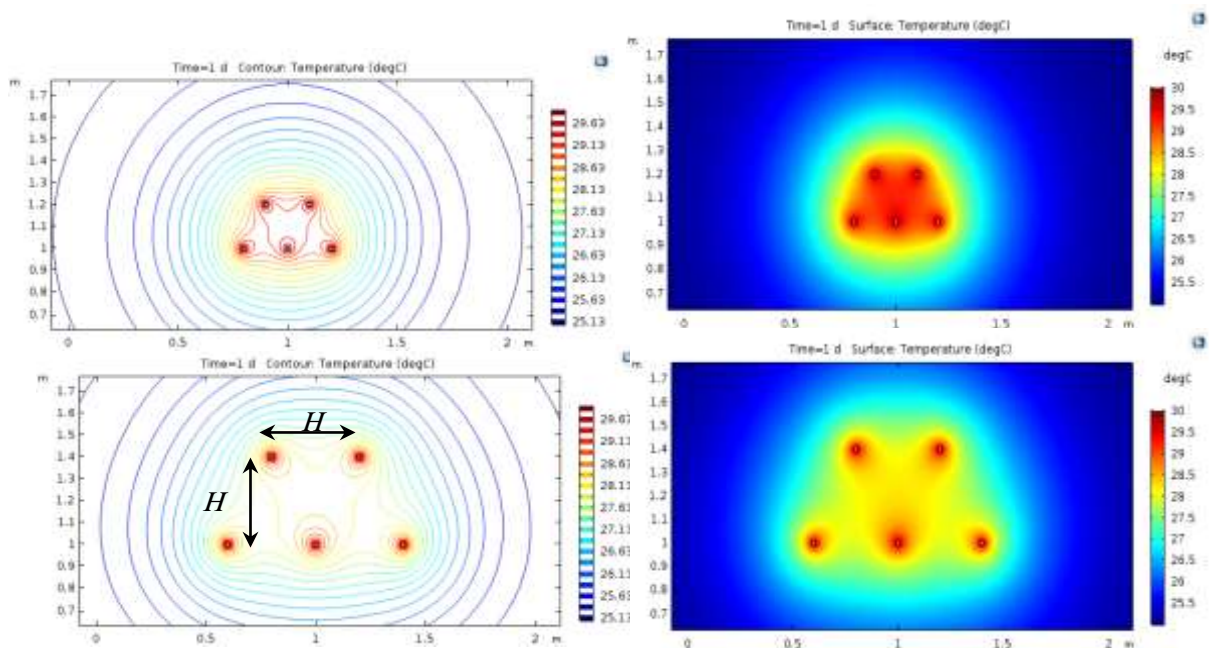
Figure 3.6 It shows the isothermal contours and temperature variation from the pipes surface through the soil at pipe surface temperature 30°C

The   Figure 3.7 the results obtained, from shows the relation between soil
temperature (Tsoil) versuse the time of operation of a horizontal GHE for a
different spaces between pipes (H). indicate that the soil temperature would
continue to rise for the soil nearby pipes during the first four hours, then it
becoming stabile at a constant temperature according to diffrents distance
between pipes ,where the space dimentions in which the mid point temperature is
close to the initial soil temperature are the best space dimentions for GHE design.
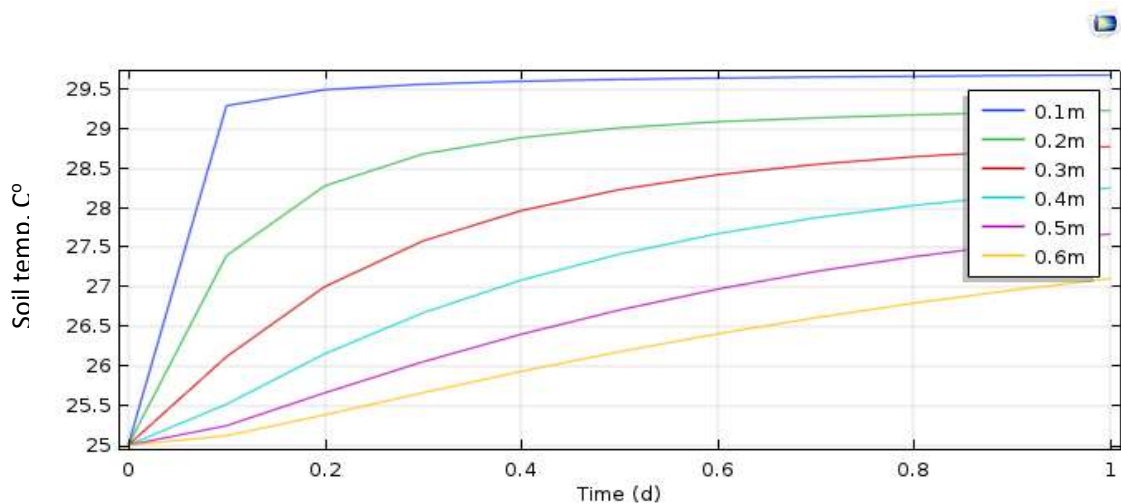
Figure 3.7 Shows the relationship between time and soil temperature at the cut point

when pipe surface temperature 30˚C

In order to clarify the appropriate dimension between the tubes for the design
of the heat exchanger, the temperature of the outer surface of the tube was raised
to 50 °C (Tpip) and at the same soil initial temperature (Tsoil) 25 °C, and Figure
3. show the the thermal lines countore and the temperature distribution of the soil
around the pipes.
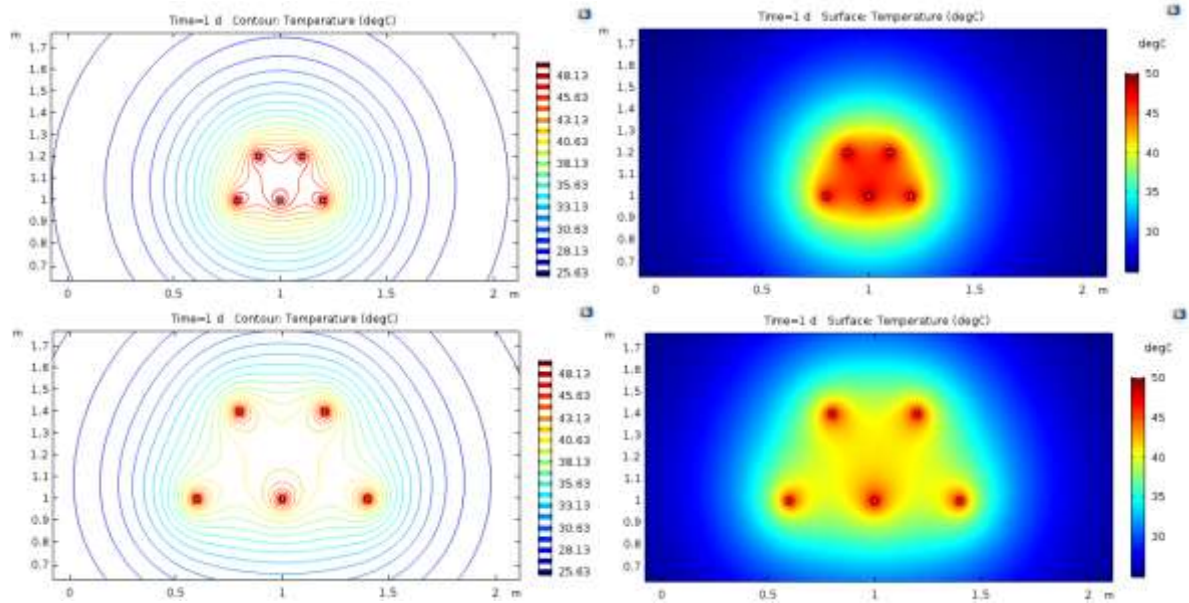
Figure 3.8 It shows the isothermal contours and temperature variation from the pipes
surface through the soil at pipe surface temperature 50˚C

Figure 3.9 of the results obtained, shows the relation between soil
temperature (Tsoil) versus the time of operation of a horizontal GHE for a
different space between pipes (H) through two days to show the stable. indicate
that the soil temperature would continue to rise for the soil nearby pipes during
the first day, then it became stable at a constant temperature according to the
different distance between pipes in the second day, best space dimensions for
GHE design when the space dimensions which the midpoint temperature is close
to the initial soil temperature.
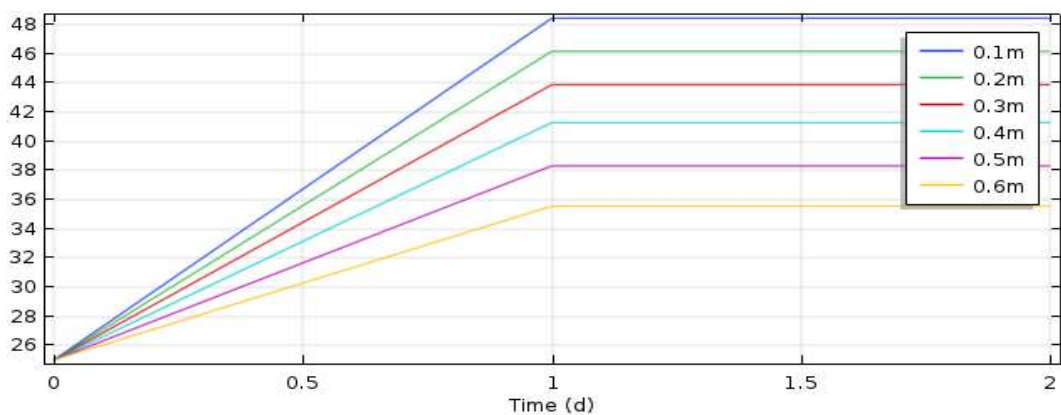
Figure 3.9 Shows the relationship between time and soil temperature at the cut point
when pipe surface temperature 50˚C

According to the above Figures 3.7 and 3.9, and the results that be explained the optimum distance (H) can be estimated roughly, it will be restricted between (0.3-0.5 m) taking into account the area that used and the efficient operation of the GHE, within the same dimensions of pipes and properties of soil that used. where it is possible to obtain a temperature of cut-point close to the temperature of the initial soil at these dimensions.

3.6   GEOTHERMAL HEAT EXCHANGER PRESSURE LOSSES

From [69] the pressure losses in the pipes of GHE can estimated by the following expression

$$\Delta p = \mathcal{F} * \frac{L}{D_i} * \frac{\rho}{2} * U^2 \ \ \dots\dots\dots \ 3.27$$

Where $\mathcal{F}$ calculated from the following formula:

$$\mathcal{F} = \{-2.0 \ log[\frac{\frac{e}{D_i}}{3.7065} - \frac{5.0452}{Re} log\left(\frac{(\frac{e}{D_i})^{1.1098}}{2.8257} + \frac{5.8506}{Re^{0.8981}}\right)]\}^{-2} \dots.3.28$$

3.7   METHODOLOGY AND ASSUMPTIONS:

In the present research, a closed system of horizontal type heat exchanger serpentine shape was tested for two layers buried in a two different depths for the same work area, using water as a heat transfer medium in a sandy soil at the Najaf state / Iraq and finding the performance of each network separately and together.

The following assumptions are considered for the line-source model in HGHEs:

- The soil are isotropic and uniform in the thermal properties.
- The change in moisture quantity is negligible.
- There is no effect of the ground water advection.
- Thermal contact resistance is negligible between the pipe surface and the ground.
- The effect of the solar variation on the ground surface is negligible.
- The heat transfer in two dimensions only.
- Neglecting the effect of the intensity of solar radiation at depths of 2-4 meters for its very slight effect

CHAPTER FOUR

EXPERIMENTAL WORK

4.1   INTRODUCTION

In This chapter, explain the practical procedures of the project, which implemented according to the theoretical basis and design dimensions mentioned in the previous chapter, and find the properties of soil in area work, in addition to the equipment used for this purpose, with a summary of the practical procedures and the time of the test.

4.2   EXPERIMENTAL ASSUMPTIONS.

After viewing a set of practical studies in previous chapters, the following factors considered:

1.   The initial temperature of the working fluid approximately between (30 – 50)°C.

2.   The volumetric flow rate of the work fluid was taken (2 - 4) ℓ/min for the single layer, and (3 - 5) ℓ/min for the double layer GHE.

3.   Measuring the thermal gradient of the soil in increment of 0.5 m from the ground surface to depth of 3.5 m along the year, used 8 thermocouples type K.

4.   The depth of burying the exchanger layers is, 2.5 m, and 3 m in succession.

5.   The ground moisture is constant at a different times. With Consideration of the absence of rain or water in the area during the study times and recording the results.

4.3   EXPERIMENTAL EQUIPMENT AND PREPARATION PROCESS

Began preparing the practical equipment in the work area by designing the pipes, burying them, and connecting the attached parts and measuring devices to be at the arrangement of the system of GHE as in the figure 4.1 below.

1	Tank
2	heater
3	Mixer
4	Water pump
5	valve
6	Flowmeter
7	Data logger
8	Temperature sensors
9	Pipes networks
10	Laptop
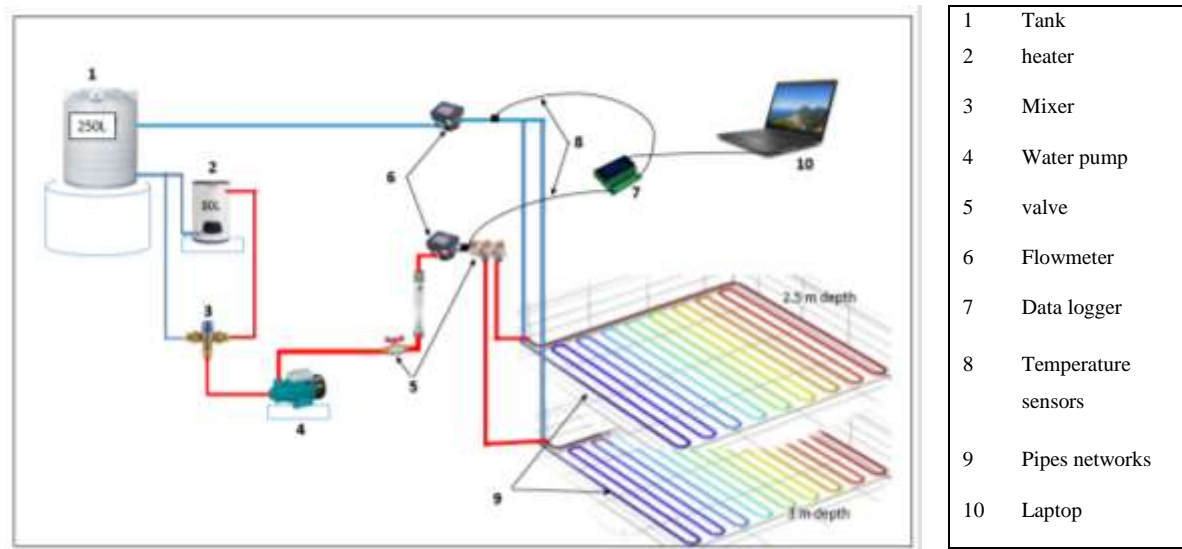
Figure 4.1: Two layer GHE entire connections.

The following are detailed steps for these experimental settings for the GHE system:

4.3.1   Site selection and preparation

The site selection for the geothermal heat exchanger burying is an important step, to insure the optimum operation. The site of suggested project of Zero Energy House in the Engineering Technical College in the Najaf holly city, is an appropriate place to burying the GHE as shown in figure 4.2, the first step is

the preparation of the site ground, to be prepared to engraving and to burying the GHE. So the selecting of the different depths taking into account the external diameter, length, design, and the distance between the pipes used in the GHE. The study area was 25 square meters ($5 \times 5m^2$).

Figure 4.2 The experimental study area.

4.3.2   Graving the study area.

In Figure 4.3 graving the study area to a depth of up to 3 meters, to ensure the depth when of the relatively stable temperature of the soil which is suitable to obtaining a nearly constant heat flux along the year.

Figure 4.3 During graving workspace by Poclain machine

During the drilling presses, it is important to measuring the soil temperature at a different depths and finally at a depth of about 3.5m by the thermal camera(with accurate ±2%), also it is useful to measures the moisture content of a soil at this depth(by device with accurate ±10%), this step completed by the digital soil moisture meter immediately after graving, as it is shown in figure 4.4 & figure 4.5

(the temperature was at 25.4 in this depth and moisture is 7%) ,to know the temperature and moisture of the initial soil at the 3 m depth below the surface of the earth, to know the type and properties of the soil by relying on them later.
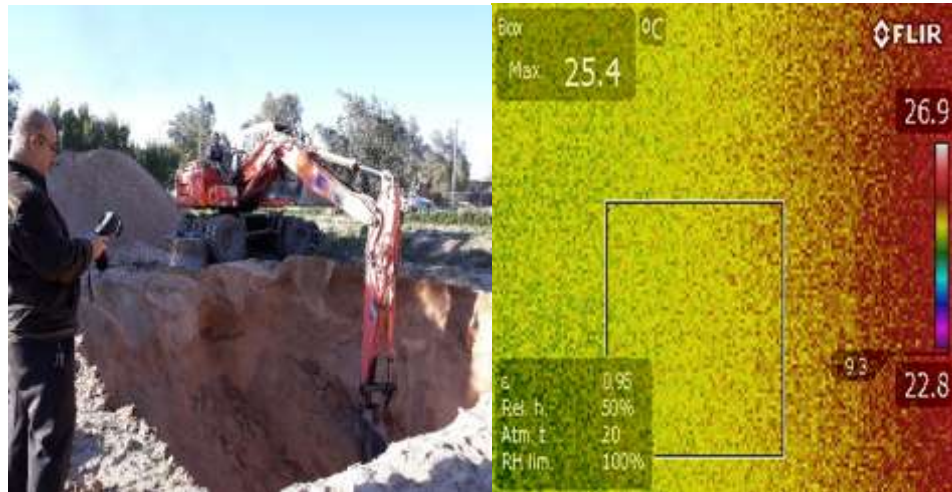
Figure 4.4: the thermal camera to measuring the soil temperature during the burying process.

Figure 4.5: measuring the moisture content in the burying site.

4.3.3   Measuring the soil thermal conductivity.

As it mentioned in the previous chapter, thermal conductivity of the soil is a critical parameter affecting the amount of energy transferred from the working fluid to the soil or vice versa. A sample of soil was taken from the depth which burying the pipes of first-layer, for measuring the thermal conductivity, in the soil

properties measurement laboratory. In the department of civil technical in Najaf Technical Institute, the thermal conductivity of soil specimen was measured according to the following steps:

a)   Preparing the sample of soil in the form of molds known dimensions (15×15 cm and thickness 5 cm) according to the dimensions of the thermal heater of the device used as shown in figure 4.6. The soil sample of sandy porous type was dried to calculate the thermal conductivity when no moisture was present.

Figure 4.6 Preparing the test sample.

b)   Placing the test sample inside the measurement device and installing a two thermocouples on the surfaces, one of them and in the top, and the other in the bottom side which is touch an electric heater. An insulators were placed around the sides of the sample to insure the isolation from the thermal effect of the surroundings figure 4.7

Figure 4.7 Placing thermostable and insulations

c)   Operating the device at relatively low heat flux, by controlling the electricity equipped, and monitoring the heat flow through the sample by connecting the thermocouples to the Data Logger as it indicated in figure 4.8.

Figure 4.8 Connecting instruments to measuring the soil thermal conductivity

d) Recording the temperature difference every 15 minutes for 4 hours when

$$Q = (V * I * cos\varphi)$$

$$Q = (10 * 0.18 * 0.85)$$

After reaching a stable heating state after about 20 minutes of operating time. Deducing the thermal conductivity value of the soil mold through the following diagram.
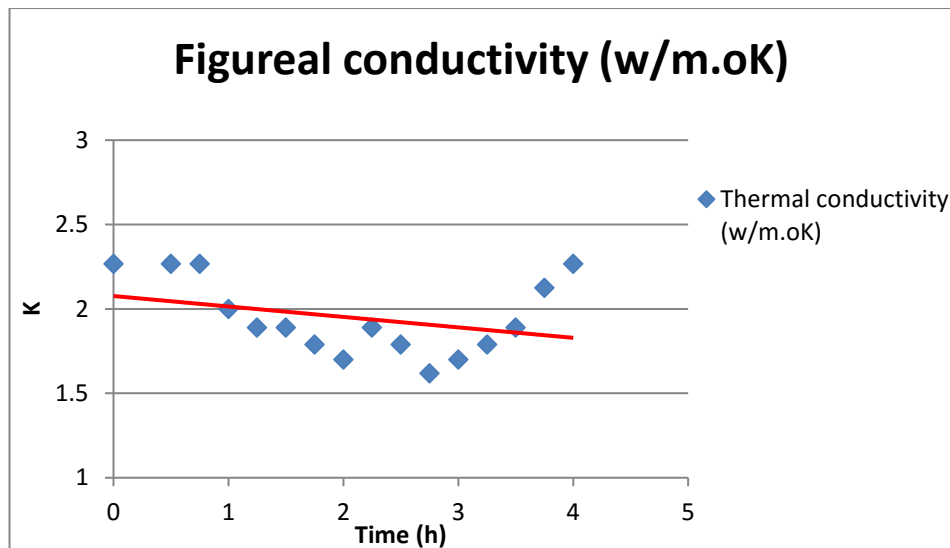
Figure 4.9 Relation between the time and thermal conductivity measured by soil labrotory test.

From the above figure 4.9, a chart showing the relationship between a set of the thermal conductivity values of the soil sample with time after a period of stability and for every 15 minutes and by fixing the heat flow value of the heater below the sample. It was concluded that the values of the thermal conductivity of the soil are restricted between (1.6 - 2.2) W / m.k . Soil thermal conductivity was practically calculated as the average of the most stable points to be (1.77) W / m.k .according to the research [70]

The type of soil in Najaf Governerat specifically (31.9760718 ° N 44.364692 ° E). Where the type of soil in the study area is sandy soil when was examined according to standard tests to be (Sand 88.13 %, Silt 6.33 %, Clay 5.54 %) ,and with a high gypsum content of up to 28%, according to laboratory studies conducted by many researchers and according to standard tests [71],[72] which depend on standardized tests to find the proportions of soil components in the south-west region of the Najaf governorate and at various depths.

After knowing the thermal conductivity and the amount of moisture of the soil, it is possible to find the thermal properties of this soil through research, [73] , To be almost as in the table (4.1) .

Table (4.1) thermal properties of soil [73]

Thermal properties of soil	Conductivity W/m.K	Dry density kg/m^3	Diffusivity m^2/day
Light sand (15% water)	1.0-2.1	1285	0.047-0.093

Depending on the thermal conductivity of the soil and the amount of moisture measured experimentally and based on the researches, managed to know the type of soil and the rest of its properties.

4.3.4   Setting sensors in the soil before burying the exchangers.

According to measures the temperature gradient of soil in the study area, it is instilled 8 thermocouple type K sensor measure range (-50~350°C), at each 0.5 m of grave depth, by setting the end of each sensor at along stick woodenly perforated each half-meter so that the sensors touch the soil and from all sides, to record the soil gradient temperature During a year in this region, as shown in figure 4.10

Figure 4.10 Setting the thermocuples to measuring the soil temperature gradient.

4.3.5   Selecting the GHE piping type.

The type of piping used as shown in, figure 4.11 was chosen according to the availability and the measurements calculated in the previous chapter, pipes were chosen from the type of polyethylene multi-layer composite pipe (MLCP), this type of pipes was used in most projects to benefit from geothermal energy directly in modern systems. This is due to the advantages offered by this discovered type of pipe.
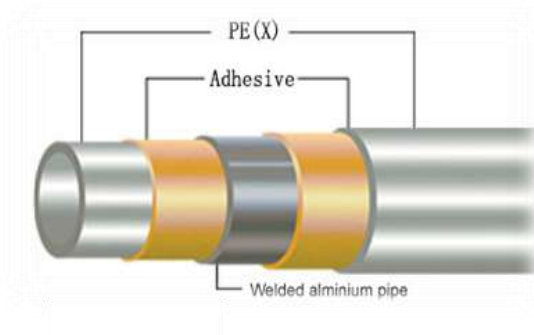
Figure 4.11 Sectional view of pipe selected.

The advantage of MLCP pipes:

- Light weight, flexible and form-stable.
- Fast and fame free installation.
- Low expansion rates, safety and clean.
- No wastage and fewer fittings than traditional installations.
- MLCP pipes have a life expectancy of minimum 50 years with correct use, and it is not affected by the different soil components compared to the metal tubes.
- Fully certified and approved across Europe.

Table (4.2): properties and dimensions of selected piping system MLCP.

Inner diameter	0.012 m
Outer diameter	0.016 m
thickness	2 mm
thermal conductivity (kp)	0.040 W/m*°k
Endurance pressure	10 bar at 70 °C
Operating temperature ranges	0 °C to 95 °C
Minimal roughness	0.0004 mm
Expansion coefficient (α)	$25 \times 10\text{-}6(\text{m/m} \times^\circ \text{K})$
Water volume	0.113 (l/m)
Roll Length	100 m

4.3.6   Forming the GHE

According to the available length, the MLCP pipes was divided and formed as a two networks in a serpentine forms, each network with a length of 100 m, the distance between pipes is 0.4 m, to bending the pipes a special tools was used, the riser pipes which appears from the surface was isolated with good insulators to maintain the temperature of the water coming out of the system constant. Shown in figure 4.12 some tools used to fixing the pipes.

Figure 4.12 bending and pipe cutting tools with some accessories that used.

The other step is to Install the first network by burying it at a depth of 3 m, and implant a (1 meter) stick vertically, where it touched the beginning pipe surface of the first network, to ensure the matching of the two layers as planned, at M side view. then burying the second layer where the view of its pipes passes through the mid-distance between the pipes of the first layer. The vertical distance between the two layers is (0.5 m)(taking into account the distance between grains and compressibility of sandy soil). this process is to make the pipes in a staggered arrangement to reduce heat accumulation around the pipes, also to make the pipes far from each other, to ensure the best heat transfer. The purpose of two layer GHE used to decrease the area required to burying the heat exchanger (preserve at long lengths of pipes with same efficient performance) as shown in figure 4.13, figure 4.14 and figure 4.15 preparation of pipelines networks.

Figure 4.13 Burying the first serpentine networks at depth of 3m.

(The matching stick was removed after burying the second network)
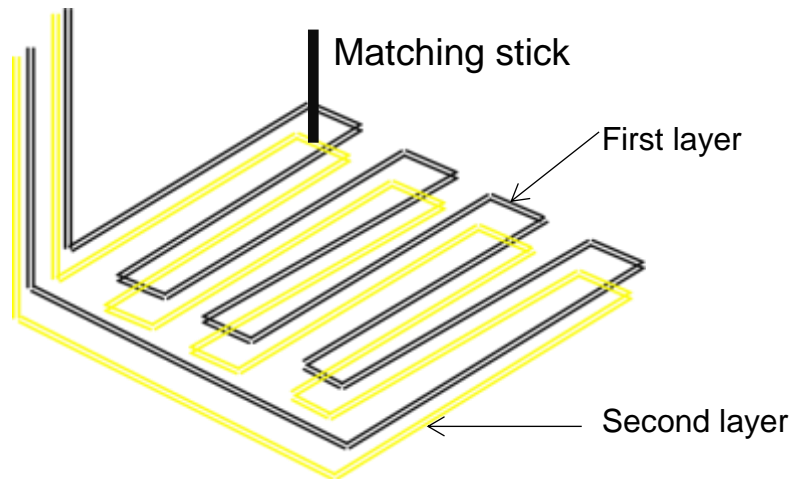
Figure 4.14 Matching the two layers of GHE.

Figure 4.15 Burying the second serpentine networks at depth 2.5m.

4.3.7 Final steps and external connections

To obtain an actual results the same soil was reused to burying the both networks and thermocouples. Now the GHE became under the ground of the test

area, and the ends of the pipes was connected to the outer part of the GHE, figure 4.16 & figure 4.17

Figure 4.16: Burying the two networks

The other parts needs of a 250 liters tank, and a 80 liters water heater supplied with a 3000 watt electric heat in element.

Figure 4.17: Expansion tank and water heater.

The other component of the external parts are a precise mixer containing a sensor to mix hot and cold water at a required temperature which ranging between (25-60) ˚C for limited approximate the temperature of water entering ,in addition to ability 0.5 hp water pump, and the connection pipes and control units inflow (valves) ,figure 4.18.

Figure 4.18 Mixer and water pump.

The control unit consists of a valve to control the flow rate, and an accurate digital flowmeter ($\pm1\%$) ,in addition to a distribution valve to control the direction of water flow and distribute it into networks to study their performance, together or individually as shown in figure 4.19. The entrance and external end of the first and second networks pipes was marked with A1, B1 and A2, B2 respectively.

Figure 4.19 Main components of control unit.

The data logger has four temperature sensors with accuracy $\pm0.5^{o}$ C, which were connected to measure the water inlet and outlet temperature ((T_{in},T_{out}) and the ambient (T_{atm}) and soil surface temperature (T_s), as shown in Figure 4.20 .

Figure 4.20: Data logger and its accessories.

Figure 4.21: Assembly of control unit.

So that the external devices and attachments are connected as shown in the Figure 4.21

Other data logger with four channels, used thermocouples type K Used to measure the soil temperature gradient at every half-meter depth, for 8 locations on different depths of soil and over the course of the year 2019. As figure 4.22.

Figure 4.22: Data logger for Soil temperature gradient.

4.4   EXPERIMENTAL WORK PROCEDURE:

At the beginning of any practical project of renewable energy or other projects that are affected by weather conditions throughout the day or months of the region in which the project is located, it is important to know the following:

4.4.1   Determine the appropriate times to record the readings.

In order to determine the appropriate time to measure the thermal gradient of the soil from a depth of 3.5 m and for every 0.5 m to the soil surface during each month and throughout the year 2019 for the region. It is necessary to know the highest and the lowest temperature of weather that the region reaches during the year, through the annual expectation of the temperature in Najaf governorate (31.9760718°N 44.364692°E) for the year 2019, as shown in figure 4.23.
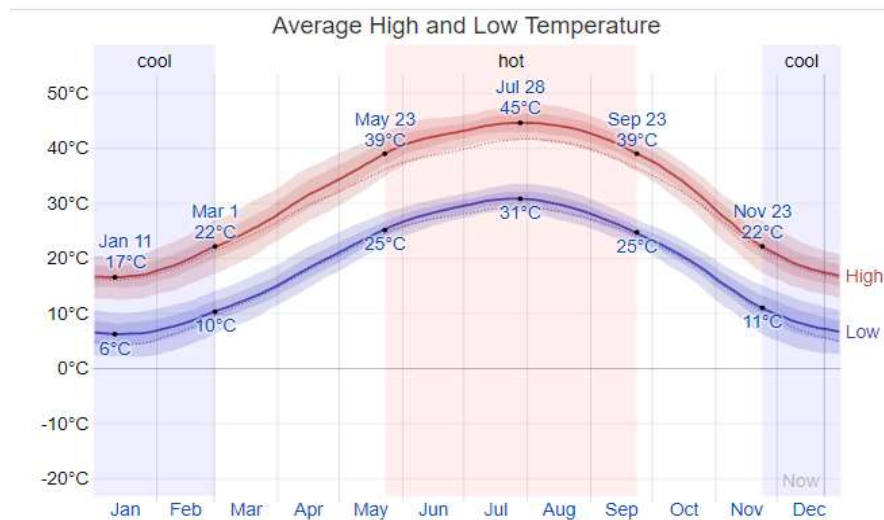
Figure 4.23: Average High and Low Temperature at Najaf in 2019 [74]

The above figure shows the maximum and minimum atmospheric temperatures for the region according to the link of weather changes during the year2019. Through it note the difference between temperatures during a year is approximately 26.5 °C (average between the highest and lowest temperature value through day and night), which is equivalent to 2.21 °C of change per month [74].

For the purpose of obtaining a noticeable change .for that reason thermal gradient readings of the soil were recorded experimental for every 15 days and for a specific time during the day at 12:00 pm. And taking an average of the soil temperature recorded during each month and from each season according to the division of seasons in the figure 4.23, we obtain a figure 4.24 of the annual gradient of the soil at different depths starting from the surface (shaded) to a depth of 3.5 m and for every 0.5 m, where the relative stability of the soil temperature results is clear between depths (2.5-3.5) m, during summer and winter seasons.
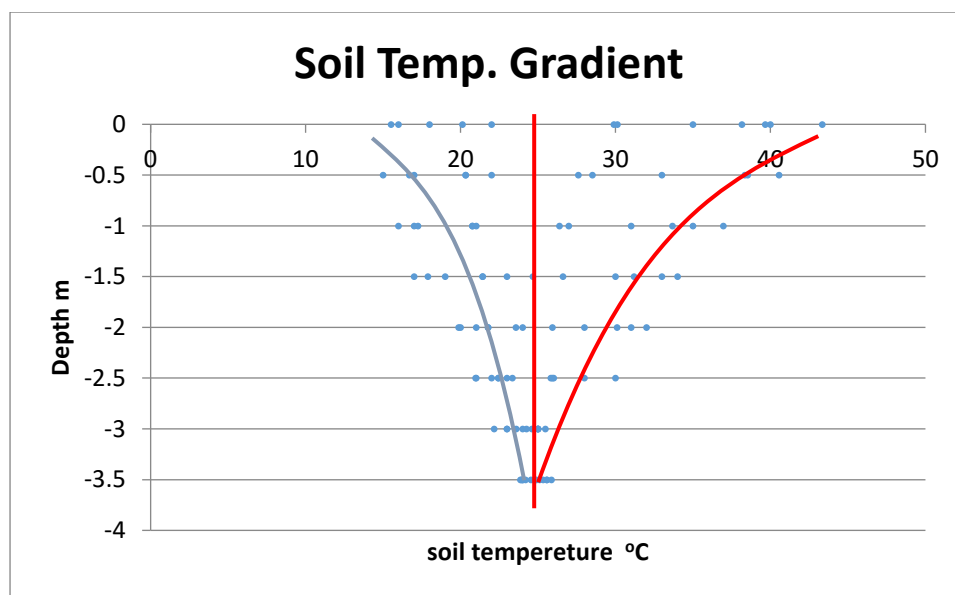
Figure 4.24: Soil temperature gradient of the test area.

The GHE operating time depends on its purpose, and because the project is for the purpose of cooling test, it was self-evident that the working time in the hottest months of this region where the ambient temperature naturally reach more than 50°C, these months were determined by the annual thermal gradient of the region's weather as it indicated in the Figure 4.23, which is from late April to mid-September, The work was done and the results were recorded in June and part of July from 2019.

4.4.2   Practical procedures of GHE system.

The GHE, has been installed and connected as it indicated in figure 4.1. and the sensors was set at the entrance and the exit of the inlet and outlet pipes, which marked A1,A2, and B1, B2, for the first and second network respectively as figure 4.25. Then the system was operated experimentally for a period of time to bleed the air from the network also to stabilize water flow inside pipes.

Figure 4.25 the inlet and outlet pipes mark in the system.

First, the performance of each network (layer of pipes) was tested separately and their results were recorded. Then the performance of the two networks (double-layers pipes) was tested together and their results were recorded, to be compared later. Valves were placed at each entrance to the network to control its closure and opening for separate and double testing with the other network. Sediment-free water (R.O.) was used in the GHE system as a circulating fluid and in a closed system. Three bands of flow were tested through the main control valve placed in front of the water flow meter to determine the measured flow values, where the flowrate values were determined after reviewing a group of researchers and according to certain hypotheses. In addition, three values of water temperature were tested. Inside and at every value of the flow. Before recording any readings, the system must reach a steady-state, and this is done by observing the stability of the temperature of the water entering the system,

and after a certain period of time, where the temperature of the water entering regulated, by the sensitive water mixer that regulated entered temperature value, and monitored in the data logger screen through The sensor installed at the inlet pipe. Taking into consideration the emptying of each layer of the water remaining inside it from the previous experiment at each subsequent test.

Practical tests started in the summer season from June to July (12/6/2019 - 22/7/2019).

The first-layer was tested performance (the water inlet valve was closed to the second-layer), which is at a depth of 3 m below the surface of the soil. The water was circulated through 100 m of pipes with a different flow at (2-3-4) ℓ/min with a change in the temperature of the water entering at each value of flow to approximately between (30-60) ˚C, the temperature of entry (T_{A1}) and exit (T_{B1}) was recorded(ambient temperature (T_{amb}) and soil surface temperature (T_s) are also recorded for every half an hour and within 6 hours of the day (7:00 am-1:00 pm), for each amount of flow, as the first network experiments lasted 9 days (26/6/2019 - 8/7/2019).

The second -layer was tested performance (the water inlet valve was closed to the first-layer), which is at a depth of 2.5 m below the surface of the soil. In the same way as the first network test, with the same flow rate, temperatures, and time, the temperature of entry (T_{A2}) and exit (T_{B2}) was recorded (Ambient temperature(T_{amb}) and soil surface temperature (T_s) are also recorded) for every half an hour and within 6 hours of the day (7:00 am-1:00 pm), for each amount of flow, as the second network experiments lasted 9 days also (12/6/2019 - 24/6/2019).

In the last, the double-layers (the water inlet valve of two layers opened together) was tested performance. The water was circulated through 200 m of pipes with a different flow at (3-4-5) ℓ/min with a change in the temperature of the water entering at each value of flow to approximately between (30-60) ˚C, the

temperature of entry (TA)and exit(TB) was recorded(Ambient temperature(Tamb) and soil surface temperature (T$_s$) are also recorded) for every half an hour and within 6 hours of the day (7:00 am-1:00 pm), for each amount of flow, as the two networks experiments lasted 9 days also(10/7/2019 - 22/7/2019).

Figure 4.26 The readings of the flowmeter and Data logger are in different circumstances

The results of the experiments were recorded and the amount of the lost heat was found at each layer and for both layers together. The Figures were drawn showing the difference in temperature degrees between entry and exit for each layer and for the double-layers. after that, the comparison was made between separate layer state and double-layers state after assume that when flowing 4 ℓ/min for the double-layer state the flow of each layer was 2 ℓ/min. Considering that the flow is divided in half between the two layers because they have the same diameter as the pipe. And as will be explained in Chapter Five.

CHAPTER FIVE

RESULTS AND DISCUSSIONS

5.1   INTRODUCTION

In the introduction to this chapter, we test a ground heat exchanger consisting of two layers of pipes, the length of each layer will be 100 meters, as a measure to reduce the area used in horizontal geothermal heat exchangers in this design, which is one of the problems of their use and reduce the cost in installing horizontal geothermal heat exchangers with the same efficiency.

The practical results depend on the rotation of water (as the only fluid used in the experiment) within the closed piping system to exploit the relative stability of the soil temperature in the depths used and exclusively in the summer season to cool the rotate fluid.

The temperature ΔT (The temperature difference between the water entering and leaving the system pipes) and coefficient of performance COP (which equals the amount of heat dissipated inside the soil over the work expended to circulate the water) were used as the general performance to test the practical results of the ground pipes system in addition to the soil gradient temperature. the experimental data were set in tables and Figures as will be shown later in this chapter.

5.2 Ground Thermal Characteristics

The geothermal heat exchanger installed in space at the Technical College of Engineering - Najaf southwest of the Najaf Governorate Center, which is located in southwestern Iraq, specifically (31.9760718 ° N 44.364692 ° E). Where the type of soil in the study area is light sandy soil.

The soil temperature varies according to the different weather conditions during the months of the year, and the change is noticeable near the soil surface and this change gradually decreases as go towards the depth to reach relative stability at certain depths, and a noticeable change may also be recorded at the surface of the soil due to the effect of air temperature on it during the day While the change is almost non-existent at depths that reach the relative stability of the temperature during day and night.

Results were recorded of the study area it was recorded soil temperature data at different depths according to the thermocouples buried in the soil and at depths (0 - 0.5 -1 - 1.5 – 2 - 2.5 – 3 - 3.5) meters from the surface of the soil and record the data through digital Datalogger, for every month for the year 2019(we record data at 12:00pm) Consequently, it made a summary of the results of the months according to the seasons of the year.
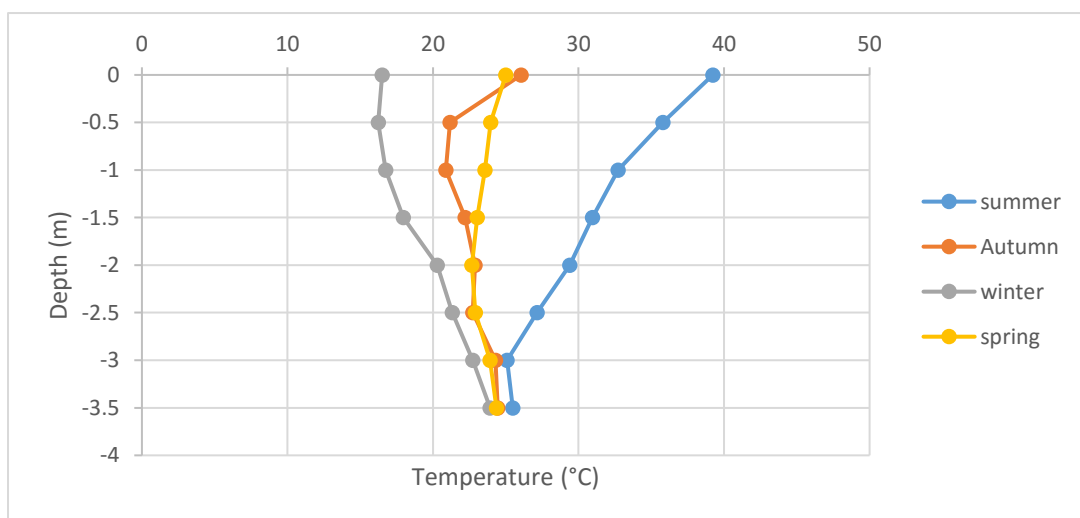
Figure 5.1: Seasonal temperature Variation at different depths for soil

Figure 5.1 shows the annual gradient of soil temperature and at different depths of the study area, by taking the outcome of the recorded readings for each month during the year 2019 and abbreviating it with four charts for the seasons of the y Where it is noticed that the temperatures in the winter season at the surface are lower than at the depths. Where that illustrate the nature of the annual temperature gradient of the study soil.

While in the spring and autumn seasons the relative convergence of the temperatures is observed at the different depths. while the summer scheme is where the temperature of the soil surface reaches 40 degrees as an average for a group of readings of the surface temperature The soil may reach higher values during specific times, while the temperatures begin to decrease relatively whenever we go to the specified depths, reaching approximately 25 degrees at a depth of 3.5 meters below the surface of the soil. Which is considered a comfortable temperature for humans.
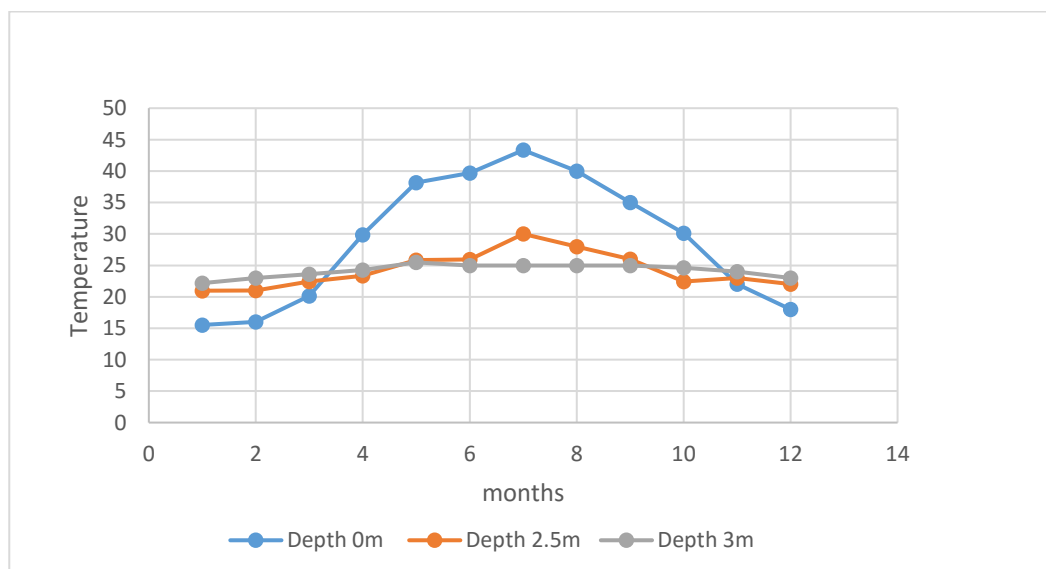
Figure 5.2: Annual change of soil temperature at various depths.

In Figure 5.2, the effect of temperature changes on the soil surface according to the change in the temperature of the atmosphere during the year 2019 with the temperature of two different depths of the soil, in which the tuned pipe-layers were installed at the two depths (2.5 &3) m in order to obtain a good heat exchange During the year (better heat dissipation).due to the slight influence of temperature and climatic conditions during the year at these depths for the study area soil.
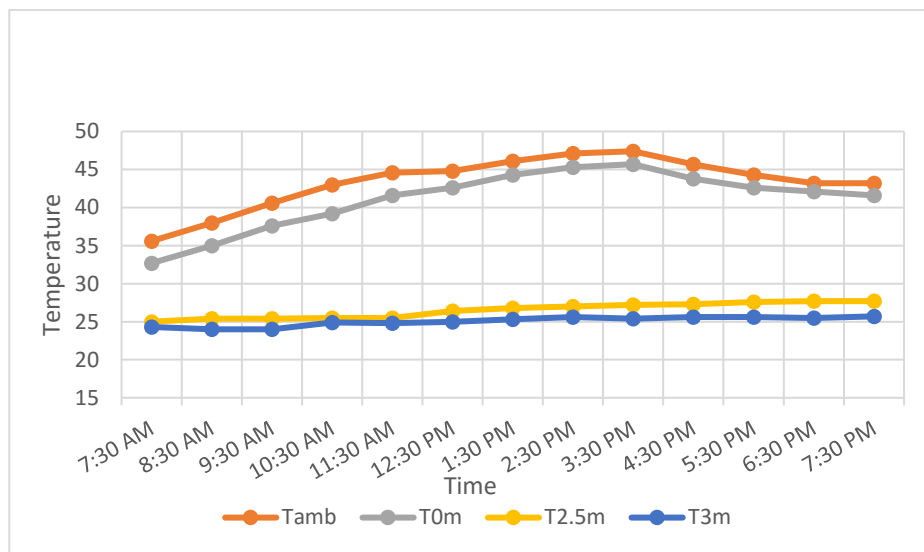
Figure 5.3: Temperature grid net with time

Figure 5.3 shows the temperature of the soil for the mentioned depths (2.5&3) m with two charts for the temperature of the soil surface and the temperature of the atmosphere surrounding the study area and during every hour of the day, and that was on 1/6/2019. Where it becomes clear the relative stability of the temperature of the depths in comparison with the temperature of the surrounding atmosphere and the temperature of the surface of the soil affected by it.

5.3 Ground Heat Exchanger GHE

Due to the high temperatures in months of the year for the specified region, and their rise to degrees approaching half the boiling degree in the summer, this led to an increase in the consumption of refrigeration systems in addition to the cost of installation and maintenance compared to the heating systems used.it had

to search for alternative methods of cooling and test it. So headed to be the purpose of the underground heat exchanger for cooling to contribute to finding a solution to this problem, hence the work on testing the underground heat exchanger in the hottest months of the year,(12/6/2019 -22/7/2019).
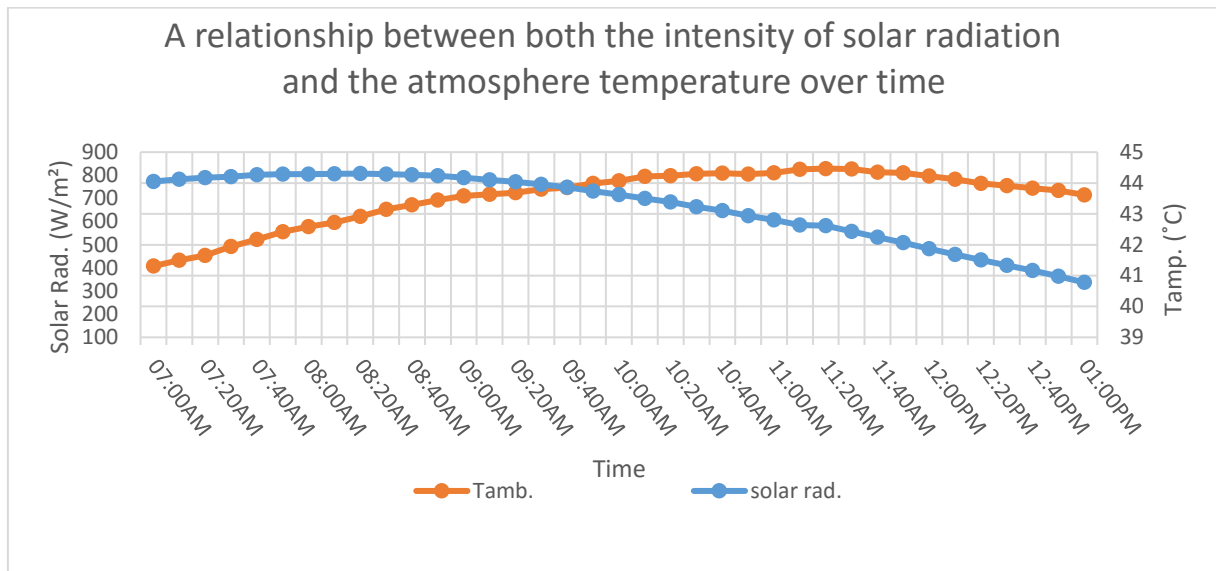
Figure 5.4: the average values of the intensity of solar radiation and the temperature of the atmosphere over time at specific days in 2019

Figure 5.4 shows the average of a set of values of the intensity of solar radiation with time, plus an average for a group of values of ambient temperature during same time and date of recording the results for testing the underground heat exchanger layers (first, second, and double layers state).

The ground heat exchanger consisting of two layers was tested for each layer separately and then for the two layers together (in case of changing the flow rate and the entry temperature of water into the ground heat exchanger). The following are tables showing the results obtained in addition to the mathematical calculations used.

Where the date and time appropriate for recording the results were recorded in each table, as the system reached stability, and both the temperature of the surrounding atmosphere and the surface of the soil and the temperature of the water entering and leaving the piping layer by means of sensors placed and a data

monitor. In addition to the calculation of the properties of water as being variable with the water bulk temperature (T_b) (in the equation 3.26) and within certain equations given in the appendix [63]. The velocity of flow(u) changes slightly with the change in the water density, which is affected by the temperature at the constant flow rate .Also, Prantel number and Nusselt number were calculated from the equations mentioned in chapter three and find ($h_{con.}$) from them, which is included in the calculation equation the fluid resistance equation ($R_{con.}$), and calculate the rest of the resistors (R_{total}) to calculate the overall heat transfer coefficient (U) which is included in the equation to calculate the rate of heat transfer (Q).

The results were as follows:

5.3.1 First-layer GHE

The results of testing the first layer of the geothermal heat exchanger, which is at a depth of 3 meters from the soil surface with length pipe 100m.

- When we test the flow rate of 2 LPM (0.0333 kg/s) we get the results as in the table below:

Table (5.1) Results of first-layer GHE at 2lpm flow

Date	26/6/2019	27/6/2019	30/6/2019
Time	8:00 AM	10:00 AM	12:00 PM
T amb.	38.1	44.9	53
T soil	37.2	44	47.7
T_{in}	33.3	40.2	58.5
T_{out}	29.9	35.1	42.4
ΔT	3.4	5.1	16.1
T_b	31.6	37.65	50.45
Cp	4178.51	4178.31	4181.24
ρ	995.14	993.05	987.72

u	0.2963	0.2969	0.2985
μ	756.317 *E-6	667.355 *E-6	524.316 *E-6
Re	4623.669	5302.384	6748.933
K w	618.007*E-3	626.957*E-3	643.603 *E-3
Pr	5.1741	4.4475	3.4063
Nu	32.2008	34.3353	38.4415
h con.	1658.361	1793.896	2061.752
R con.	0.016003	0.014794	0.012872
R pipe	11.45 *E-3	11.45 *E-3	11.45 *E-3
R soil	0.59556582	0.59556582	0.59556582
R total	0.623021447	0.621812347	0.619890328
U	0.319482719	0.320103946	0.321096453
ΔP	0.139041346	0.1340214	0.126016301
Q	473.52	710.31	2243.93
Power	358.6	358.6	358.6
COP	1.320479418	1.980795939	6.257474563

After the system reached a state of stability every day and for the same flow, the results of the entry temperature ranged between (30-60) ˚C and the exit temperature, which was between (30-50) ˚C and noting the differences between them, where the highest temperature difference was (16.1˚C) and higher. The rate of heat transfer (2243.93 W) for this flow and the difference in the temperature of the inlet water. This is due to the high temperature of the inlet water and the difference between it and the initial soil temperature. In addition to measuring the current consumed at this flow to be (1.63 A). The highest value (COP) (6.26) is also recorded. Due to the higher temperature difference and the heat transfer rate compared to the consumption rate.

- When we test the flow rate of 3 LPM (0.05 kg/s) we get the results as in the table below:

Table (5.2) Results of first-layer GHE at 3lpm flow

Date	1/7/2019	2/7/2019	3/7/2019
Time	8:00 AM	10:00 AM	12:00 PM
$T_{amb.}$	38.3	44	48.6
T soil	36.1	41.5	45.9
T_{in}	33.1	43	55.3
T_{out}	30.9	37.8	44.8
ΔT	2.2	5.2	10.5
$T_{b.}$	32	40.4	50.05
Cp	4178.127988	4178.699153	4181.108121
ρ	995.0097486	992.0015525	987.8992633
u	0.444539667	0.445887712	0.447739277
μ	758.132*E-6	629.886*E-6	527.698*E-6
Re	7001.226894	8426.696384	10058.51055
K w	618.620486*E-3	630.795158*E-3	643.129607*E-3
Pr	5.120382334	4.172674515	3.430665071
Nu	44.73607472	48.79530826	53.01127784
$h_{con.}$	2306.221025	2564.987014	2841.093523
$R_{con.}$	0.011507691	0.01034675	0.009341219
R_{pipe}	11.45 *E-3	11.45 *E-3	11.45 *E-3
R_{soil}	0.59556582	0.59556582	0.59556582
R_{total}	0.618525822	0.617364881	0.616359351
U	0.321804812	0.322409959	0.322935939
ΔP	0.278650377	0.265868748	0.254776355
Q	459.59	1086.46	2195.08

Power	363	363	363
COP	1.26609939	2.993007658	6.047057199

After the system reached a state of relative stability for every day, where the entry temperature was recorded for the first, second, and third day to be roughly between (30-60) ˚C and the exit temperature was roughly between (30-50) ˚C, where the temperature gradient from low to medium then high during the three days respectively. Noting the differences between them, where the highest temperature difference was (10.5 ˚C) and higher. The rate of heat transfer (2195.08W) for this flow and the difference in the temperature of the inlet water. This is due to the high temperature of the inlet water and the difference between it and the initial soil temperature. In addition to measuring the current consumed at this flow to be (1.65 A). The highest value (COP) (6.05) is also recorded. Due to the higher temperature difference and the heat transfer rate compared to the consumption rate.

- When we test the flow rate of 4 LPM (0.06667 kg/s)   we get the results as in the table below:

Table (5.3) Results of first-layer GHE at 4lpm flow

Date	4/7/2019	7/7/2019	8/7/2019
Time	8:00 AM	10:00 AM	12:00 PM
$T_{amb.}$	35.7	43.6	49.5
T_{soil}	34.6	38.4	43.1
T_{in}	32.9	42.8	50.9
T_{out}	30.6	38.1	42.7
ΔT	2.3	4.7	8.2
$T_{b.}$	31.75	40.45	46.8
C_p	4178.142479	4178.707624	4180.140817

ρ	995.090321	991.9819894	989.3516429
u	0.592671563	0.594528673	0.596109321
μ	762.61*E-6	629.242*E-6	557.505*E-6
Re	9280.156068	11247.08649	12694.30509
K w	618.2376*E-3	630.8636*E-3	639.1727*E-3
Pr	5.153833264	4.167967325	3.646040973
Nu	56.1579401	61.45216043	65.0371415
$h_{con.}$	2893.246011	3230.661028	3464.164227
$R_{con.}$	0.009172838	0.008214814	0.007661091
R_{pipe}	11.45 *E-3	11.45 *E-3	11.45 *E-3
R_{soil}	0.59556	0.59556	0.59556
R_{total}	0.61619097	0.615232945	0.614679223
U	0.323024185	0.32352719	0.323818633
ΔP	0.459278146	0.438168752	0.425906517
Q	501.37	1197.81	1560.64
Power	367.4	367.4	367.4
COP	1.743735747	3.56376807	6.219770405

As the system reaches stability when the entry temperature is low faster, while the system needs more time to stabilize when the inlet water temperature rises, so the results were recorded for different days and different times. Noting the differences between them, where the highest temperature difference was (8.2 ˚C) and higher. The rate of heat transfer (1560.64 W) for this flow and the difference in the temperature of the inlet water .This is due to the high temperature of the inlet water and the difference between it and the initial soil temperature. In addition to measuring the current consumed at this flow to be (1.67 A). The highest value (COP) (6.22) is also recorded. Due to the higher temperature difference and the heat transfer rate compared to the consumption rate.

It is also noted from the tables above that the values of the heat transfer rate converge upon increasing the flow with change in temperature different.

To more clearly demonstrate the changing effects on results with Figures, for every half hour within six hours of the day ,we can divide them into:

- **The effect of temperature change at entry**

Here are three Figures in each graph showing the difference between the entry and exit temperature of the heat exchanger when the input temperature changes to several values that are approximate to (30, 40, 50) ˚C and when stabilizing the water flow values to (2,3,4) l/min.

Figure 5.5: the relationship between temperature difference and time when flowrate

$2 \, \ell/min$ and for the first-layer

Figure 5.5 shows that when the flow is constant at 2 l/min, we note that the temperature change is in three patterns. The first is when the rate of the temperature of entering the water is close to 30 ˚C, where the rate of change is (3.48)˚C, and the second is when the rate of the temperature of the inlet water is close to For 40 ˚C where the rate of change is recorded by (5.45)˚C. The highest values of the outcome of the temperature difference (15.8) ˚C are recorded when the inlet water is at a temperature close to 50 ˚C, due to the large difference

between the temperature of the surface of the pipe and the initial degree of the soil at this depth and because the flow rate allows Slow flow, which saves time to cool the water inside the pipes.

Figure 5.6 the relationship between temperature difference and time when flowrate $3 \, \ell/min$ and for the first-layer

Figure 5.6 shows that when the flow is constant at 2l/min, we note that the temperature change takes place in three modes. The first is when the average inlet water temperature is about 30 ˚C, where the rate of change is (2.42) ˚C. And the second is when the average inlet water temperature is close to 40 ˚C where the rate of change is recorded by (4.77) ˚C where it is slightly turbulent. The highest values of the temperature difference result (8.98) ˚C are recorded when the inlet water is at a temperature close to 50 ˚C, and the turbulence is observed at the initial points where the flow needs time to stabilize ,due to the increase in the flow rate and the high temperature of the water inside the pipes. The high difference is due to the large difference between the surface temperature of the tube and the initial temperature of the soil at this depth, which allows cooling the water circulated inside the pipes.
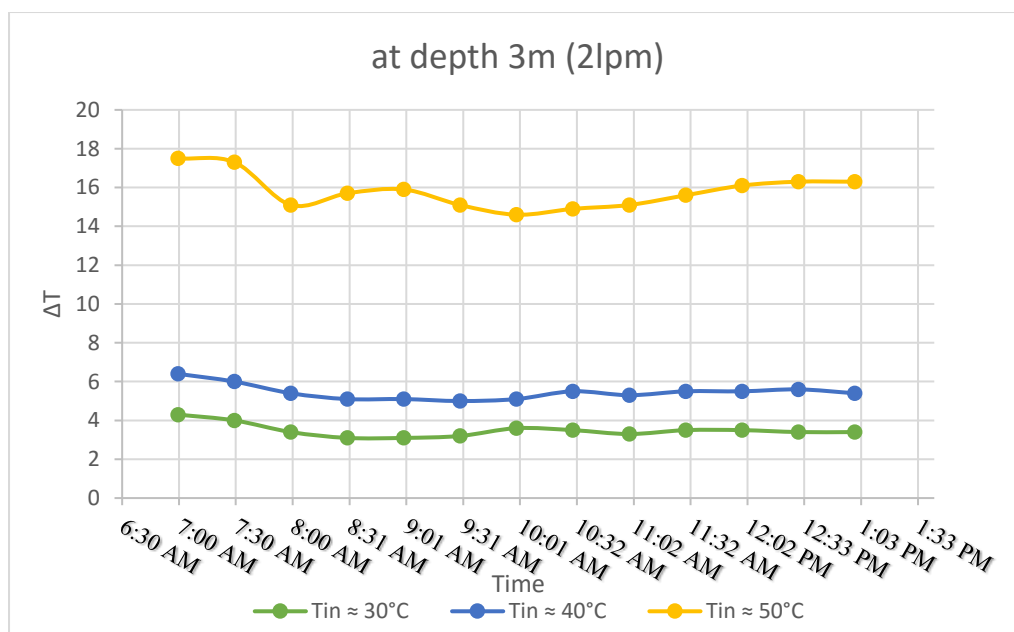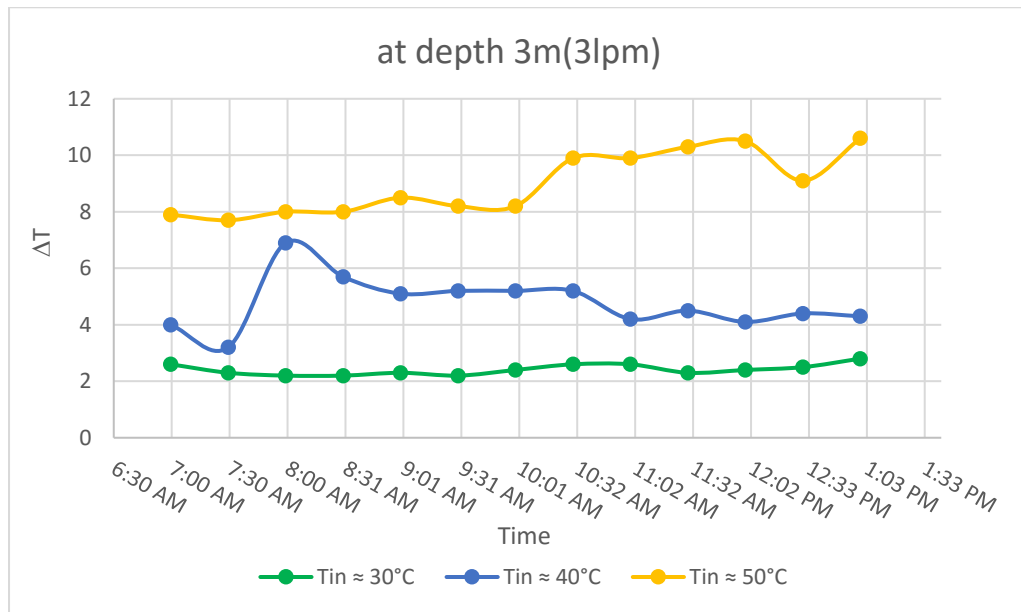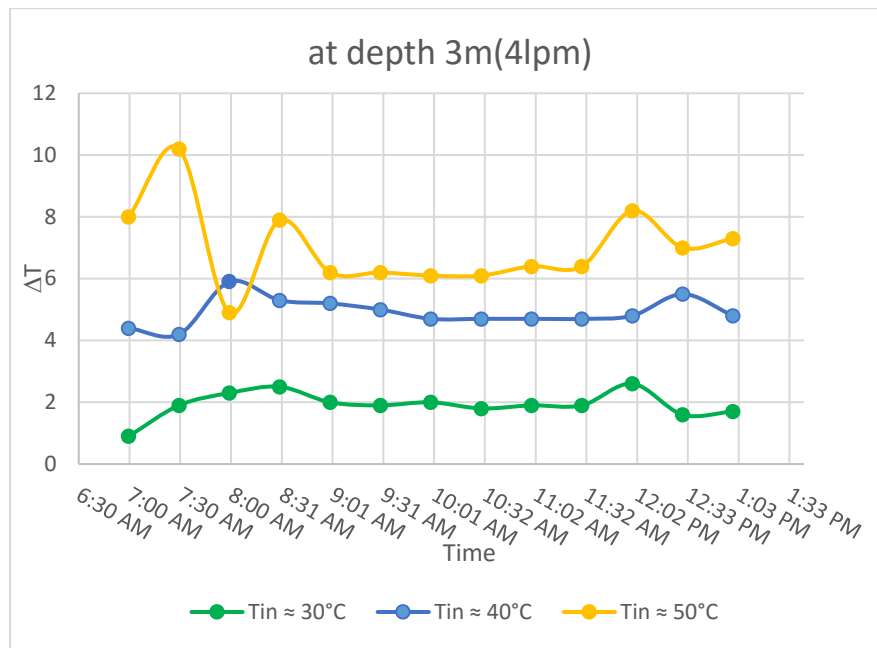
Figure 5.7: the relationship between temperature difference and time when flowrate
4 ℓ/min and for the first-layer

Figure 5.7 shows the temperature difference values of the circulating water inside the pipes in three levels over time at the constant flow rate 4 l/min .Where the first scheme is when the inlet temperature is close to 30 ° C, the difference is little (1.92) ° C due to the slight difference between the temperature of the inlet water and the soil surrounding the tube at that depth, while it begins to settle after that, then is disturbed in the last hour due to the high temperature of the water circulating inside the pipes. The second scheme, when the inlet temperature is close to 40 ° C, where it is stable on the result of the temperature difference (4.92) ° C with little turbulence at the end due to the high temperature of the water circulating While the third chart shows that when the entry temperature is close to 50 ° C, with temperature difference (6.99) ° C the turbulence is clear at the beginning due to the speed of the flow, while it takes stability, it returns to turbulence slightly at the last hour due to the high temperature of the circulating water and the change of its properties.

▪ **Flux effect**

The following are chars that show the effect of changing the flow of water inside the pipes at a temperature relatively of the water entering, through the amount of heat transfer rate to the soil (in watt unit).

Where; q_1, q_2, q_3 are heat transfer rate at temperature of the water entering is approximate close to ≈30, 40 and 50°C respectively.

Figure 5.8 the relationship between heat transfer rate and time when inlet water temperature approximate 30°C and for the first-layer

In Figure 5.8 above, when the incoming water temperature is approximately 30 ° C, the average heat transfer rate is three plots at each flow rate. The first diagram shows heat transfer values whose rate is (482.8 W) with slight turbulence at constant flow (2 l/min) .While the randomness of the water movement increases slightly when the flow increases to record the rate of heat transfer (499.9W) at constant flow (3l/min). While the third chart shows the turbulence about an hour (8:00AM) due to the increase in the flow to the constant value (4l/min) so that the movement of water inside the pipelines will be turbulent, as well as at about the clock (11:30). We notice the disturbance in the values of the transmitted temperature due to the high temperature of the

water and the different properties of it, to record the rate of heat transfer (555.7W).

Figure 5.9 the relationship between heat transfer rate and time when inlet water temperature approximate 40°C and for the first-layer

In the above Figure 5.9, when the incoming water temperature is approximately 40˚C, the average heat transfer for the first chart when constant flow rate at (2 l/min) it seems almost stable to be (755.4W).Whereas when the constant flow values rise to (3 -4) l /min, it is noticed at the hour (8:00 AM) that the values rise suddenly due to disturbance in the flow, while the values are in contradiction before that. the scheme is at the flow (3 l/min) it is with high values after that begins to decrease due to the low temperature of the inlet water A little bit about it at the beginning, due to the surrounding conditions, to be recorded as an outcome of values (983.6W). While the scheme at flow (4 l/min) reaches the stability phase and then is slightly turbulent at the end due to the high temperature of the circulating water to record an average of the sum of the values of the heat transfer rate (1365.3 W).
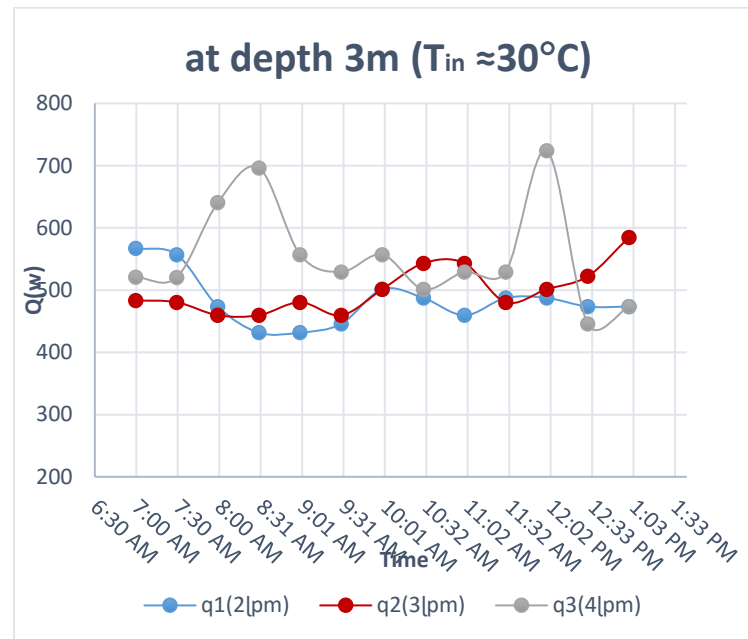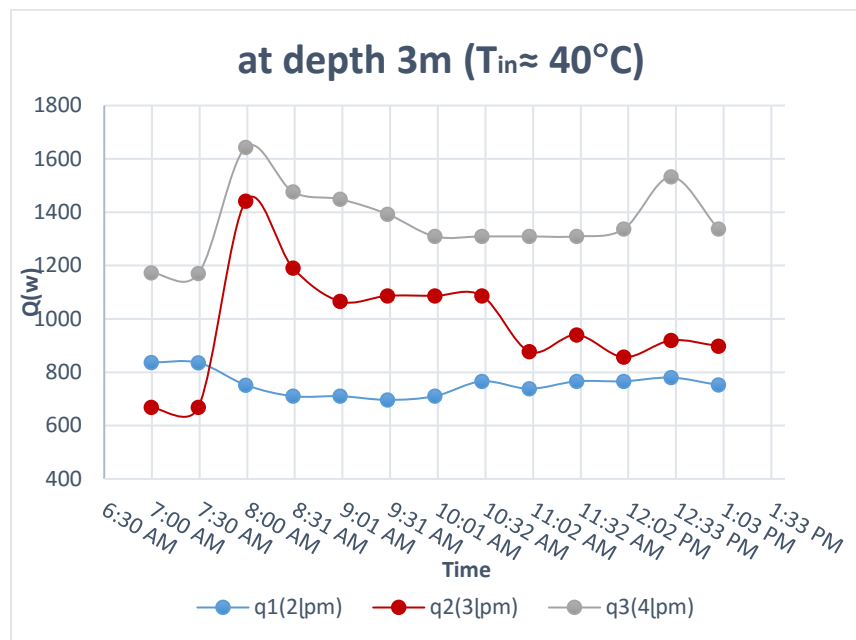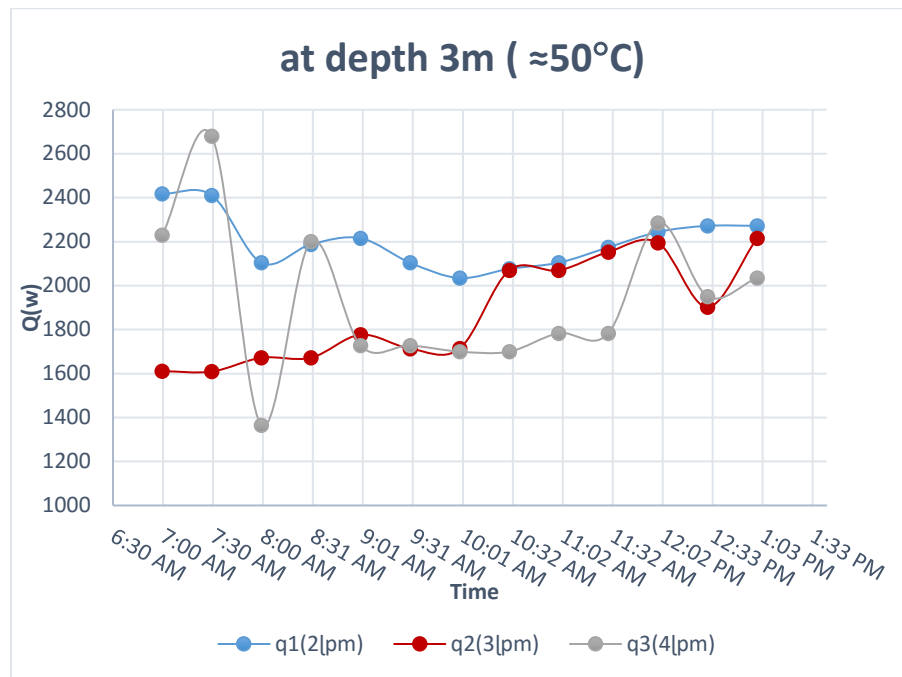
Figure 5.10: the relationship between heat transfer rate and time when inlet water temperature approximate 50°C and for the first-layer

In the above Figure 5.10, when the incoming water temperature is approximately 50 ˚C, the average heat transfer rate in three charts for every value of constant flowrate 2,3, and 4 l/min respectively. As it becomes clear that the highest values of the heat transfer rate can be obtained, which is (2201.28W) when the flow is (2l/min). While the turbulence in the values is clear when the flow (3 l/min) where it is oscillating between the lowest values of the start of the scheme, but after an hour (10:00AM) begins to rise and converges from the values of the temperature at the flow (2 l/min) to be recorded as an average (1874.8W) due to the high temperature of the inlet water, and the difference between it and the temperature of the soil increases At that depth and increased flow rate also affect turbulence. observe the large fluctuation of the values of the heat transfer rate when increasing the flow to (4 l/min), where random values ranging from the highest and lowest values are recorded so that their rate is (1935.97 W) the stability is between hours (11:00am-12:00pm) and the fluctuation is due to the high temperature of the inlet water, which causes its properties to change and increases the randomness of the flow with Increase the flow rate at this layer.

▪ **The effect of performance coefficient (COP) of GHE**

The following are three charts that show the relationship between the performance coefficient values of the first stratum with time according to the difference in temperature difference values between the incoming and outgoing water for each diagram, and with constant flow rates 2, 3, and 4 l/min.

Figure 5.11:COP values with time at inlet temperature approximate 30 ˚C and at three constant flow rates.

In figure 5.11, we note the convergence of the performance parameter values according to the difference in flow when the inlet temperature is close to 30 ° C. The average of values at flow (2 l/min) is (1.35), while (1.38) at flow (3 l/min). At the flow (4 l/min) it is noticed that the values are lower at the start. and began slightly be high to be the average values of the performance factor (1.4), due to the proportionality between the temperature difference and the rate of flow, to the electrical consumption.

Figure 5.12 COP values with time at inlet temperature approximate 40 ˚C and at three constant flow rates.

In figure 5.12, three plots of the performance parameter values of the system are shown with time at each constant flow rate value, and when the inlet water temperature is approximately 40 ° C. The average of values at flow (2 l/min) is (2.1). Whereas when the flow rate is (3 l/min), the beginning of the scheme is a few values due to the increase in flow, then it starts to rise at the hour (8:00 am), the highest value is recorded, then the relative stability begins. For circulating water at this flow, the resulting values are (2.75). The third chart is at the constant flow value (4 l/min), where it records the highest values of the performance parameter despite the disturbance occurring at the beginning and end of the scheme and is at a rate (3.75) due to the direct proportion between the increase in flow and the amount of heat dissipation in addition to the temperature difference values and the rate of electricity consumption at this flow.
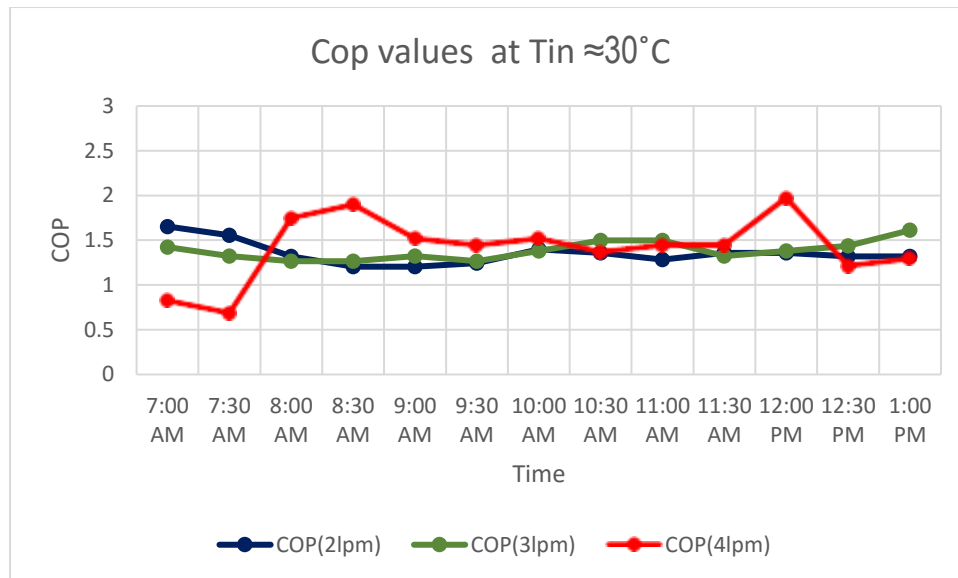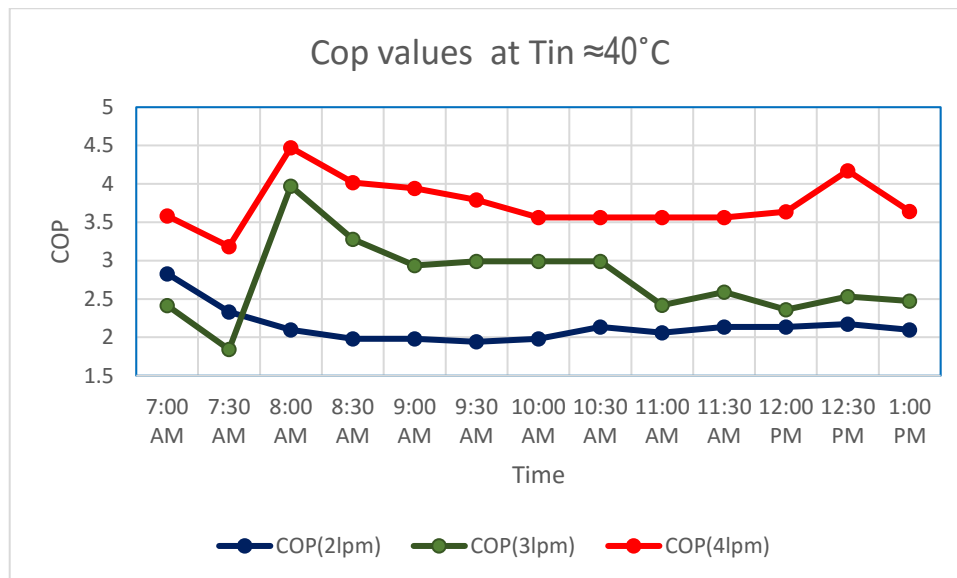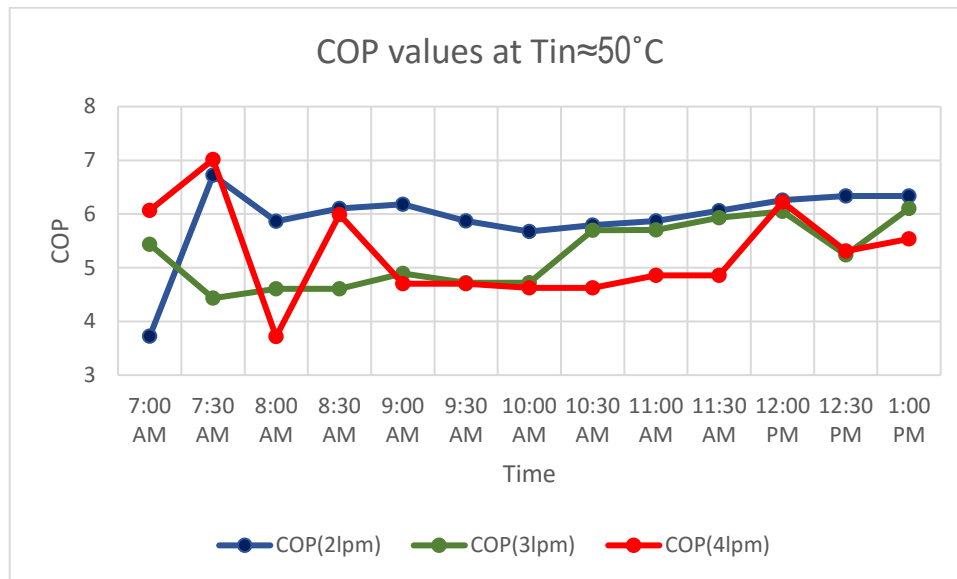
Figure 5.13 COP values with time at inlet temperature approximate 50 ˚C and at three constant flow rates.

In figure 5.13, three plots of the performance parameter values of the system are shown with time at each constant flow rate value, and when the inlet water temperature is approximately **5**0 ° C. Notice the turbulence and instability of the charts until the hour (8:30 am). Record the average values of the performance parameter (5.9) at the flow (2 l/min). While at the flow (3 l/min) with alternating values that are few at the beginning of the scheme, it starts to rise at the hour (10:30 am) to be its rate (5.2) due to the availability of more time for heat exchange at this flow. While the chart at the flow (4 l/min) is turbulent at the beginning, it reaches the stability phase between the hours (9:00-11:30) am to record an average of (5.25) values less than the rest of the flow values due to the lack of time for heat exchange for the speed of the flow of water in addition to the amount of electrical consumption greater at this amount of flow.

5.3.2 Second-Layer GHE

The results of testing the second layer of the geothermal heat exchanger, which is at a depth of 2.5 meters from the soil surface. Length of pipes 100 m.

- When we test the flow rate of 2 LPM (0.0333 kg/s) we get the results as in the table below:

Table (5.4) Results of second-layer GHE at 2lpm flow

Date	12/6/2019	13/6/2019	16/6/2019
Time	8:00 AM	10:00 AM	12:00 PM
$T_{amb.}$	33.6	39.6	43.6
T_{soil}	32.8	37.2	40.4
T_{in}	29.6	41.8	53.4
T_{out}	26.6	31.1	39.8
ΔT	3	5.7	13.6
$T_{b.}$	28.1	36.45	46.6
Cp	4178.625189	4178.200705	4180.085997
ρ	996.2029043	993.4867822	989.4387501
u	0.296004827	0.296814083	0.298028421
μ	832.784*E-6	685.029*E-6	559.481*E-6
Re	4249.086402	5165.577989	6324.73212
$K\,w$	612.513*E-3	625.236*E-3	638.922*E-3
Pr	5.681334696	4.577766531	3.660349679
Nu	30.95276128	33.91712767	37.29222687
$h_{con.}$	1579.914102	1767.186553	1985.570988
$R_{con.}$	0.016797925	0.015017814	0.013366069
R_{pipe}	11.45 *E-3	11.45 *E-3	11.45 *E-3
R_{soil}	0.590615748	0.590615748	0.590615748
R_{total}	0.607413673	0.605633561	0.603981816

U	0.327691975	0.328655145	0.329553938
ΔP	0.142308091	0.134953323	0.128061057
Q	417.86	1490.22	1894.97
Power	358.6	358.6	358.6
COP	1.165260789	4.155674618	5.284362294

After the system reached a state of stability every day and for the same flow, the results of the entry temperature ranged between (29-55) ˚C and the exit temperature, which was between (26-40) ˚C and noting the differences between them, where the highest temperature difference was (13.6˚C) and higher. The rate of heat transfer (1894.97 W) for this flow and the difference in the temperature of the inlet water. This is due to the high temperature of the inlet water and the difference between it and the initial soil temperature. In addition to measuring the current consumed at this flow to be (1.63 A). The highest value (COP) (5.3) is also recorded. Due to the higher temperature difference and the heat transfer rate compared to the consumption rate in this conditions.

- When we test the flow rate of 3 LPM (0.05 kg/s) we get the results as in the table below:

Table (5.5) Results of second-layer GHE at 3lpm flow

Date	17/6/2019	18/6/2019	19/6/2019
Time	8:00 AM	10:00 AM	12:00 PM
$T_{amb.}$	34.1	41.5	48.9
T_{soil}	32.2	37.4	44.3
T_{in}	34.5	42.7	52.1
T_{out}	31.9	38	43.8
ΔT	2.6	4.7	8.3
T_b	33.2	40.35	47.95

Cp	4178.087957	4178.690732	4180.466884
ρ	994.6154611	992.021097	988.845614
u	0.444715892	0.445878927	0.447310779
μ	737.202*E-6	630.531*E-6	546.469*E-6
Re	7200.001391	8418.077978	9712.998764
K w	620.441*E-3	630.726*E-3	640.595*E-3
Pr	4.96435859	4.177391763	3.566206384
Nu	45.32656871	48.77190884	52.15217733
h$_{con.}$	2343.540984	2563.478552	2784.038784
R$_{con.}$	0.011324435	0.010352838	0.009532654
R$_{pipe}$	11.45 *E-3	11.45 *E-3	11.45 *E-3
R$_{soil}$	0.579163436	0.57916	0.57916
R$_{total}$	0.601940183	0.600968586	0.600148402
U	0.330671704	0.331206307	0.331658945
ΔP	0.276644912	0.265936121	0.256874431
Q	543.15	981.99	1734.89
Power	363	363	363
COP	1.496284943	2.705213008	4.779321644

After the system reached a state of relative stability for every day, where the entry temperature was recorded for the first, second, and third day to be roughly between (30-53) ˚C and the exit temperature was roughly between (30-45) ˚C, where the temperature gradient from low to medium then high during the three days respectively. Noting the differences between them, where the highest temperature difference was (8.3 ˚C) and higher. The rate of heat transfer (1734.9 W) for this flow and the difference in the temperature of the inlet water. This is due to the high temperature of the inlet water and the difference between it and the initial soil temperature. In addition to measuring the current consumed at this

flow to be (1.65 A). The highest value (COP) (4.78) is also recorded. Due to the higher temperature difference and the heat transfer rate compared to the consumption rate.

- When we test the flow rate of 4 LPM (0.06667 kg/s) we get the results as in the table below:

Table (5.6) Results of second-layer GHE at 4lpm flow

Date	20/6/2019	23/6/2019	24/6/2019
Time	8:00 AM	10:00 AM	12:00 PM
$T_{amb.}$	34.6	42	46.3
T_{soil}	33.5	38.5	39.9
T_{in}	35	43	50.3
T_{out}	32.9	38.9	44.3
ΔT	2.1	4.1	6
$T_{b.}$	33.95	40.95	47.3
C_p	4178.086559	4178.795034	4180.280334
ρ	994.3627832	991.7853378	989.1327071
u	0.593105199	0.594646557	0.596241265
μ	724.586*E-6	622.878*E-6	552.639*E-6
Re	9767.146777	11361.99729	12806.0845
K w	621.566*E-3	631.545*E-3	639.794*E-3
Pr	4.870575543	4.121444883	3.610824123
Nu	57.51963116	61.74565897	65.30445768
$h_{con.}$	2979.354081	3249.600062	3481.786426
$R_{con.}$	0.008907729	0.008166937	0.007622317
R_{pipe}	11.45 *E-3	11.45 *E-3	11.45 *E-3
R_{soil}	0.57916	0.57916	0.57916
R_{total}	0.599523477	0.598782685	0.598238064

U	0.332004657	0.332415401	0.332718023
ΔP	0.453469725	0.437107563	0.425051185
Q	584.93	1142.20	1672.11
Power	367.4	367.4	367.4
COP	1.592085243	3.108883985	4.551203412

As the system reaches stability when the entry temperature is low faster, while the system needs more time to stabilize when the inlet water temperature rises, so the results were recorded for different days and different times. Noting the differences between them, where the highest temperature difference was (6 °C) and higher. The rate of heat transfer (1672 W) for this flow and the difference in the temperature of the inlet water. This is due to the high temperature of the inlet water and the difference between it and the initial soil temperature. In addition to measuring the current consumed at this flow to be (1.67 A). The highest value (COP) (4.55) is also recorded. Due to the higher temperature difference and the heat transfer rate compared to the consumption rate.

It is also noted from the tables above that the values of the heat transfer rate converge upon increasing the flow with a change in temperature difference for water circulating in pipes of second-layer at depth 2.5 m from the surface.in addition that results are less than of the first-layer because of the temperature of the soil in this depth and weather conditions at the surrounding in thes dates.

To more clearly demonstrate the changing effects on results with Figures, for every half hour within six hours of the day ,we can divide them into:

▪   **The effect of temperature change at entry**

Here are three Figures in each graph showing the difference between the entry and exit temperature of the heat exchanger when the input temperature changes to several values that are approximate to (30, 40, 50) ˚C and when stabilizing the water flow values to (2,3,4) l/min.

Figure 5.14: the relationship between temperature difference and time when flowrate $2\ \ell/min$ and for the second-layer

In the above Figure 5. 14 when the flow is constant at 2l/min, notice that the temperature change is in three patterns. The first is when the rate of the temperature of entering the water is close to 30 ˚C, where the rate of change is (3.32)˚C, and the second is when the rate of the temperature of the inlet water is close to For 40 ˚C where the rate of change is recorded by (5.72)˚C.at the beginning of the first and second schemes ,the values are almost equal due to the instability of the system in this point .The highest values of the outcome of the temperature difference (13.41) ˚C are recorded when the inlet water is at a temperature close to 50 ˚C, due to the large difference between the temperature of the surface of the pipe and the initial degree of the soil at this depth and because the flow rate allows Slow flow, which saves time to cool the water inside the pipes.
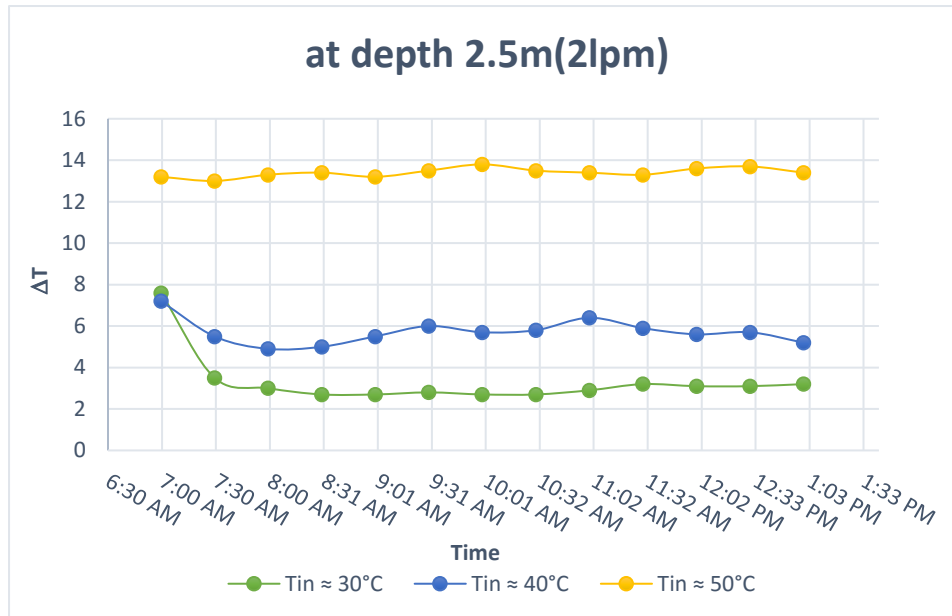
Figure 5.15: the relationship between temperature difference and time when flowrate

3 ℓ/min and for the second-layer

In the above Figure 5. 15 shows that when the flow is constant at 2l/min, we note that the temperature change takes place in three modes. The first is when the average inlet water temperature is about 30 ˚C, where the rate of change is (2.6) ˚C. And the second is when the average inlet water temperature is close to 40 ˚C where the rate of change is recorded by (4.7) ˚C where it is slightly turbulent. The highest values of the temperature difference result (8.3) ˚C are recorded when the inlet water is at a temperature close to 50 ˚C, due to the increase in the flow rate and the high temperature of the water inside the pipes. The high difference is due to the large difference between the surface temperature of the tube and the initial temperature of the soil at this depth, which allows cooling the water circulated inside the second-layer of pipes.
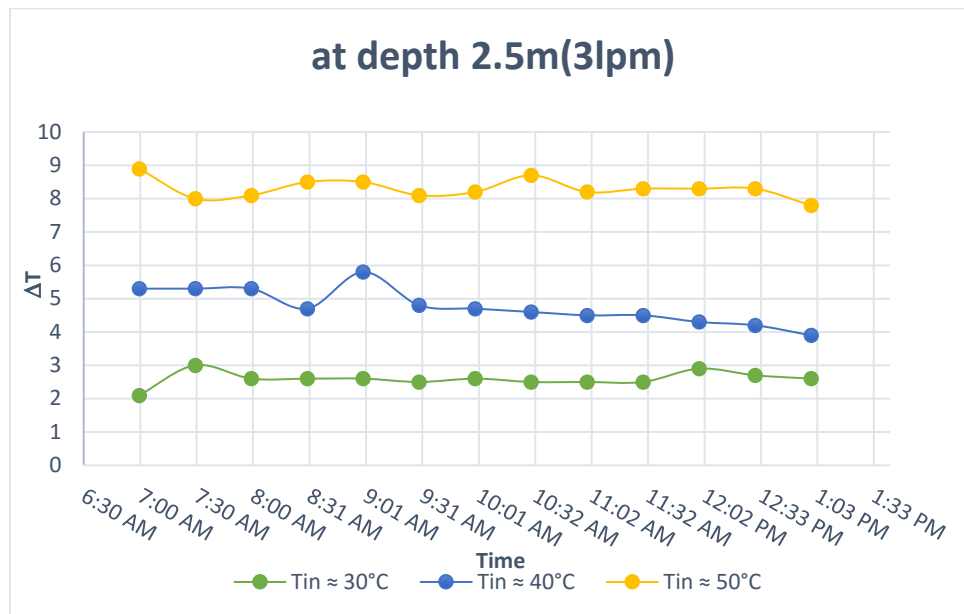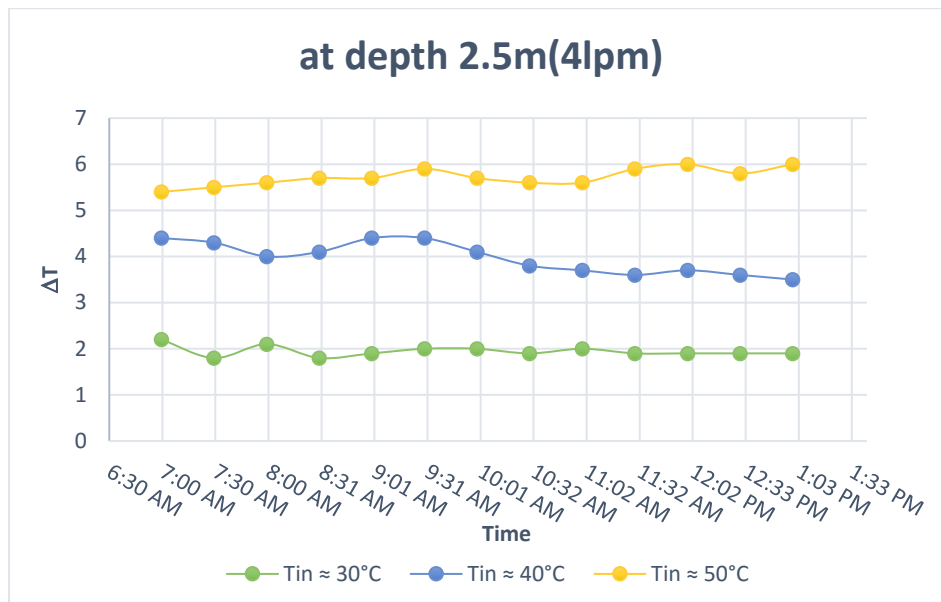
Figure 5.16: the relationship between temperature difference and time when flowrate $4\ \ell/min$ and for the second-layer

In the above 5.16 when the flow is constant at 4 l/min, notice that the temperature change is in three patterns. The first is when the rate of the temperature of entering the water is close to 30 ˚C, where the rate of change is (1.9)˚C, and the second is when the rate of the temperature of the inlet water is close to For 40 ˚C where the rate of change is recorded by (3.97)˚C. The highest values of the outcome of the temperature difference (5.7) ˚C are recorded when the inlet water is at a temperature close to 50 ˚C, due to the large difference between the temperature of the surface of the pipe and the initial degree of the soil at 2.5m depth and due to the speed of the flow, where the heat dissipation time is less to cool the water inside the pipes.

Flux effect:

The following are chars that show the effect of changing the flow of water inside the pipes at a temperature relatively of the water entering, through the amount of heat transfer rate to the soil (in watt unit).

Where; q_1, q_2, q_3 are heat transfer rate at temperature of the water entering is approximate close to ≈30, 40 and 50°C respectively.

Figure 5.17: the relationship between heat transfer rate and time when inlet water
temperature approximate 30°C and for the second-layer

In the Figure 5.17, when the incoming water temperature is approximately 30˚C, the average heat transfer rate in the scheme when the flow is constant to 2 l/min is (432.1 W).the value sloping from the highest value at (7:00-8:00) AM hours, where it begins with turbulent at beginning values and this due to the instability of the system at the beginning and to the temperature difference between circulating water and soil at this flow. While the scheme at flow (3 and 4 l/min) disturbed more in the hour (7:00-8:30)AM and began slightly turbulent after that at due to the unsteady system, it recorded an average of the sum of the values of the heat transfer rate (541.5 W) and (542.1W) respectively.

Figure 5.18: the relationship between heat transfer rate and time when inlet water

temperature approximate 40°C and for the second-layer

In figure 5.18, there are three plots of the values of the heat transfer rate with time. When the entry temperature is approximate nearly 40 °C .The first diagram is a flow (2l/min) where it is slightly sloping at its beginning with slight perturbation to record the result of values (1493.4 W). While the flow is (3l/min) less than it with disturbance of the values at the clock (9:00) am .To record the result of the values (994.9W). While it is noticed when the flow is raised to (4l/min), the result is (1105.7 W) values. The reason for the decline of the three diagrams to lower values after the hour (11:30) am is due to the thermal accumulation that reduces the temperature difference value of the circulating water.
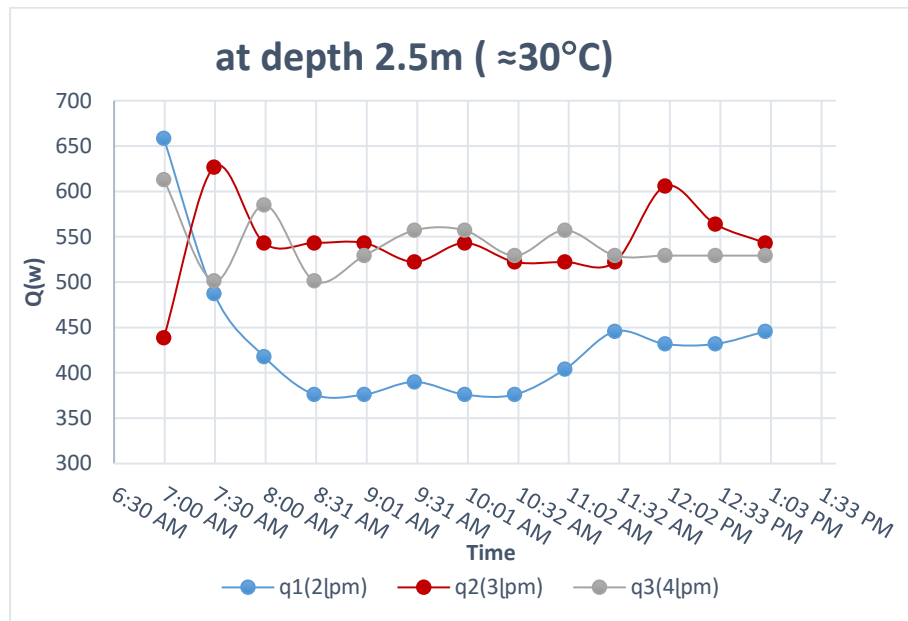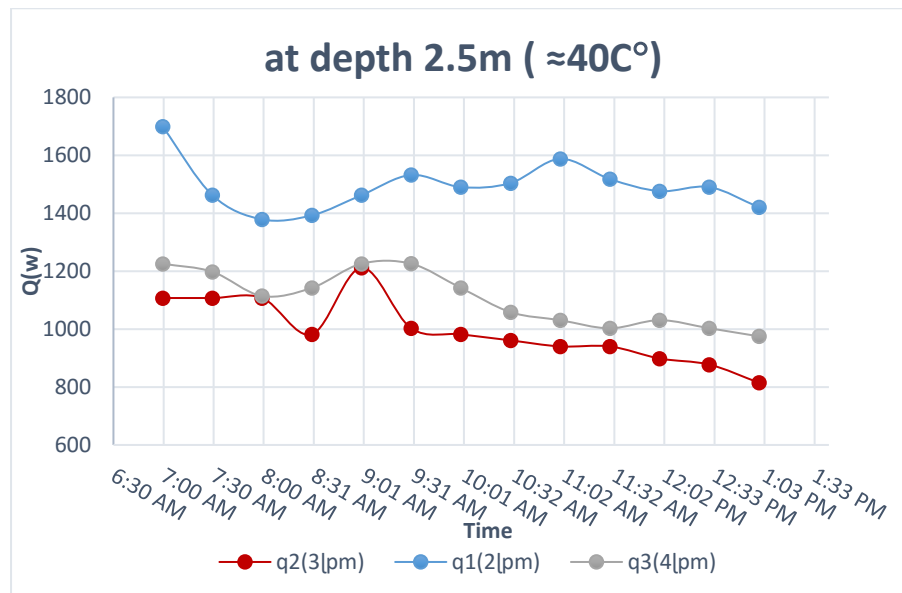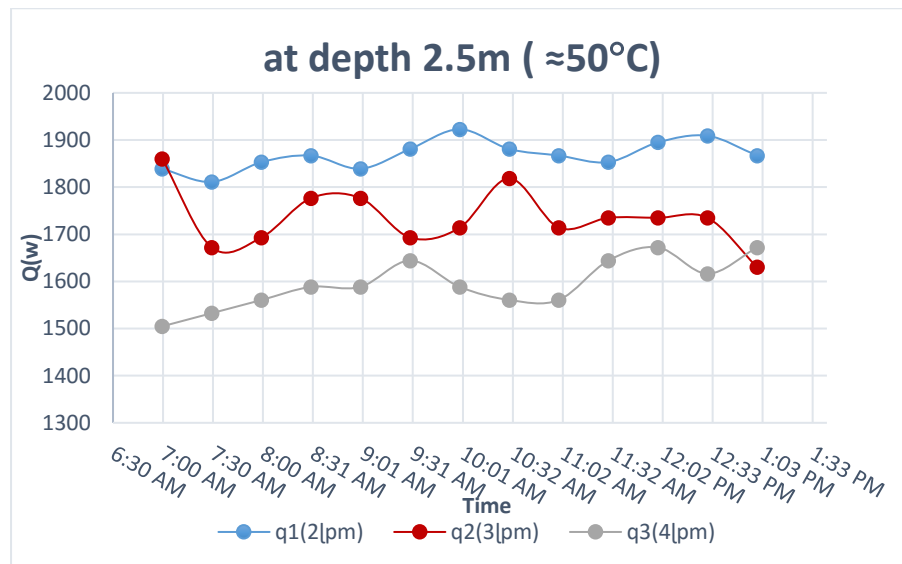
Figure 5.19: the relationship between heat transfer rate and time when inlet water temperature approximate 50°C and for the second-layer

In Figure 5.19, there are three heat transfer rate plots over time. When the entry temperature is approximate nearly 50 °C .The first plot is flow (2 l/min) where there is a slight disturbance to record the result of values (1868.1 W). While the flow (3l/min) from it with disturbance in the values to record the result of the values (1734.8 W), where the highest value is recorded at the beginning due to instability, while the value decreases after an hour (1:00)pm due to the decrease in the temperature difference. While it is observed when the flux is raised to (4l/min), the average of the values is (1594.9 W) with little turbulence. The cause of thermal accumulation reduces the value of the temperature difference of circulating water.

▪   **The effect of performance coefficient (COP) of GHE**

The following are three charts that show the relationship between the performance coefficient values of the second stratum with time according to the difference in temperature difference values between the incoming and outgoing water for each diagram, and with constant flow rates 2, 3, and 4 l/min.

Figure 5.20: COP values with time at inlet temperature approximate 30 ˚C and at three constant flow rates.

In figure 5.20, there are three diagrams for the performance parameter values, which differ at each constant value of the flow, and at the inlet water temperature approximately close to 30 ° C. Records different values for the charts at an hour (7:00)am due to the instability of the system. Record the sum of the values of (1.49) and (1.47) at flow (3l/min) and (4l/min) respectively. While the decreases slightly at flowrate (2l/min) to be recorded as a rate (1.25) due to the slow flow of water at this flow.

Figure 5.21 COP values with time at inlet temperature approximate 30 ˚C and at three constant flow rates.

In figure 5.21, there are three diagrams for the performance parameter values, which differ at each constant value of the flow, and at the inlet water temperature approximately close to 40 ° C. Note when flowing (2l/min) the highest average values recorded, which (4.2) . While it is noted when flowing (3l/min), a disturbance is recorded at an hour (9:00) am, to be recorded as the average values (2.7). When the flow (4l/min), the rate of the performance parameter (3) is recorded. It is noted that the values of the two diagrams are decreased at the runoff (3l/min) and (4l/min) due to the lower temperature difference of the incoming and outgoing water.
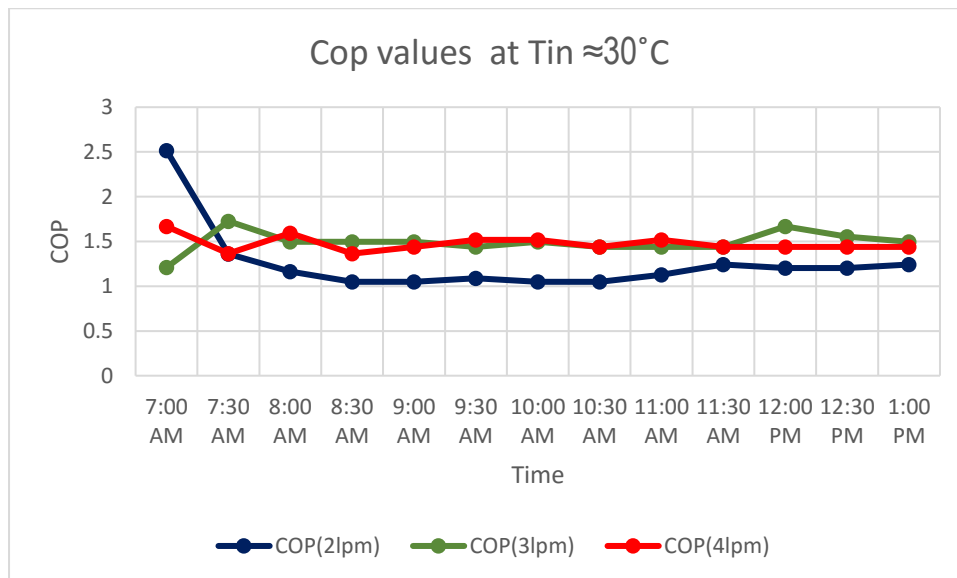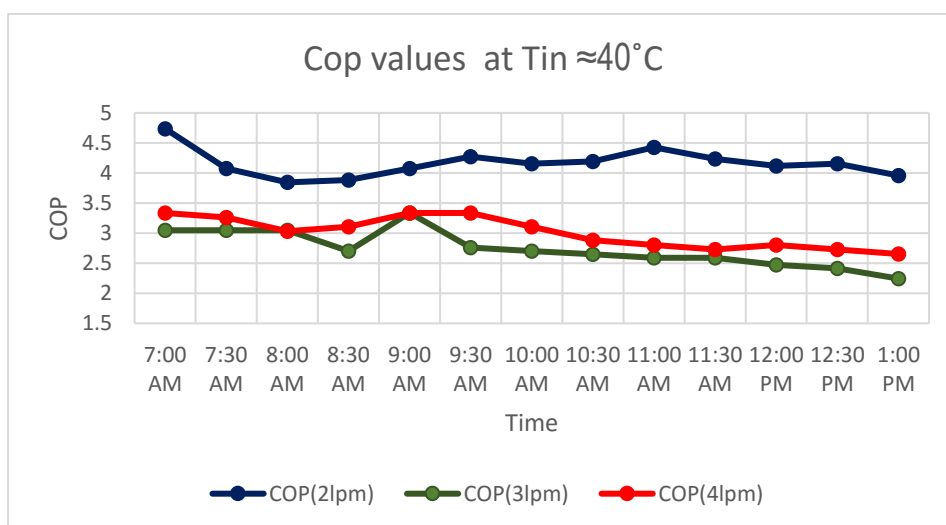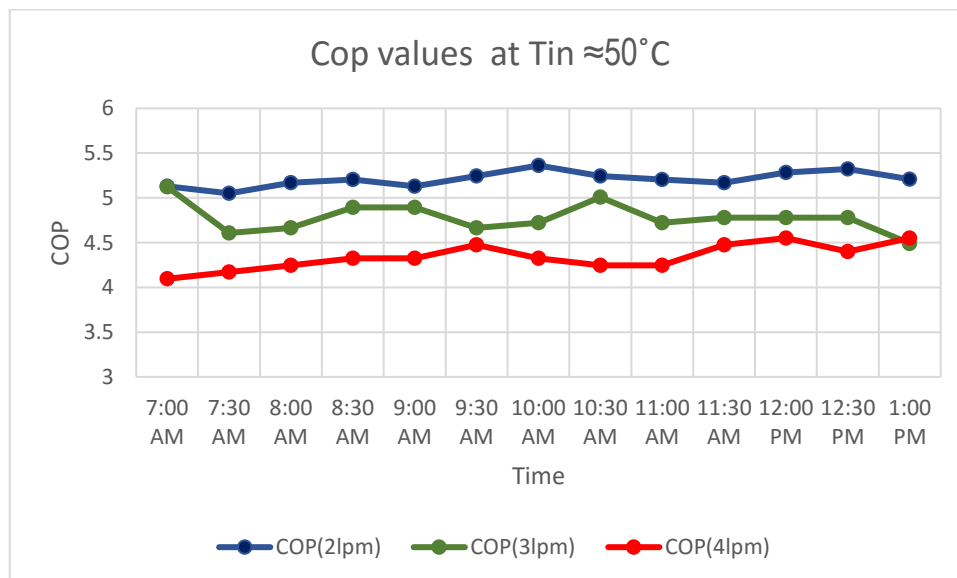

Figure 5.22 COP values with time at inlet temperature approximate 30 ˚C and at three constant flow rates.

In figure 5.22, there are three diagrams for the performance parameter values, which differ at each constant value of the flow, and at the inlet water temperature approximately close to 50 ° C. Record the highest values of the performance parameter at flow (2l/min) to be (5.2). Following the chart at flow comes (3l/min) to be (4.78). While the lowest values are recorded at flow (4l/min) to be the average values of performance coefficient (4.3). This is due to the increase in the rate of electricity consumption with the increase in flow.

5.3.3 Double-Layers GHE

The results of the two-layer test together for the ground heat exchanger at depth 2.5m and 3m.when length of pipes become 200m. When operating the system as two layers together, the increase in the length of the pipes allows more time for heat exchange, as the flow rate is less than it is in the single-layer separately, so the flow rates 3, 4, and 5 l/min were taken for testing according to the hypothesis of equations explained in the appendix.

- When we test the flow rate of 3 LPM (0.05 kg/s) we get the results as in the table below:

Table (5.7) Results of double-layers GHE at 3lpm flow

Date	10/7/2019	11/7/2019	14/7/2019
Time	**8:00 AM**	**10:00 AM**	**12:00 PM**
$T_{amb.}$	38.9	45.4	47.8
T_{soil}	37.3	42	44.3
T_{in}	34.3	44.1	53.1
T_{out}	29.7	33.6	36.6
ΔT	4.6	10.5	16.5
T_b	32	38.85	44.85
C_p	4178.127988	4178.461966	4179.631227
ρ	995.0097486	992.598689	990.189402

u	0.444539667	0.44561947	0.446703733
μ	758.132*E-6	650.496*E-6	577.521*E-6
Re	7001.226894	8159.702035	9190.751574
K w	618.6204*E-3	628.6493*E-3	636.70253*E-3
Pr	5.120382334	4.32367253	3.791136919
Nu	44.73607472	48.0643545	50.82056613
h$_{con.}$	2306.221025	2517.968713	2696.465218
R$_{con.}$	0.011507691	0.010539955	0.009842248
R$_{pipe}$	11.45 *E-3	11.45 *E-3	11.45 *E-3
R$_{soil}$	0.59556582	0.59556582	0.59556582
R$_{total}$	0.618525822	0.617558087	0.616860379
U	0.160902406	0.161154546	0.161336822
ΔP	0.557300754	0.536011618	0.520574292
Q	960.97	2193.69	3448.20
Power	363	363	363
COP	2.647298725	6.043230117	9.499161879

After operating the two layers together at the aforementioned flow, it is possible to reach a steady-state in a short time when the inlet water temperature is approximately close to 30 ° C. While it takes more time for the entry of water at a temperature close to 40 ° C. And it takes more time to reach stability due to the high temperature of the inlet water to about 50 ° C. When the inlet water temperature is between (30-55) ° C during the three days, the outgoing water temperature is between (29-37) ° C when climatic conditions are for the days in which the results are recorded and the aforementioned time. Where we notice the highest temperature difference (16.5)° C, which was obtained when the inlet water temperature was high due to the large difference between the temperature of the piping surface and the soil at the depths (2.5&3)m in addition to slow flow velocity which provides time for heat dissipation. After finding the set of results

and recording them in the above table, we notice that the highest value of the heat transfer rate is recorded (3448.2 W) due to the high-temperature difference. While the highest value of the performance coefficient of the double-layer system is recorded to be (9.49), due to the lack of current consumed (1.65 A) at the aforementioned flow, in addition to the value of the high heat transfer rate obtained, which is approximately (1 ton refrigeration).

- When we test the flow rate of 4 LPM (0.06667 kg/s) we get the results as in the table below:

Table (5.8) Results of double-layers GHE at 4lpm flow

Date	15/7/2019	16/7/2019	17/7/2019
Time	8:00 AM	10:00 AM	12:00 PM
$T_{amb.}$	41	47	48.9
T_{soil}	38.5	43.9	45.8
T_{in}	33.3	45.2	50.5
T_{out}	30.3	35.3	38.5
ΔT	3	7.9	12
T_b	31.8	40.25	44.5
Cp	4178.139406	4178.674038	4179.545828
ρ	995.0742502	992.06013	990.3370166
u	0.592681135	0.594481845	0.595516199
μ	761.711*E-6	631.824*E-6	581.295*E-6
Re	9291.107088	11201.12203	12174.79101
K w	618.314*E-3	630.589*E-3	636.2515*E-3
Pr	5.147116609	4.186856506	3.818533374
Nu	56.1889622	61.33430972	63.77728469
$h_{con.}$	2895.20324	3223.064254	3381.532792

R_{con.}	0.009166637	0.008234176	0.007848298
R_{pipe}	11.45*E-3	11.45*E-3	11.45*E-3
R_{soil}	0.59556582	0.59556582	0.59556582
R_{total}	0.616184769	0.615252308	0.61486643
U	0.161513718	0.161758504	0.161860021
ΔP	0.918285286	0.87719571	0.860091339
Q	835.63	2757.92	3343.64
Power	367.4	367.4	367.4
COP	2.274436258	7.506600068	9.100807465

After operating the two layers together at the aforementioned flow, it is possible to reach a steady-state in a short time when the inlet water temperature is approximately close to 30 ° C. While it takes more time for the entry of water at a temperature close to 40 ° C. And it takes more time to reach stability due to the high temperature of the inlet water to about 50 ° C. When the inlet water temperature is between (30-51) ° C during the three days, the outgoing water temperature is between (30-40) ° C when climatic conditions are for the days in which the results are recorded and the aforementioned time. Where we notice the highest temperature difference (12)° C, which was obtained when the inlet water temperature was high due to the large difference between the temperature of the piping surface and the soil at the depths (2.5&3)m in addition to flow velocity which provides time for heat dissipation. After finding the set of results and recording them in the above table, we notice that the highest value of the heat transfer rate is recorded (3343.6 W) due to the high-temperature difference. While the highest value of the performance coefficient of the double-layer system is recorded to be (9.1), due to the current consumed (1.67 A) at the aforementioned flow, in addition to the value of the high heat transfer rate obtained.

- When we test the flow rate of 5 LPM (0.08333 kg/s) we get the results as in the table below:

Table (5.9) Results of double-layers GHE at 5lpm flow

Date	18/7/2019	21/7/2019	22/7/2019
Time	**8:00 AM**	**10:00 AM**	**12:00 PM**
$T_{amb.}$	44	47	49.4
T_{soil}	43.2	46.6	47.1
T_{in}	36.7	45.8	51.5
T_{out}	35.6	39.1	41
ΔT	1.1	6.7	10.5
$T_{b.}$	36.15	42.45	46.25
C_p	4178.17798	4179.0855	4179.991438
ρ	993.5945923	991.1843838	989.5905418
u	0.741954693	0.743758863	0.744956767
μ	689.578*E-6	604.553*E-6	562.981*E-6
Re	12828.75143	14632.99487	15713.5302
$K w$	624.803*E-3	633.563*E-3	638.483*E-3
Pr	4.611344309	3.987731892	3.685699345
Nu	70.37584355	74.85351479	77.39320276
$h_{con.}$	3664.250988	3952.035958	4117.855916
$R_{con.}$	0.007242757	0.006715343	0.006444926
R_{pipe}	11.45 *E-3	11.45 *E-3	11.45 *E-3
R_{soil}	0.59556582	0.59556582	0.59556582
R_{total}	0.614260888	0.613733475	0.613463058
U	0.162019583	0.162158815	0.162230295
ΔP	1.321725335	1.28164211	1.261080322
Q	383.00	1643.49	1783.54
Power	371.8	2333.32	3657.49
COP	1.030122776	6.275747008	9.837257956

After operating the two layers together at the aforementioned flow, it is possible to reach a steady-state in a short time when the inlet water temperature is approximately close to 30 ° C. While it takes more time for the entry of water at a temperature close to 40 ° C. And it takes more time to reach stability due to the high temperature of the inlet water to about 50 ° C. When the inlet water temperature is between (35-52) ° C during the three days, the outgoing water temperature is between (35-42) ° C when climatic conditions are for the days in which the results are recorded and the aforementioned time. Where we notice the highest temperature difference (10.5)° C, which was obtained when the inlet water temperature was high due to the large difference between the temperature of the piping surface and the soil at the depths (2.5&3)m. After finding the set of results and recording them in the above table, we notice that the highest value of the heat transfer rate is recorded (3657.49 W) which is approximately (1 ton refrigeration).due to the temperature difference and high value of flow rate. While the highest value of the performance coefficient of the double-layer system is recorded to be (9.8), due to the current consumed (1.69 A) at the aforementioned flow, in addition to the value of the high heat transfer rate obtained.

To more clearly demonstrate the changing effects on results with Figures, for every half hour within six hours of the day ,we can divide them into:

- **The effect of temperature change at entry**

Here are three Figures in each graph showing the difference between the entry and exit temperature of the heat exchanger when the input temperature changes to several values that are close to 30, 40 and 50°C and when stabilizing the water flow values to different values.

Figure 5.23: the relationship between temperature difference and time when flowrate
$3 \, \ell/min$ and for the double-layers

In the above Figure 5.23 when the flow is constant at 3l/min, Note that the rate of change in temperature 4.1, 11.22, and 15.9 °C for the inlet water temperature values approximate approaching 30, 40, and 50°C respectively, at steady flow (3l/min). Due to slow flow rate and availability of exchange time in addition to the large difference between the inlet water temperature and the initial soil temperature at depths (3&2.5) meters

Figure 5.24: the relationship between temperature difference and time when flowrate

$4 \ \ell/min$ and for the double-layers

In the Figure 5.24 when the flow is constant at 4 l/min, notice that the temperature change is in three patterns. The first is when the rate of the temperature of entering the water is close to 30 ˚C, where the rate of change is (3.29)˚C, and the second is when the rate of the temperature of the inlet water is close to For 40 ˚C where the rate of change is recorded by (8.32)˚C. The highest values of the outcome of the temperature difference (11.2) ˚C are recorded when the inlet water is at a temperature close to 50 ˚C, due to the large difference between the temperature of the surface of the pipe and the initial degree of the soil at 2.5&3m depths and due to the speed of the flow, where the heat dissipation the water inside the pipes.
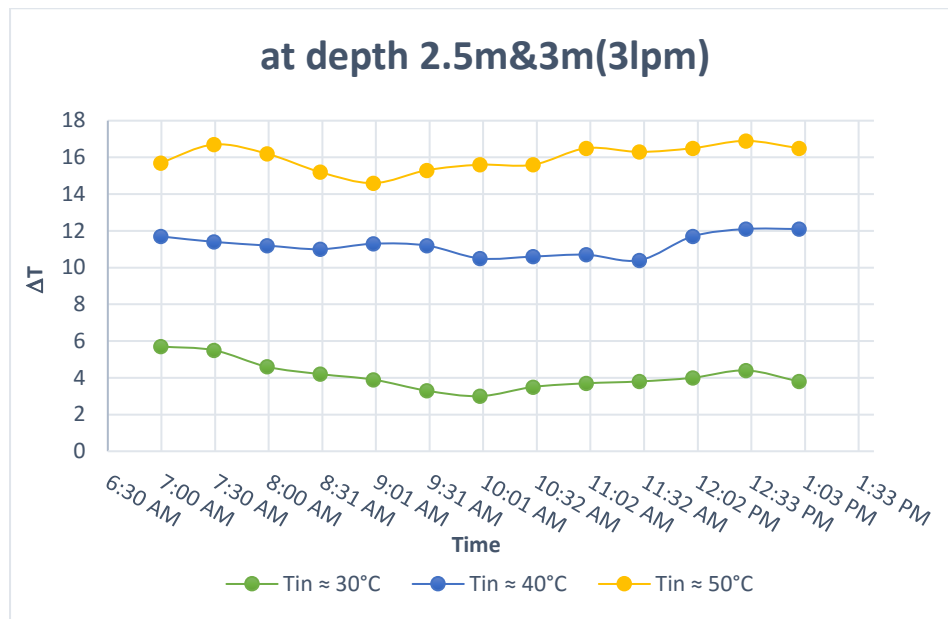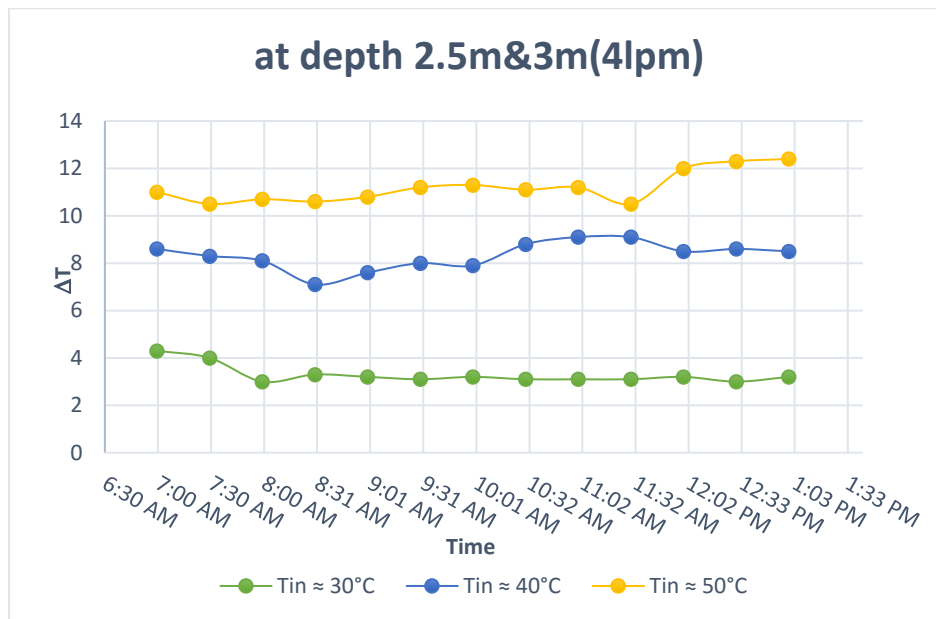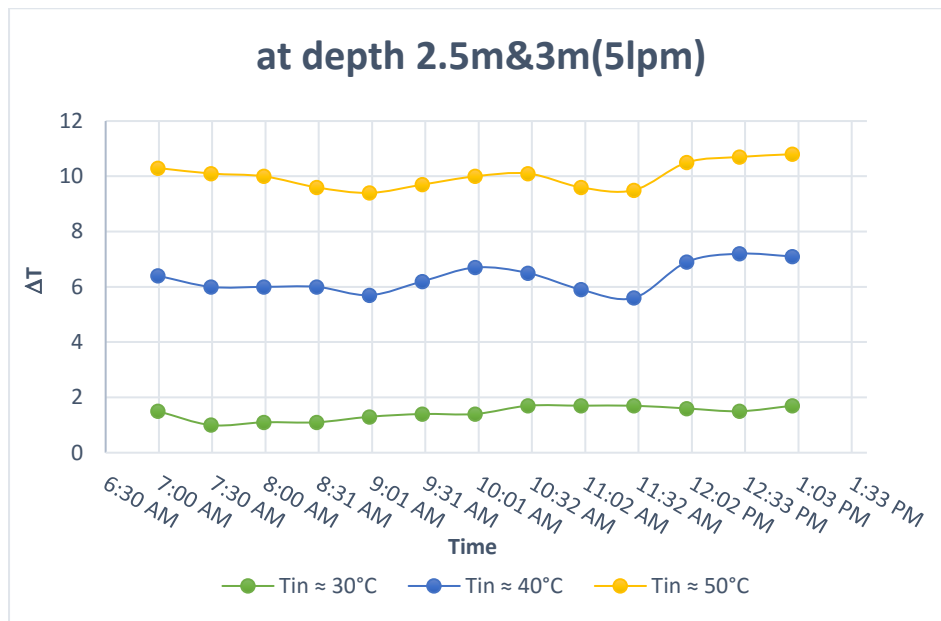
Figure 5.25: the relationship between temperature difference and time when flowrate

5 ℓ/min and for the double-layers

In the Figure 5.25, Notice that the rate of change in temperature from high to low 1.4, 6.3 and 10 °C for the approximate inlet water temperature values approaches 30, 40 and 50, respectively, at steady flow (5l/min). Because of the speed of flow at the rate of flow and the lack of time for heat exchange in addition to the large difference between the temperature of the inlet water and the initial soil temperature at depths of (2.5&3) meters for high temperatures. After the piping system reached to stay-state.

- **Flux effect**

The following are chars that show the effect of changing the flow of water inside the pipes at a temperature relatively of the water entering, through the amount of heat transfer rate to the soil (in watt unit).

Where; q1, q2, q3 are heat transfer rate at temperature of the water entering is approximate close to ≈30, 40 and 50˚C respectively.

Figure 5.26: the relationship between heat transfer rate and time when inlet water temperature approximate 30°C and for the double-layers

In Figure 5.26 shows charts at an entry temperature close to 30 ° C. The first plot is at flow (3l/min), where it descends from the highest values at the hour (7:00am) to the lowest value at the hour (10:00)am, after which it begins to rise .the average become (854.9 W). This disturbance in the plot is due to dividing the flow into two networks, and The high difference temperature of the soil at the depths is compared with the temperature of the inlet water. As for the scheme at the flow (4l/min), the beginning of the scheme is with turbulent values due to the lack of stability until the hour (8:30) am to record (910.6 W). While the scheme at the flow (5l/min) is graduated from a few values at the beginning, it was started by stabilizing to record the result (487.5 W) due to the high flow, which does not provide sufficient time for heat dissipation.
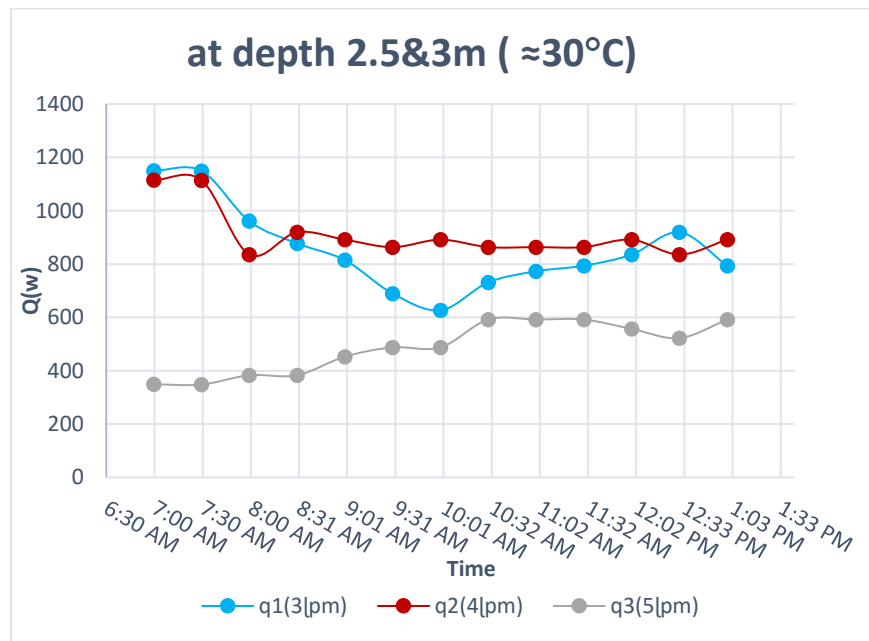
Figure 5.27:the relationship between heat transfer rate and time when inlet water temperature approximate 40°C and for the double-layers

In the Figure 5.27, shows the graphs at an entry temperature approaching 40 ° C. The overall values in the charts are turbulent. The highest sum of the values of the heat transfer at flow(4l/min) is recorded (2869.5 W) due to the dependence of the values on the amount of flow and the temperature difference between the incoming and outgoing water, while the average values of (2340 W) at the flow (3l/min). A disturbance of the values is observed at the flow chart (5l/min), and they rise at the clock (10:00 am), to record as a result the values of (2191.4 W). It is noticed that the values be rise at the two planners at the flowrates (3l/min) and (5l/min) after the hour (12:00 am), due to the availability of more time for heat dissipation with the higher temperature of entering the water to give a greater temperature difference.
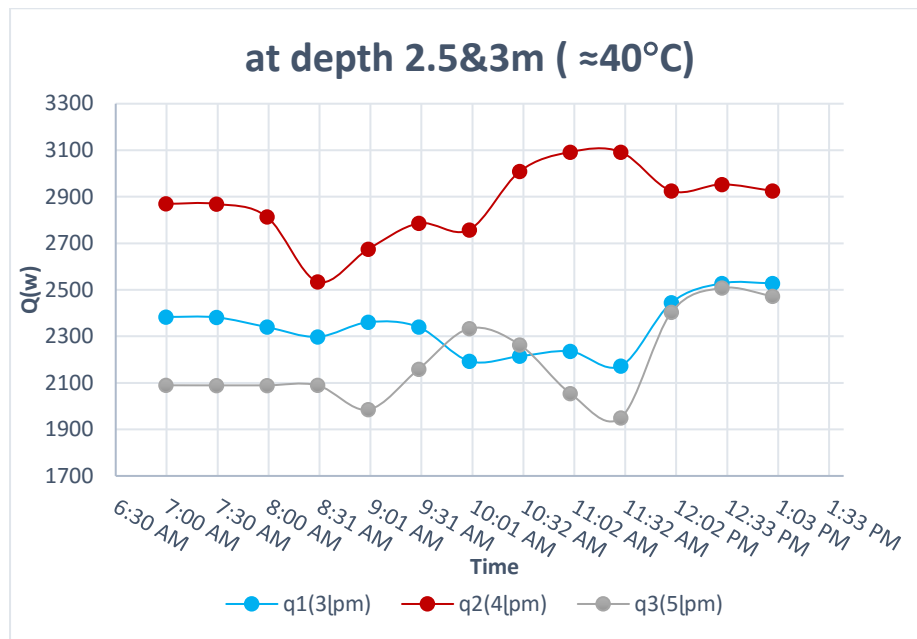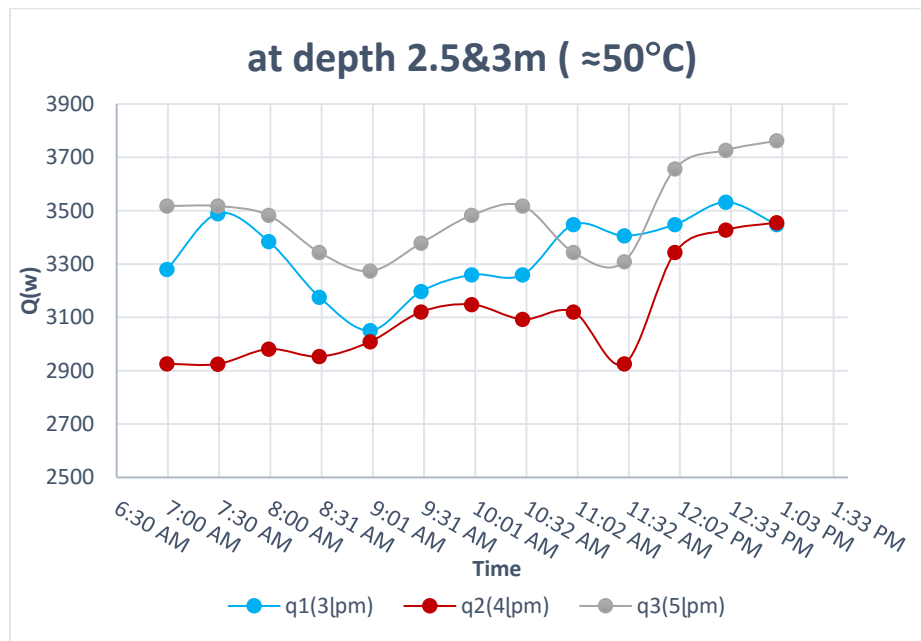
Figure 5.28 the relationship between heat transfer rate and time when inlet water temperature approximate 50°C and for the double-layers

In the Figure 5.28, when the inlet water temperature rises to about 50 °C or slightly higher or slightly lower. shows charts at each flow and notes the highest rate of heat transfer values that are (3485.7W) at flow (5l/min) due to the direct mathematical proportion between the amount of flow and the heat transferred, with the observation of turbulence and the rise of the values after The time (11:30) am, due to the increase in the temperature of the circulating water. While the diagram at constant flow (3l/min) records the average values of (3337.1 W) due to the slow flow velocity which saves time for heat dissipation. Whereas the scheme records when the flow (4l/min) average values of (3109.9 W) gradually increase due to the increase in the temperature difference with the increase in the temperature of the circulating water inside the two layers.

- **The effect of performance coefficient (COP)of GHE:**

The following are three charts that show the relationship between the performance coefficient values of the two stratum with time according to the difference in temperature difference values between the incoming and outgoing water for each diagram, and with constant flow rates 2, 3, and 4 l/min.

Figure 5.29 COP values with time at inlet temperature approximate 30 ˚C and at three constant flow rates.

In Figure 5.29, three plots of the performance parameter values are shown in two layers with time . in which the plot at flow (4l/min) records the highest result of the values reaching (2.48), followed by the scheme at flow (3l/min), where the average values of (2.36) are recorded. It is also noticed that the previous two charts start with high values due to instability, after which the values converge, while the lowest values of the performance coefficient of the system are recorded at the flow (5l/min) the amount of (1.3), due to the high flow, which increases the electricity consumption compared with the temperature difference of the circulating water inside the system.

Figure 5.30 COP values with time at inlet temperature approximate 40 ˚C and at three constant flow rates.

In Figure 5.30, three charts of the performance of coefficient values are shown in two layers with time at water entered temperature approximate close to 40˚C. in which the chart at flow (4l/min) records the highest result of the values reaching (7.8), followed by the scheme at flow (3l/min), where the average values of (6.4) are recorded. While the lowest values of the performance coefficient of the system are recorded at the flow (5l/min) to be (5.9), due to the high flow, which increases the electricity consumption compared with the temperature difference of the circulating water inside the system. With noticing the disturbance in charts due to divided water flow inside two layers of pipes.
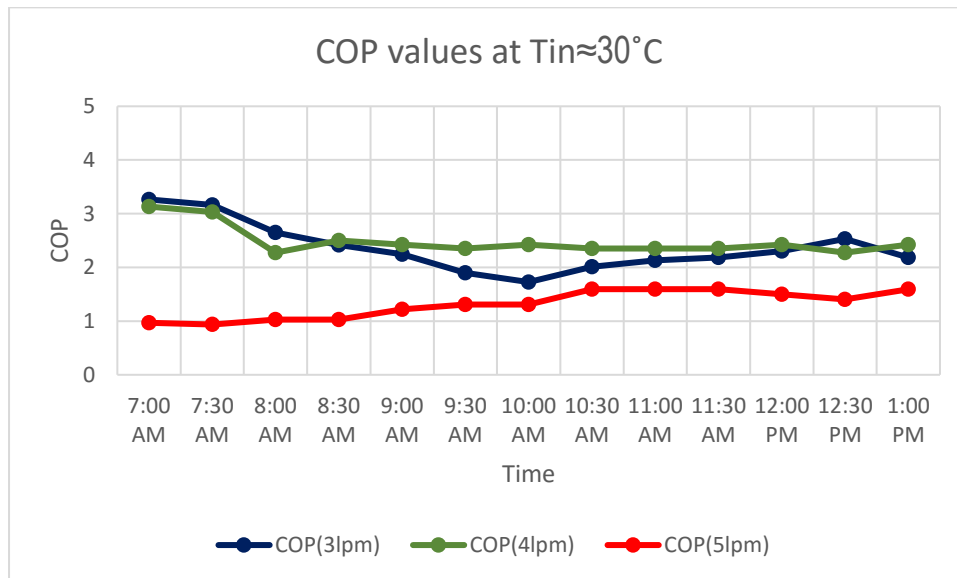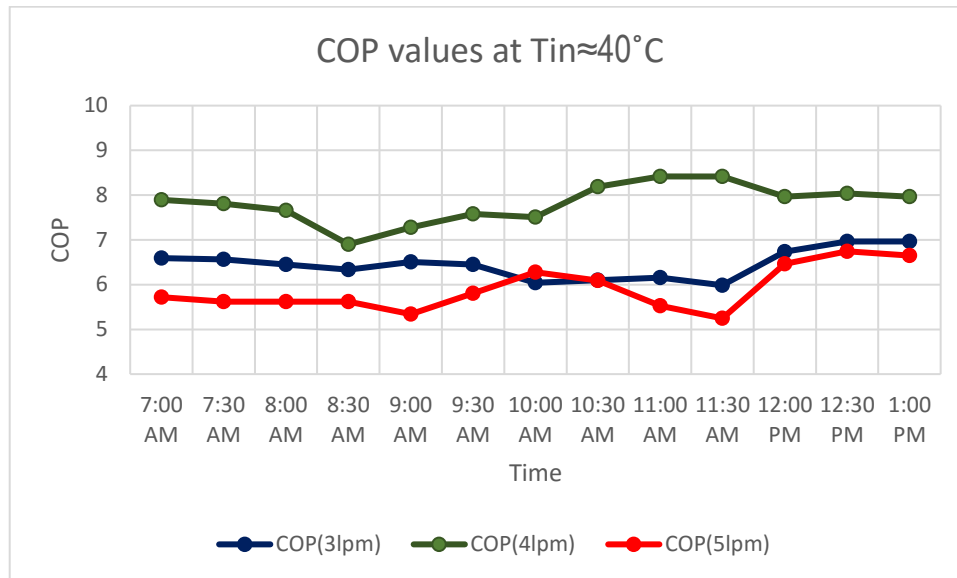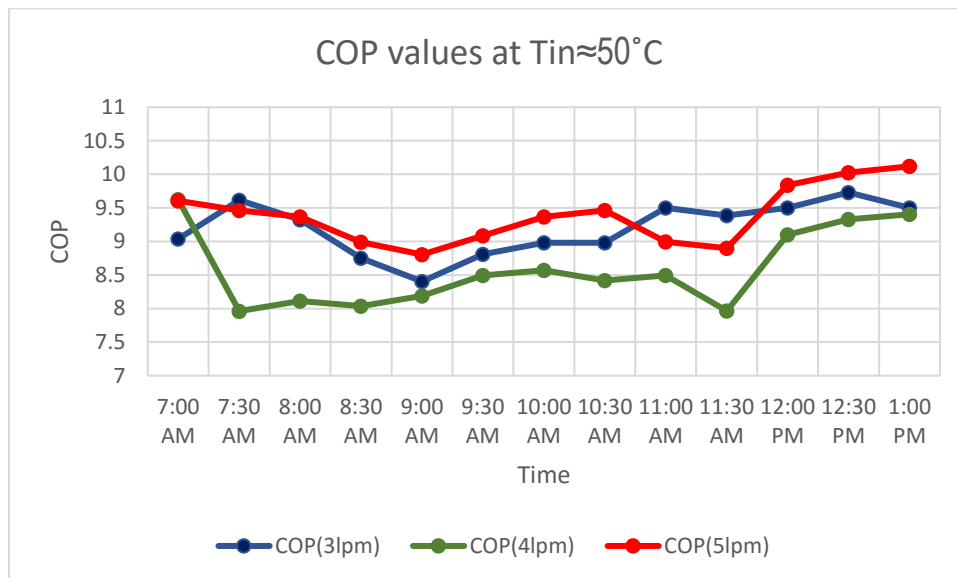
Figure 5.31 COP values with time at inlet temperature approximate 50 ˚C and at three constant flow rates.

In Figure 5.31, three charts of the performance of coefficient values are shown in two layers with time. When the temperature of water entered is close to 50˚C. A slight slope of the values until the hour (9:00) am is observed in the chart when flowing (5l/min), after which the values are disturbed, and then the chart begins to rise to register as a rate (9.4), while the values are disturbed up and down in the chart when the flow (3l/min) is recorded as the average (9.1). While the lowest values of the rate are (8.6) where the flow (4l/min). It is noticed that the performance coefficient is high after the hour (12:00 pm) due to the high temperature and the accompanying rise in the difference between the temperature of entering and exiting the water inside the system.

5.4 A comparison between the results of the layers of the pipes of GHEs

To compare the results of the two layers of pipes separately with the results of the two layers of pipes together, their results were taken at two joint flow rate between them where the water was entered with the flow of 2 l/min for each layer separately and be 4 l/min as a total flow rate for both layers as well, with a change in the temperature of the water entering at each flow For approximately 30,40 and 50 ˚C.

The difference can be seen in the values of each heat transfer rate (Q) for every layer and for two-layers.

Where; the first-layer GHE can be represented by the number 1

Second-layer GHE can be represented by the number 2

The double-layers GHE can be represented by the number 3

Figure 5.32: a comparison of the heat transfer rate with time for each layer separately and for double- layers at inlet temperature approximate 30°C.

The Figure 5.32 shows the values of the heat transfer rate when the temperature of entering water approximately 30°C degrees, in the two-layer chart, the value of heat transfer rate at the beginning be high and stoop upon hour (8:00 am)to record highest the average value (910.7W) compared with each separate

layer . While the first and second layer recording the convergent average values (482.9 W) and (432.1 W) respectively, at same conditions, due high flowrate and effect on the rate of the heat transfer value
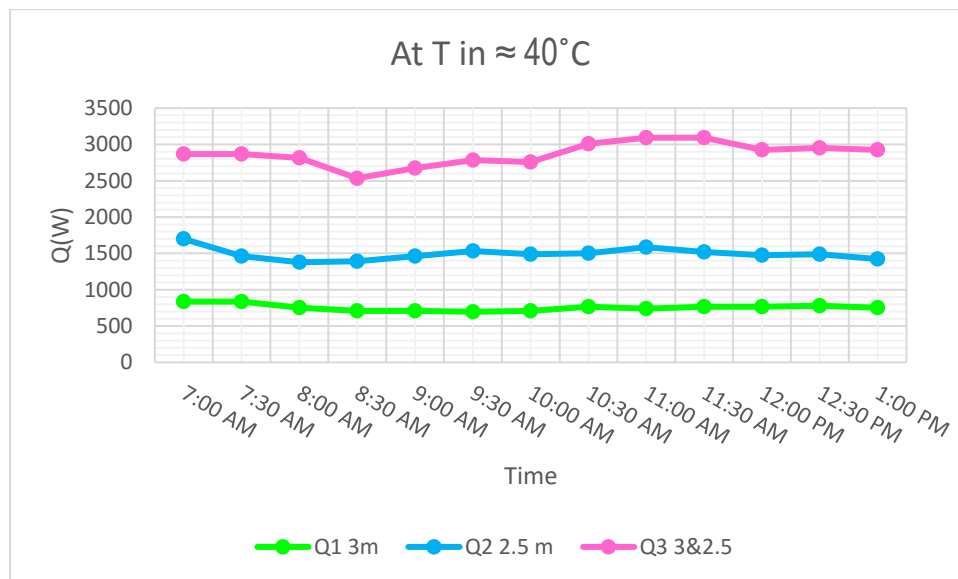
Figure 5.33: a comparison of the heat transfer rate with time for each layer separately and for double- layers at inlet temperature approximate 40°C.

The Figure 5.33 shows the values of the heat transfer rate when the temperature of entering water approximately 40°C degrees, Where the two layers recorded together with the highest value, reaching an average of (2869.47 W), after which the second layer recorded a rate of (1493.4 W) due to the moisture of the soil at the depth (2.5m) in the test day, then the first layer recorded a rate of heat transfer of (755.39 W).
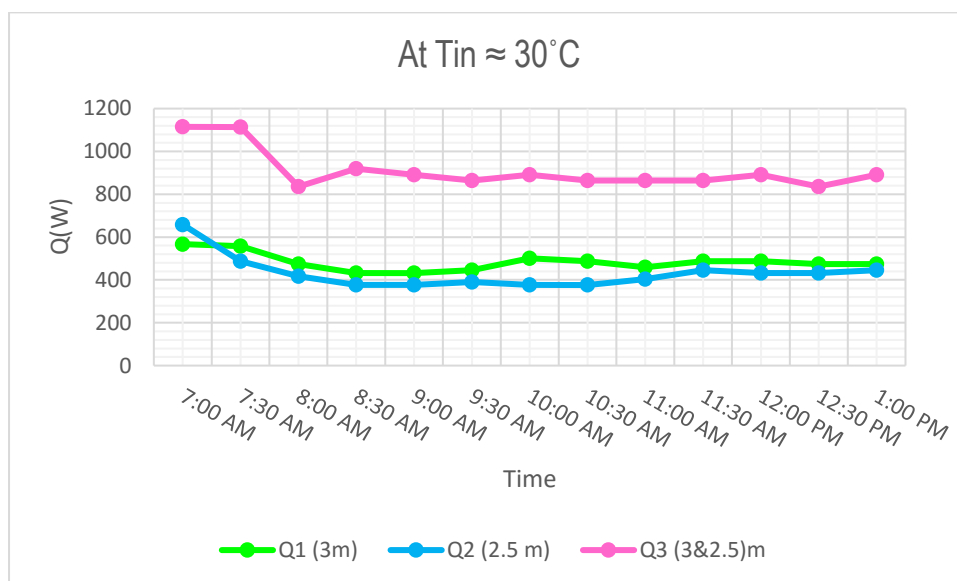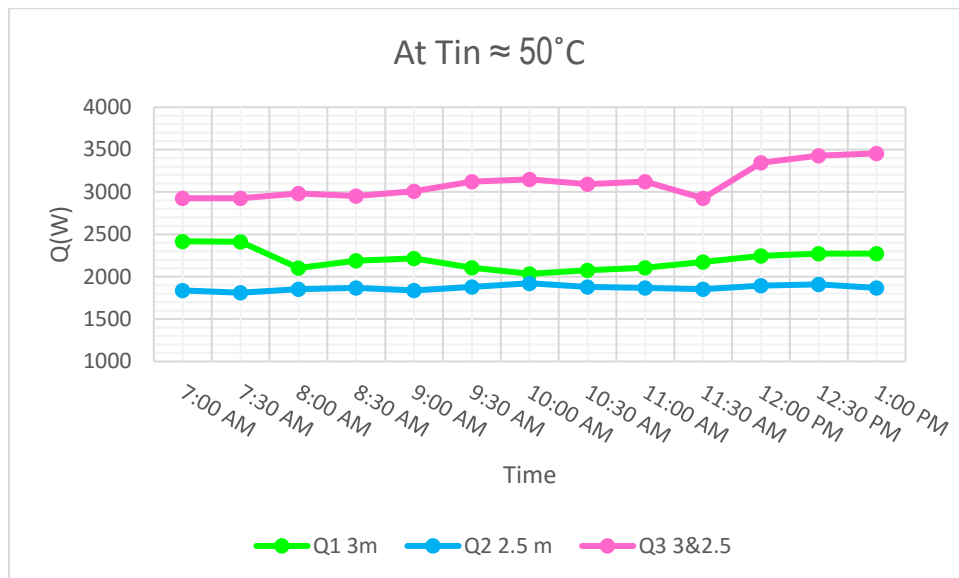
Figure 5.34 a comparison of the heat transfer rate with time for each layer separately and for double- layers at inlet temperature approximate 50°C.

The Figure 5.34 shows the values of the heat transfer rate when the incoming water temperature of approximately 50°C, Where the two layers were recorded together with the highest value reaching the average (3109.9 W), while the heat transfer rate values were (2201.3 W) and (1868.1W) for the first and second mesh, respectively. Due to the high flow rate of the two layers together, which increases the value of the dissipated heat rate from water inside pipes to soil.

The comparison can also be noticed when testing the same values of flow and temperature of the incoming water for the two layers together and then for each layer separately through the performance of the coefficient of the pipes layer, as in the following diagrams:
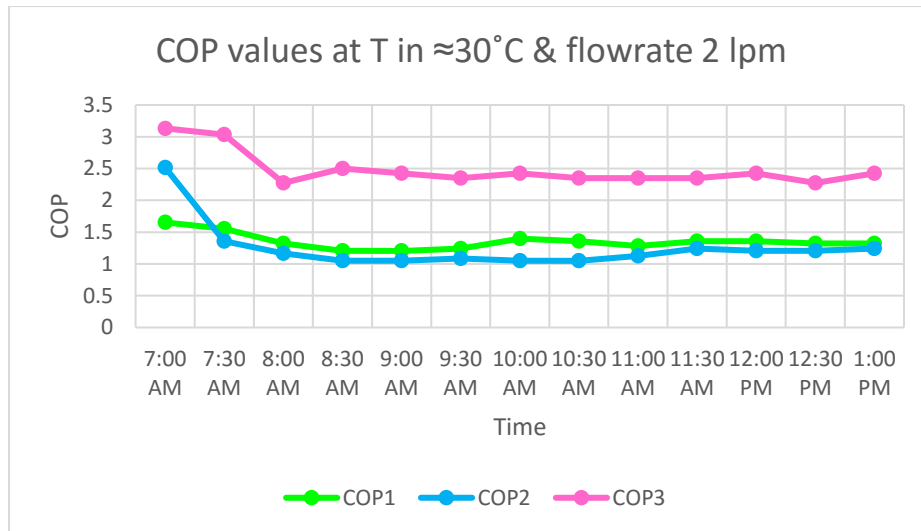
Figure 5.35comparison COP values with time at inlet temperature approximate 30 ˚C for each layer separate and with double-layers.

The Figure 5.35 shows an illustration of three charts of the performance coefficient values the highest COP values at the lowest in the case of double layers and at each layer separately during a specified time when the inlet water temperature is approximately 30 ° C. Where the average values of the performance coefficient values of the two layers together have the highest values reaching (2.48) due to the increase in the amount of circulating water and the increase in the length of the pipes, which allows for better heat dissipation compared to the separate layers. Where the first and second grid recorded rates (1.35) and (1.26) respectively. A disturbance in the values is observed at the beginning of the charts due to time of the steady-state.
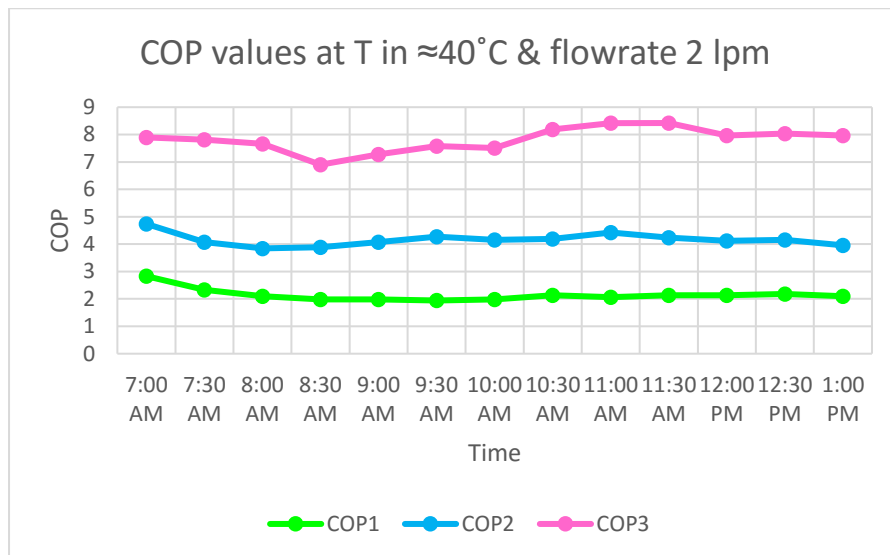
Figure 5.36: comparison COP values with time at inlet temperature approximate 40 ˚C for each layer separate and with double-layers.
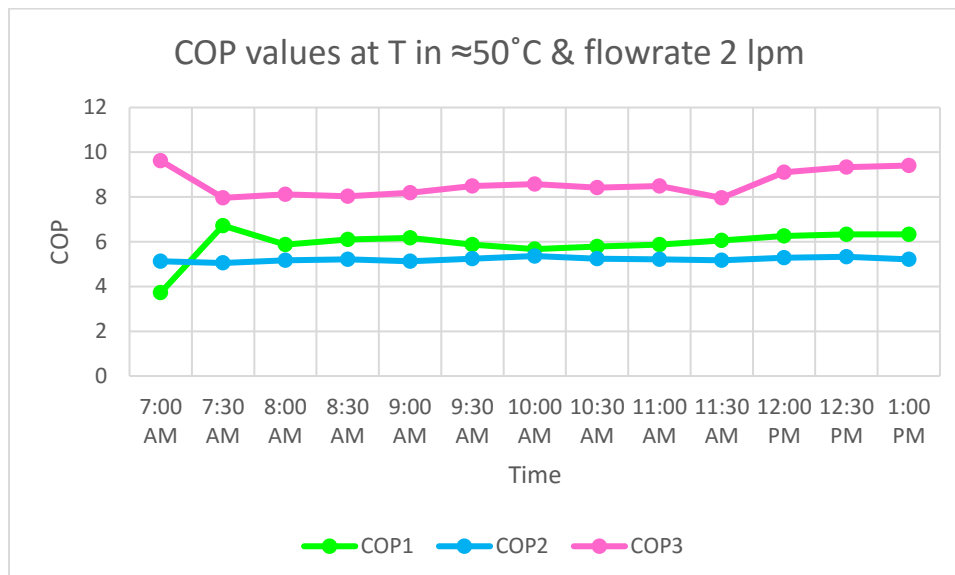
Figure 5.37comparison COP values with time at inlet temperature approximate 50 ˚C for each layer separate and with double-layers.

In Figure 5.36 an illustration of three charts of the performance coefficient values in the case of double layers and at each layer separately during a specified time when the inlet water temperature is approximately 40 ° C. Where the average values of the performance coefficient values of the two layers together have the highest values reaching (7.82) due to the increase in the amount of circulating water and the increase in the length of the pipes, which allows for better heat

dissipation compared to the separate layers. Where the first and second grid recorded rates (2.14) and (4.16) respectively. Due to the moisture of the soil at the depth (2.5m) in the test day.

While the Figure 5.37 shows the three diagrams, where a disturbance and difference in the initial values is observed due to the time of the system to reach a stable state. Where the highest values of the average performance coefficient are recorded at both layers (8.59). While the values of the first and second layers are close to each other due to the convergence of temperature at these depths, to record (5.9) and (5.2) as the average values of their performance coefficient respectively. Because of the increase in the flow rate of the two layers together compared with the separate layers.

CHAPTER SIX

CONCLUSIONS AND RECOMMENDATIONS

6.1 Conclusions

Conclude from the results recorded in the previous chapter the following:

1) With regard to thermal sensors for soils with the aforementioned characteristics in the previous chapter, and for the different depths that gradient at every half meter from the surface of the earth, down to a depth of 3.5 meters. Notice the large effect with a temperature of atmosphere and weather conditions, to the surface soil temperature, and it was observed with and this effect gradually decreases with increasing depth. The average annual temperature was for two depths (2.5 m) and (3 m) are (22.2˚C) and (22.1˚C) respectively.

2) The relative stability of the temperature at specific depths during the seasons of the year and its stability during the hour of day at a certain temperature with a noticeable change in the ambient temperature.

3) It describes the performance of GHE in a two-layer case better than piping system due to the increase in the length of the tube and the division of the flow rate within the two clusters to achieve a slow speed in the flow of water circulating inside the closed system, which saves time for better dissipating the water temperature through the soil.

4) The higher the temperature of the water entering the system, the higher the temperature difference between entering and exiting the circulating water inside the pipes. This is to increase the difference between the temperature of the surface of the tube and the temperature of the soil at the specified depths (which is characterized by the relative stability of the temperature with different weather conditions).

5) The lower the water flow rate inside the pipes decreased the velocity of the water. which leads the higher the difference in temperature of the circulating water due to the availability of time for heat exchange between the tube surface and the soil, and vice versa.

6) When testing the first piping layer that is located at a depth of (3m), the highest rate of heat transfer (2410.58W) is recorded at the temperature difference (17.3) ˚C and by constant flow (2 l/min). This was in the hour (7:30) am of the date (30/6/2019). While the second layer, which is located at a depth of (2.5 m) when tested separately, recorded the highest heat transfer rate (1922.7W) at the temperature difference (13.8) ˚C and constant flow (2 l/min). This was in the hour (10:00) pm of the date (16/6/2019). Whereas the rate of heat transfer is approximately one refrigeration ton when the two layers are tested together to record (3531.89W) at the temperature difference (16.9) ˚C and with the constant flow (3 l/min) in the hour (12:30) pm from the date (14/7/2019).Because of the direct proportionality of the heat transfer rate with both the temperature difference of the circulating water and the amount of flow.

7) he highest performance coefficient values (COP) for the first layer, second layer, and two-layers heat exchanger are 5.9,5.2 and 8.58 respectively, at the same conditions. According to the rate of increased flow, which leads to a little increase in electricity consumption, to the values of the heat transfer rate recorded that affect directly on performance coefficient values.

6.2 Recommendations for future works

1.   A large difference can be obtained for transferring heat when misleading the area or plant planting, where increasing the moisture increases the thermal conductivity of the soil.

2.   Heat transfer can be increasing in the soil around the tubes by mixing them with components that improve the heat transfer properties of the surrounding soil.

3.   The circulating water inside the pipes can be replaced with another fluid and compare the performance of the underground exchanger. (fluid with a freezing factor above zero)

4.   The two-layer heat exchanger can be operated alternately to avoid thermal accumulation in the soil around the tubes which occurs over time.

5.   It is possible to make the underground heat exchanger as open system and compare the performance of the exchanger.

6.   The heat exchanger can be tested in the case of drawing heat from the soil to warm the fluid circulating inside the pipes and test its performance in the winter season.

7.   In addition to the proposal to design a heat pump to take advantage of the transfer of heat to and from the soil to use the system to cool and heat rooms.

8.   The system can be tested by introducing water at high temperatures above 50° C and with flow values less than 2 l/min to achieve a greater difference in temperature degrees, which increases the rate of heat transfer to the system.

References

References

[1] .Banerjee, R. (2015). Importance of Energy Conservation. International Journal of Innovatice Research in Advanced Engineering, 2(4), 186–190.

[2]. https://www.bbc.com/timelines/zqgxtfr

[3]. https://quranenc.com/ar/browse/english_saheeh/16

[4]. Santamouris M., Mihalakaha G., Balaras C.A., Argirioua A.D. and Vallinaras M., Use of buried pipes for energy conservation in cooling of agricultural greenhouse, Solar Energy, 35, 111 .(1995)

[5]. Zhu, J., Hu, K., Lu, X., Huang, X., Liu, K., & Wu, X. (2015). A review of geothermal energy resources, development, and applications in China: Current status and prospects. Energy, 93(December), 466–483. https://doi.org/10.1016/j.energy.2015.08.098

[6].Doeff, M. M. (2012). Encyclopedia of Sustainability Science and Technology - Battery Cathode Materials, (January 2012). https://doi.org/10.1007/978-1-4419-0851-3

[7]. Miller, C. C. (2006). Chapter two. Forbes (Vol. 178).

[8]. Florides, G., & Kalogirou, S. (2007). Ground heat exchangers-A review of systems, models and applications. Renewable Energy, 32. https://doi.org/10.1016/j.renene.2006.12.014

[9].Alghannam, A. (2012). "Investigations of performance of earth tube heat exchanger of sandy soil in hot arid climate." Journal of Applied Sciences Research(June): 3044-3052".

[10].Yusof, T., et al. (2015). "A review of ground heat exchangers for cooling application in the Malaysian climate." Journal of Mechanical Engineering and Sciences: 1426-1439.

[11] Muntadher M. Ali, Dhafer Manea Hachim, Hassanain Hammed, "Numerical Investigation for Single Slope Solar Still Performance with Optimal Amount of Nano-PCM", Journal of Advanced Research in Fluid Mechanics and Thermal Sciences Vol. 63, Issue 2, pp. 302-316, 2019.

References

[12] Hiba Q.Mohammed, Ali Sh. Baqir, Hasan S.Khwayyir, " Effects of Air Bubble Injection on the Efficiency of a Flat Plate Solar Collector: An Experimental Study for the Open Flow System" Journal of Engineering and Applied Sciences, Vol. 15 No. 7, pp. 1703-1708

[13] Hasan S.Khwayyir, Ali Sh. Baqir, Hiba Q.Mohammed, "Effect of Air Bubble Injection on the Thermal Performance of a Flat Plate Solar Collector", Thermal Science and Engineering progress, https://doi.org/10.1016/j.tsep.2019.100476.

[14] Hassanain Hammed, Hayder Aziz Neema, "Experimental Study for Productivity Enhancement of a Parabolic Solar Concentrator System", AlQadisiya Journal for Engineering sciences, Vol. 4, No. 2, pp 37-41, 2011.

[15] Hassanain Hammed, Ahmed H. Ali, Zaid M. Al-Dulaimi, "EXPERIMENTAL INVESTIGATION OF THE ENHANCEMENT PARAMETERS ON THE PERFORMANCE OF SINGLE-SLOPE SOLAR STILL", nternational Journal of Latest Trends in Engineering and Technology Vol.(10)Issue(3), pp.139-145

[16] Dhafer Manea. H. Al-Shamkhi, "Experimental Study of the Performance of Low Cost Solar Water Heater in Najaf City", International Journal of Mechanical & Mechatronics Engineering IJMME-IJENS, Vol. 16, Issue 1, pp. 109-121, 2018.

[17] Ali Sh. Baqir, Hameed B. mahood, "Optimisation and evaluation of NTU and effectiveness of a helical coil tube heat exchanger with air injection", Thermal Science and Engineering Progress Volume 14, December 2019

[18] Nawfel M. Baqer, Ali Shakir Baqir, "Numerical Investigation for Enhancement of Heat Transfer in Internally Finned Tubes Using ANSYSCFX Program, "

[19] Ali Majeed Abed AL –Kreem, Ahmad Hashim Yousif, Ali Shakir Baqir, "Study the effect of twisted tapes on thermal performance solar collector with using curvature vortex generators," Technology of Kansai University, Volume 62, Issue 07, PP. 3631-3643,2020.

References

[20] Basil N. Merzha, Majid H. Majeed, Fouad A. Saleh, Experimental study of flat plate solar collector performance with twisted heat pipe, IOP Conference Series: Materials Science and Engineering 518 (3), 032035 (2019)

[21] Basil N. Merzha, Majid H. Majeed, and Fouad A. Saleh, Numerical study of flat plate solar collector performance with square shape wicked evaporator, Al-Qadisiyah Journal for Engineering Sciences 12 (2), 90-97. (2019)

[22]. Kharseh, M. and L. Altorkmany (2012). "How global warming and building envelope will change buildings energy use in central Europe." Applied energy 97: 999-1004.

[23]. Kharseh, M., et al. (2015). "Analysis of the effect of global climate change on ground source heat pump systems in different climate categories." Renewable Energy 78: 219-225.

[24]. Sivasakthivel, T., et al. (2015). "Study of technical, economical and environmental viability of ground source heat pump system for Himalayan cities of India." Renewable and Sustainable Energy Reviews 48: 452-462

[25]. Esen, H., et al. (2007). "A techno-economic comparison of ground-coupled and air-coupled heat pump system for space cooling." Building and environment 42(5): 1955-1965.

[26]. Demir, H., et al. (2009). "Heat transfer of horizontal parallel pipe ground heat exchanger and experimental verification." Applied Thermal Engineering 29(2-3): 224-233.

[27]. Eicker, U. and C. Vorschulze (2009). "Potential of geothermal heat exchangers for office building climatisation." Renewable Energy 34(4): 1126-1133.

[28]. Shua'a, A. K. M. and N. S. Sabeeh (2009). Analysis The Performance of Underground Heat Exchanger. Second Scientific Conference of the College of Engineering, University of Al-Qadisiya

[29]. Ozgener, L. and O. Ozgener (2010). "An experimental study of the exergetic performance of an underground air tunnel system for greenhouse cooling." Renewable Energy 35(12): 2804-2811.

[30]. Fujii, H., et al. (2010). Field tests of horizontal ground heat exchangers. 4th World Geothermal Congress.

[31]. Miyara, A., et al. (2011). "Experimental study of several types of ground heat exchanger using a steel pile foundation." Renewable Energy 36(2): 764-771.

[32]. Wu, Y., et al. (2011). "Prediction of the thermal performance of horizontal-coupled ground-source heat exchangers." International Journal of Low-Carbon Technologies 6(4): 261-269.

[33]. Zukowski, M., et al. (2011). Assessment of the cooling potential of an earth-tube heat exchanger in residential buildings. Environmental Engineering. Proceedings of the International Conference on Environmental Engineering. ICEE, Citeseer.

[34]. Congedo, P., et al. (2012). "CFD simulations of horizontal ground heat exchangers: A comparison among different configurations." Applied Thermal Engineering 33: 24-32.

[35]. Naili, N., et al. (2012). "Experimental analysis of horizontal ground heat exchanger for Northern Tunisia".

[36]. Abdul Rahman O. Alghannam"Investigations of Performance of Earth Tube Heat Exchanger of Sandy Soil in Hot Arid Climate" Journal of Applied Sciences Research, 8(6): 3044-3052, 2012.

[37]. Naili, N., et al. (2013). "In-field performance analysis of ground source cooling system with horizontal ground heat exchanger in Tunisia." Energy 61: 319-331.

[38]. Nikiforova, T., et al. (2013). "Methods and results of experimental researches of thermal conductivity of soils." Energy Procedia 42.(0)

[39]. NAILI, N., et al. (2013). "Experimental performance of horizontal ground heat exchanger for space cooling".

[40]. Bošnjaković, M., et al. (2013). THE GREENHOUSES SOIL HEATING BY GEOTHERMAL ENERGY. 5th International Scientific and Expert Conference TEAM 2013 Technique, Education, Agriculture & Management.

References

[41].Chen, J., et al. (2015). "Simulation and experimental analysis of optimal buried depth of the vertical U-tube ground heat exchanger for a ground-coupled heat pump system." Renewable Energy 73: 46-54.

[42].Boughanmi, H., et al. (2015). "Thermal performance of a conic basket heat exchanger coupled to a geothermal heat pump for greenhouse cooling under Tunisian climate." Energy and Buildings 104: 87-96.

[43].Naili, N., et al. (2016). "Assessment of surface geothermal energy for air conditioning in northern Tunisia: Direct test and deployment of ground source heat pump system." Energy and Buildings 111: 207-217.

[44].Patel, R. D. and P. Ramana (2016). "Experimental performance of buried tube heat exchanger validated by simulation performance in heating climate condition." Indian Journal of Science and Technology 9(33): 1-6.

[45].Sivasakthivel, T., et al. (2017). "Experimental thermal performance analysis of ground heat exchangers for space heating and cooling applications." Renewable Energy 113: 1168-1181.

[46].Song, X., et al. (2017). "Heat extraction performance simulation for various configurations of a downhole heat exchanger geothermal system." Energy 141: 1489-1503.

[47] .Ceylan, H. (2017). "Toprak Isı Değiştiricisi Uzunluğunun Kondenser Sıcaklığı ile Değişimi Üzerine Deneysel Çalışma." Mühendis ve Makina 58(688): 39-51.

[48].Popovici, C. G., et al. (2017). "Innovative Solutions for Geothermal Heat Exchangers." Energy Procedia 112: 434-441.

[49].Neupauer, K., et al. (2018). "Study of ground heat exchangers in the form of parallel horizontal pipes embedded in the ground." Energies 11(3): 491.

[50].Habibi, M. and A. Hakkaki-Fard (2018). "Evaluation and improvement of the thermal performance of different types of horizontal ground heat exchangers based on techno-economic analysis." Energy Conversion and Management 171: 1177-1192.

[51].Min-Jun Kima, Seung-Rae Leea, SeokYoonb, Jun-SeoJeona" An applicable design method for horizontal spiral-coil-type ground heat Exchangers" ELSVEIR. Geothermics 72 (2018) 338–347

[52]. Gao, J., et al. (2018). "Ground heat exchangers: Applications, technology integration and potentials for zero energy buildings." Renewable Energy 128: 337-349.

[53]. Revesz, A., et al. (2018). "Modelling of Heat Energy Recovery Potential form Underground Railways with Nearby Vertical Ground Heat Exchangers in an Urban Environment." Applied Thermal Engineering.

[54]. Hassanzadeh, R., et al. (2018). "A new idea for improving the horizontal straight ground source heat exchangers performance." Sustainable Energy Technologies and Assessments 25: 138-145.

[55]. Omer, A. (2018). "Heat exchanger technology and applications: ground source heat pump system for buildings heating and cooling." MOJ App Bio Biomech 2: 92-107.

[56]. Shi, Y., et al. (2018). "Numerical investigation on heat extraction performance of a downhole heat exchanger geothermal system." Applied Thermal Engineering 134: 513-526.

[57]. Boughanmi, H., et al. (2018). "A performance of a heat pump system connected a new conic helicoidal geothermal heat exchanger for a greenhouse heating in the north of Tunisia." Solar Energy 171: 343-353.

[58]. Noorollahi, Y., et al. (2018). "The effects of ground heat exchanger parameters changes on geothermal heat pump performance–A review." Applied Thermal Engineering 129: 1645-1658.

[59]. Lamarche, L. (2019). "Horizontal ground heat exchangers modelling." Applied Thermal Engineering 155: 534-545.

[60]. Atwany, H., et al. (2019). "Performance of earth-water heat exchanger for cooling applications.

[61]. William E. Glassley Geothermal Energy: Renewable Energy and the Environment , by Taylor and Francis Group, LLC(2010)،

[62]. Marc A. Rosen and Seama Koohi – Fayegh, Geothermal Energy Sustainable Heating and Cooling Using the Ground, University of Ontario Institute of Technology, Oshawa, Canada first edition, John Wiley & Sons, Ltd(2017) ،

[63]. Heat Pumps: The Definitive Guide For 2019 from https://www.everysolarthing.com/blog/heat-pumps/

[64]. Holman J. and Bhattacharyya S., Heat transfer, ninth edition, Tata Mc Graw-Hill, New Delhi.(2008) ،

[65]. Said, Habib, & Mokheimer. (2009). Horizontal Ground Heat Exchanger Design for Ground-Coupled Heat Pumps. Ecologic Vehicles - Renewable Energies - Monaco.

[66]. Lund, J. W. (2001). Design of Closed-Loop Geothermal Heat Exchangers in the U . S . Europe, 1–13.

[67]. Abbas Khalaf Mohammed Shua'ab&NawrasShareefSabeeh" Analysis The Performance of Underground Heat Exchanger" Second Scientific Conference of the College of Engineering - University of Al-Qadisiya Held on 19-20 Oct. 2009.

[68]. Haq, H., Martinkauppi, B., & Hiltunen, E. (2017). Analysis of ground heat exchanger for a ground source heat pump : A study of an existing system to find optimal borehole length to enhance the coefficient of performance. WEAS Transactions on Heat and Mass Transfer, 12(April), 38–47.

[69]. Merci, B. (2016). Introduction to fluid mechanics. SFPE Handbook of Fire Protection Engineering, Fifth Edition. https://doi.org/10.1007/978-1-4939-2565-0_1

[70]. Blázquez, C. S., Martín, A. F., Nieto, I. M., & González-Aguilera, D. (2017). Measuring of thermal conductivities of soils and rocks to be used in the calculation of A geothermal installation. Energies, 10(6). https://doi.org/10.3390/en10060795

[71]. Al-Dabbas, M. A., Schanz, T., & Yassen, M. J. (2012). Proposed engineering of Gypsiferous soil classification. Arabian Journal of Geosciences, 5(1), 111–119. https://doi.org/10.1007/s12517-010-0183-

[72]. Ali, T. S., & Fakhraldin, M. K. (2016). Soil parameters analysis of Al-Najaf City in Iraq: case study. J Geotech Eng, 3(1), 1987–2394.

[73]. Ming Zhong Zhao ; Simulation of Earth-To-Air Heat Exchanger Systems Thesis in the deparment of bulding,civila and environmental engineering at Concordia university montreal;Canada;2004

References

[74] weatherspark.com. from https://weatherspark.com/y/103207/Average-Weather-in-Najaf-Iraq-Year-Round.

[75] W.P. Graebel," Advanved fluid mechanics",ISBN: 978-0-12-370885-4,2007

[76] Glassley, W. E. (2014). Geothermal energy: renewable energy and the environment, CRC press.

Appendix (A)

Calibrations

Table.A-1 Calibration for water flow meter

General flow	1	2	3	4	5
Dig.flowmeter	1.349	2.039	3.029	4.209	4.955
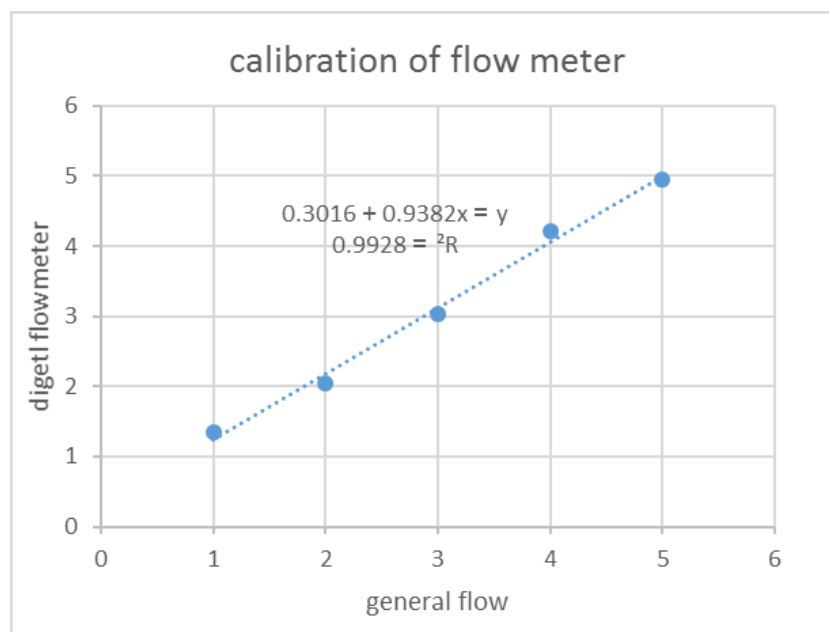
Fig.A-1: Calibration for water flow meter.

Table.A-2: Calibration for temperature sensors.

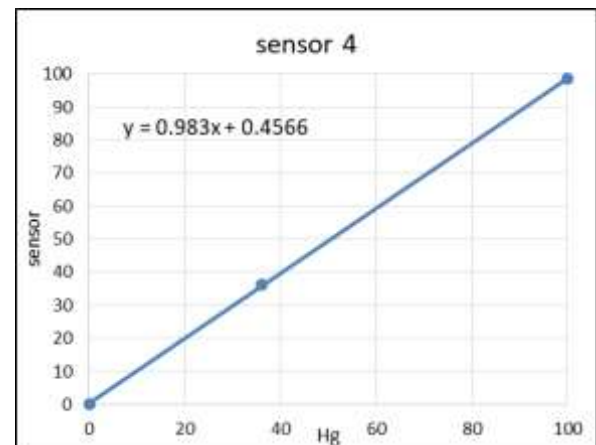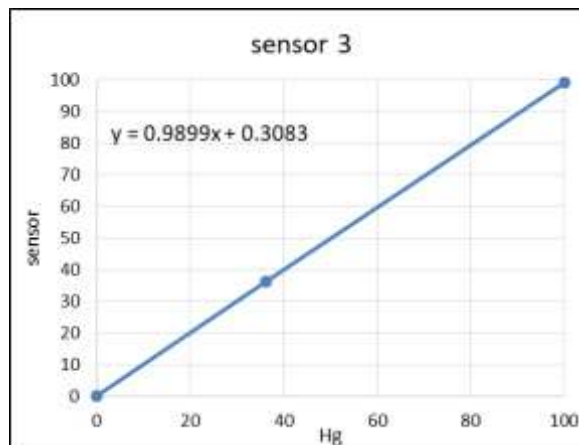| Device No.	Freezing temperature = 0 C°	Human body temperature = 37 C°	Boiling temperature = 100 C°
Hg thermometer	0	36.09	100
Sensor 1	0.19	36.2	98.8
Sensor 2	0.12	36.1	98.92
Sensor 3	0.17	36.25	99.22
Sensor 4	0.21	36.32	98.62
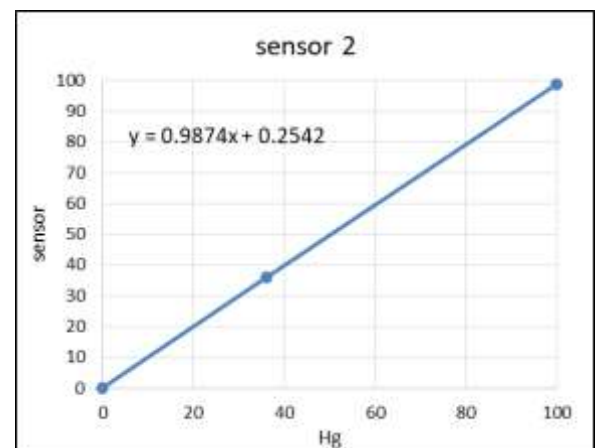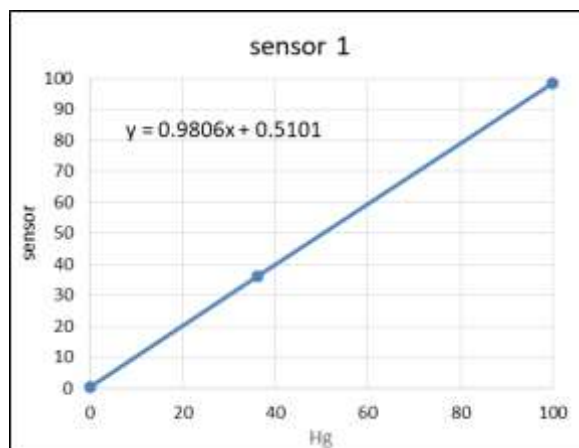
Fig.A-2: Temperature sensors calibration curves

Table.A-3: Calibration for temperature thermocouples of thermal conductivity device

Hg thermometer	15	23	34	40	52
Thermocouple 1	16	22	33.7	39.3	51.6
Thermocouple 2	15.6	21.8	33.4	38.8	51.2
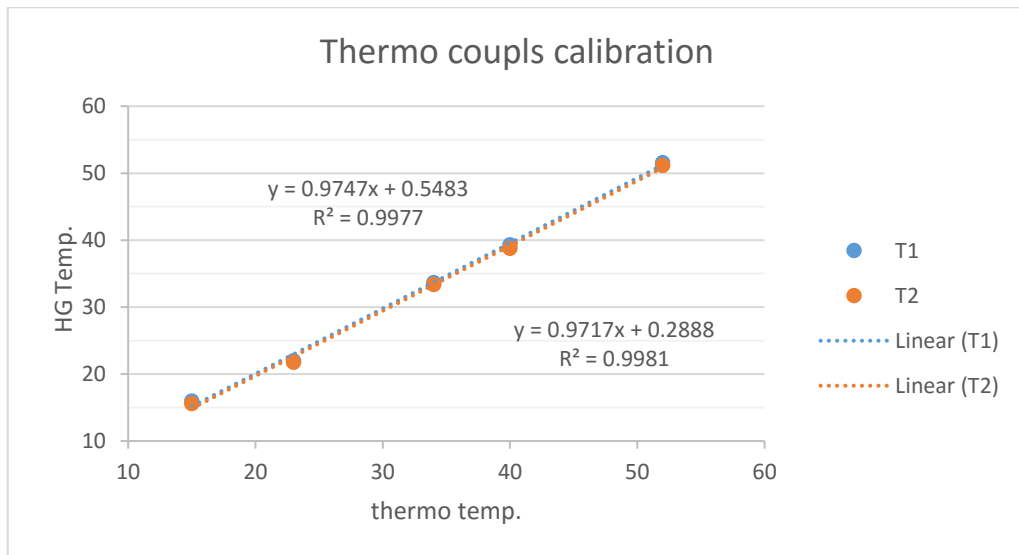
Fig.A-3

Table.A-4: Calibration for thermocouples for soil thermal gradient

Hg thermometer	0.2	19	32	65	86
Thermocouple 1	0.2	20.4	34.7	63	84.8
Thermocouple 2	0.2	20.9	34.5	69.5	87.5
Thermocouple 3	0	20.5	34.2	66.6	80.8
Thermocouple 4	0	20.6	34.3	69.3	87
Thermocouple 5	0	20	33.1	65.5	86.2
Thermocouple 6	0	20.1	33.3	63.6	84.7
Thermocouple 7	0.1	19.8	34.2	64.9	86.2
Thermocouple 8	0.2	21.6	34.1	63.4	85.9

Fig.A-4

جدول (1) تحليل الخصائص الفيزيائية والكيميائية لترب منطقة الدراسة

CaSo4	CaCO3	K	Na	Mg	Ca	PH	EC	العضوية	النسجة	التحليل الميكانيكي			الاحداثيات		الموقع
										طين	غرين	رمل	دائرة العرض	خط الطول الموقع	
1.52	8.8	3.14	28.88	2.61	9.84	7.8	11.13	0.09	رملة	5.5	6.36	88.14	32.15	44.12	B1
1.47	8.81	3.15	19.99	2.59	9.83	7.8	11.2	0.07	رملة	5.47	6.37	88.16	32.10	43.45	B2
1.49	8.89	3.15	28.88	2.59	9.83	7.8	11.13	0.05	رملة	5.54	6.33	88.13	32.01	44.20	B3
1.71	8.3	0.71	55.31	3.56	9.57	8.5	16.52	0.06	رملة مزيجة	7.05	16.43	76.52	31.47	44.85	B4
1.68	8.9	0.7	28.06	3.59	9.58	8.4	11.13	0.05	رملة مزيجة	7.05	16.47	76.48	31.26	44.25	B5
1.69	8.91	0.69	28.06	3.58	9.58	8.5	11.1	0.03	رملة مزيجة	7.06	16.43	76.51	30.58	43.28	B6
1.7	8.89	0.69	28.06	3.57	9.57	8.5	11.11	0.06	رملة مزيجة	7.05	16.43	76.52	31.23	43.45	B7
1.7	8.91	0.68	28.06	3.57	9.55	8.4	11.12	0.04	رملة مزيجة	7.06	16.47	76.47	30.36	43.4	B8
1.73	8.93	0.68	28.07	3.56	9.57	8.4	11.11	0.07	رملة مزيجة	7.08	16.43	76.49	31.05	44.33	B9
1.69	8.89	0.68	28.05	3.58	9.56	8.5	11.11	0.03	رملة مزيجة	7.06	16.47	76.47	32.05	44.12	B10
1.7	8.88	0.71	28.04	3.57	9.55	8.5	11.13	0.06	رملة مزيجة	7.09	16.43	76.48	31.45	43.49	B11
1.72	8.89	0.69	28.08	3.58	9.57	8.5	11.11	0.06	رملة مزيجة	7.06	16.45	76.49	31.19	44.39	B12
1.71	8.91	0.7	28.06	3.58	9.59	8.5	11.13	0.07	رملة مزيجة	7.07	16.46	76.47	31.13	43.59	B13
1.69	8.9	0.72	28.06	3.58	9.58	8.5	11.12	0.04	رملة مزيجة	7.08	16.44	76.48	31.49	43.25	B14
1.68	8.9	0.71	28.06	3.57	9.55	8.4	11.13	0.05	رملة مزيجة	7.05	16.46	76.49	31.06	43.46	B15
1.69	8.92	0.78	28.07	3.59	9.56	8.4	11.13	0.06	رملة مزيجة	7.06	16.43	76.51	31.23	43.30	B16
1.7	8.3	0.7	28.06	3.56	9.57	8.4	11.1	0.05	رملة مزيجة	7.06	16.45	76.49	31.18	43.18	B17
1.71	8.89	0.69	28.04	3.58	9.56	8.5	11.12	0.06	رملة مزيجة	7.07	16.48	76.45	31.15	43.27	B18
1.71	8.89	0.69	28.04	3.58	9.56	8.5	11.12	0.05	رملة مزيجة	7.07	16.48	76.45	31.12	43.29	B19
1.71	8.89	0.72	28.08	3.59	9.57	8.5	11.12	0.04	رملة مزيجة	7.02	16.47	76.51	31.15	43.09	B20

المصادر : 1. مختبر السيطرة النوعية ، جامعة الكوفة، 2011/3/22.

2. مختبرات البحوث العلمية ، محافظة القادسية ، 2011/4/12 .

3. مختبر تحاليل التربة ، المعهد التقني ، النجف ، 2012/3/24.
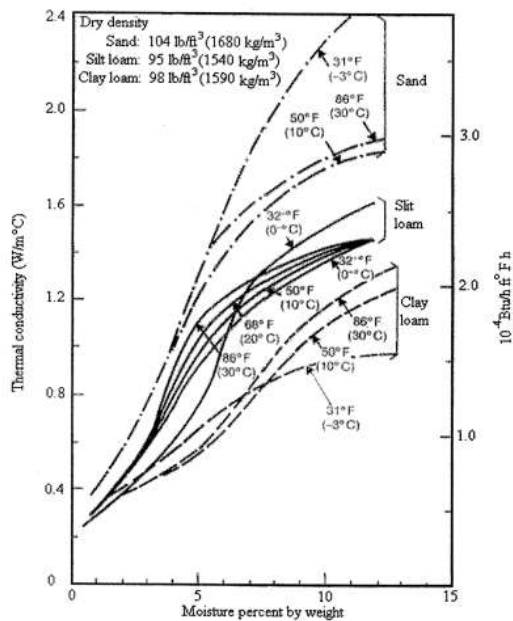
	Dry Density, kg/m³	Conductivity, W/(m·K)	Diffusivity, m²/day
Soils			
Heavy clay (15% water)	1925	1.4 – 1.9	0.042 – 0.061
Heavy clay (5% water)	1925	1.0 – 1.4	0.047 – 0.061
Light clay (15% water)	1285	0.7 – 1.0	0.055 – 0.047
Light clay (5% water)	1285	0.5 – 0.9	0.056 – 0.056
Heavy sand (15% water)	1925	2.8 – 3.8	0.084 – 0.11
Heavy sand (5% water)	1925	2.1 – 2.3	0.093 – 0.14
Light sand (15% water)	1285	1.0 – 2.1	0.047 – 0.093
Light sand (5% water)	1285	0.9 – 1.9	0.055 – 0.12
Rocks			
Granite	2650	2.3 – 3.7	0.084 – 0.13
Limestone	2400 – 2800	2.4 – 3.8	0.084 – 0.13
Sandstone	2570 – 2730	2.1 – 3.5	0.65 – 0.11
Wet shale		1.4 – 2.4	0.065 – 0.084
Dry shale		1.0 – 2.1	0.055 – 0.074
Grouts/Backfills			
Bentonite (20% soilds)		0.73 – 0.75	
Cement		0.70 – 0.78	
20% Bent.-40% SiO₂ sand		1.48	
Concrete (50% SiO₂ sand)		2.1 – 2.8	

From the book of geothermal energy [76] we can assume the following:

$(T_{in} - T_{out}) = 10°C$

1 refrigeration ton = 3504 w

$\dot{m} = 0.083865$ kg/s

$\dot{V} = 5.0319$ LPM

0.5 refrigeration ton = 1752 w

$\dot{m} = 0.041933$ kg/s

$\dot{V} = 2.5159$ LPM

L = 234.586 m   for Q=1 refrigeration ton

L = 117.293 m   for Q=0.5 refrigeration ton

We used 200m length of pipe at two layers each layer have 100 m ,so that's probably the rate of heat transfer Q become less than 3504w for two layers and less than 1752 w for one layer.

The estimation of the present research problem, needs to estimate the properties of the used working fluid. The variation of fluid temperature leads to variation in its properties such as the density, viscosity, specific heat and the thermal conductivity [75]. In this study, the mentioned properties are estimated based on the following empirical formulas:

$$c_p = -0.00000003136\ T_b^5 + 0.00001113\ T_b^4 - 0.00149\ T_b^3 + 0.1025 - 3.323\ T_b + 4217.8$$

$$\mu = -0.00000000254\ T_b^3 + 0.00000057\ T_b^2 - 0.0000465\ T_b + 0.001746$$

$$K = -0.000009484\ T_b^2 - 0.002136\ T_b + 0.56$$

$$\rho = -0.000000179\ T_b^4 + 0.0000512\ T_b^3 - 0.008172 T_b^2 + 0.0659\ T_b + 999.78$$

Where:

T_b: fluid bulk temperature (˚C).

Appendix

الخلاصة

تم اختبار عدة تقنيات لنقل الحرارة وعلى مدى سنوات لغرض الحصول على نقل جيد للحرارة وتكلفة تشغيل منخفضة ، ومن هذه التقنيات المبادلات الحرارية تحت الأرض لأنواع وأغراض مختلفة لاستخدامها والتي تعتمد على نقل حرارة السوائل بداخلها إلى أعماق التربة والعكس صحيح.

تم تصميم واختبار المبادل الحراري الأفقي تحت الأرض ذو الطبقتين كنظام مغلق لتقليل المساحة المطلوبة. تركيب مبادلات حرارية أفقية بطبقة واحدة ، يحتاج إلى مساحة كافية لدفن المبادل ، مما يزيد من التكلفة الاقتصادية لهذا النوع من المبادلات الحرارية تحت الأرض والتي تعد أحد عيوب المبادلات الحرارية الأفقية (عدم وجود مساحة كافية في بعض الأحيان) . تم تسجيل انحدار درجة حرارة التربة خلال العام ، ولوحظ ثباتها النسبي على العمق المحدد من 2 م إلى 3.5 م ، بالإضافة إلى قياس التوصيل الحراري لعينة من نفس التربة ومعرفة خصائصها.تم استخدام انابيب من نوع بولي اثلين متعدد الطبقات و بقطر خارجي 16 مم وبسمك 2 مم وبطول 100 م لكل طبقة.

تم تصميم شبكتين على شكل اعوج طول كل شبكة 100 متر ، حيث تواجه انابيب الشبكتين بعضها البعض بترتيب متدرج) على شكل (V لزيادة مساحة التلامس للأنابيب للحصول على نقل حرارة أكبر . وباستخدام برنامج COMSOL ، بافتراض نظام ثنائي الأبعاد وإدخال خصائص التصميم للأنابيب والتربة ، تم اقتراح المسافة المثلى بين الأنابيب لتكون (0.3-0.5) متر,وتم اختيار البعد 0.4متر لتصميم المبادل الحراري الارضيGHE .

تم دفن الطبقة الأولى من أنابيب النظام على عمق 3 أمتار والطبقة الثانية من أنابيب النظام على عمق 2.5 متر من سطح الأرض ، وتم إجراء الاختبارات على كل طبقة على حدة ثم للطبقتين معًا ، عن طريق تغيير درجة حرارة الماء الداخل من 30 و 40 و 50 درجة مئوية تقريبا وبمعدلات تدفق مختلفة من 2 و 3 و 4 و 5 لتر / دقيقة والتي تم تحقيقها في الفترة (2019/6/12 - 2019/7/22). لغرض التبريد في أشد شهور المنطقة حرارة.

عند تشغيل النظام في وضع الطبقة المزدوجة ، تم الحصول على فرق درجة حرارة عالية (المتوسط 15.96 درجة مئوية) ، وعند تشغيل النظام بوضع طبقة واحدة ، يكون اعلى متوسط

فرق درجة الحرارة الناتج (15.8) و (13.4) درجة مئوية بالنسبة الطبقة الأولى والثانية ، على التوالي ، في ظل ظروف مختلفة

من أجل تسجيل معامل الأداء (COP) ، تم اختبار النظام لكلا الطبقتين لتسجيل أعلى قيمة ، وكان 8.59 (COP) في وضع التشغيل ثنائي الطبقات و 5.9 ، 5.2 للطبقتين الأولى والثانية الطبقات على التوالي في نفس الظروف ، بسبب زيادة التدفق عند اختبار كل طبقة أنبوب على حدة ، مقارنة باختبار الطبقات المزدوجة معًا.

دراسة تجريبية لمبادل حراري تحت الأرض بطبقتين

رسالة مقدمة الى

قسم هندسة تقنيات ميكانيك القوى كجزء من متطلبات نيل درجة الماجستير في تكنلوجيا الحراريات في هندسة تقنيات ميكانيك القوى

تقدم بها

زهراء صالح عبد زيد

بكالوريوس في هندسة تقنيات السيارات

بإشراف

الاستاذ المساعد الدكتور	الاستاذ المساعد الدكتور
علي نجاح كاظم	**تحسين علي حسين**

اغسطس – 2020